SONNE-Berichte

Biogeochemistry/atmosphere processes in the Bay of Bengal: A contribution to the 2nd International Indian Ocean Expedition

Cruise No. SO305

10 April – 22 May 2024

Colombo (Sri Lanka) – Singapore (Singapore)

BIOCAT-IIOE2

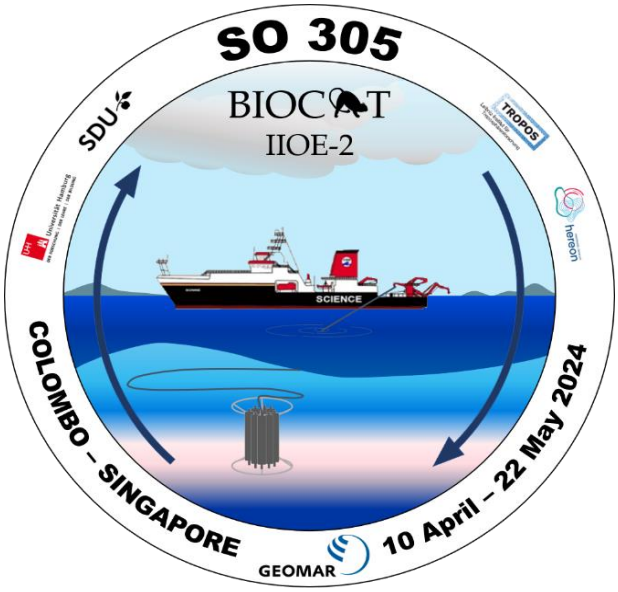

Hermann W. Bange, Ina Stoltenberg, Tjark Andersch, Damian Arévalo-Martínez, Elliot Atlas, Arun Babu Suja, Antoine Barbot, Theresa Barthelmeß, Kevin Becker, Dennis Booge, Laura Bristow, Anja Conventz, Rena Czeschel, Kirstin Dähnke, Shravan Deshmukh, Felix Duerkop, Paula Eisnecker, Anja Engel, Bert Engelen, Hendrik Feil, Victor Fernández-Juárez, Albert Firus, Martin Frank, Birgit Gaye, Martha Gledhill, Sandra Golde, Hendrik Großelindemann, Edmund Hathorne, Silvia Henning, Isabell Hentschel, Hartmut Herrmann, Riel Ingeniero, Mats Jacobsen, Rainer Kiko, Niko Lahajnar, Kira Lange, Carolin Löscher, Christa Marandino, Clara McKellar, Julia Mickenbecker, Mario Müller, Thomas Müller, Leandro Nazzari, Lubrina Nielsen, Jule Ploschke, Mira Pohlker, Benjamin Pontiller, Laurent Poulain, Birgit Quack, René Rabe, Jon Roa, Sönke Rolfes, Tina Sanders, Isabell Schlangen, Leon Schmidt, Gesa Schulz, Marcel Sommer, Bo Thamdrup, Jannis Usinger, Laurenz van Bonn, Manuela van Pinxteren and Qingwen Zhong

Prof. Dr. Hermann W. Bange

GEOMAR Helmholtz Centre for Ocean Research Kiel

2024

Table of Contents

1 Cruise Summary

1.1 Summary in English

The overarching goal of SO305 BIOCAT-IIOE2 was to quantify key (micro)biological processes in the water column and ocean/atmosphere exchange fluxes to assess their impacts on the oxygen minimum zone (OMZ) of the Bay of Bengal. To this end, we conducted a measurement campaign with the research vessel (RV) SONNE from 10 April to 22 May 2024 (SO305) as part of the BIOCAT-IIOE2 project, covering the main carbon and nitrogen cycle processes and physical processes in the water column. The oceanic measurements were complemented by an intensive atmospheric measurement program to investigate the effects of atmospheric inputs on water column processes. During SO305 the GEOMAR Helmholtz Centre for Ocean Research Kiel, the University of Hamburg, the Helmholtz Centre Hereon (Geesthacht), the Leibniz Institute for Tropospheric Research (TROPOS, Leipzig), the University of Oldenburg and the University of Southern Denmark (SDU, Odense, DK) were collaborating. A team of 39 scientists, students and technicians made measurements in the water column and in the atmosphere at 33 regular CTD stations and five 24h-stations along a cruise track from the eastern equatorial Indian Ocean to the central Bay of Bengal. The results of SO305 BIOCAT-IIOE2 will contribute to a significantly improved assessment of the future impacts of global climate change and pollution for the ecosystems and the OMZ of the Bay of Bengal.

1.2 Zusammenfassung

Das übergeordnete Ziel von SO305 BIOCAT-IIOE2 war, die wichtigsten (mikro)biologischen Prozesse in der Wassersäule und die Austauschflüsse zwischen Ozean und Atmosphäre zu quantifizieren, um ihre Auswirkungen auf die Sauerstoffminimumzone (SMZ) des Golfs von Bengalen zu bewerten. Zu diesem Zweck haben wir vom 10. April bis zum 22. Mai 2024 eine Messkampagne mit dem Forschungsschiff (FS) SONNE durchgeführt (SO305), die die wichtigsten Prozesse des Kohlenstoff- und Stickstoffkreislaufs sowie physikalische Prozesse in der Wassersäule erfasste. Die ozeanischen Messungen wurden durch ein intensives atmosphärisches Messprogramm ergänzt, um die Auswirkungen der atmosphärischen Einflüsse auf die Prozesse in der Wassersäule zu untersuchen. Während SO305 haben das GEOMAR Helmholtz-Zentrum für Ozeanforschung Kiel, die Universität Hamburg, das Helmholtz-Zentrum Hereon (Geesthacht), das Leibniz-Institut für Troposphärenforschung (TROPOS, Leipzig), der Universität Oldenburg und der University of Southern Denmark (SDU, Odense, DK) zusammengearbeitet. Ein Team von 39 Wissenschaftlern/innen, Studenten/innen und Technikern/innen führte Messungen in der Wassersäule und in der Atmosphäre an 33 CTD-Stationen und fünf 24-Stunden-Stationen entlang einer Fahrtroute vom östlichen äquatorialen Indischen Ozean zum zentralen Golf von Bengalen durch. Die Ergebnisse von SO305 BIOCAT-IIOE2 werden dazu beitragen, die künftigen Auswirkungen des globalen Klimawandels und der Umweltverschmutzung auf die Ökosysteme und die SMZ des Golfs von Bengalen wesentlich besser einschätzen zu können.

2 Participants

2.1 Principal Investigators

Name	Institution
Bange, Hermann, Prof. Dr.	GEOMAR
Gaye, Birgit, Dr.	Univ. Hamburg
Löscher, Carolin, Prof. Dr.	SDU
van Pinxteren, Manuela, Dr.	TROPOS

Fig. 2.1 Participants of SO305 BIOCAT-IIOE2 on 09 April 2024; in front of RV SONNE before departure from Colombo, Sri Lanka. In the front, sitting, from left to right: Qingwen Zhong, Jon Roa, Gesa Schulz, Anja Conventz, Isabell Schlangen, René Rabe, Arun Babu Suja, Shravan Deshmukh, Lubrina Nielsen, Jule Ploschke and Riel Ingeniero. In the back, standing, from left to right: Hermann Bange, Felix Duerkop, Marcel Sommer, Antoine Barbot, Albert Firus, Ina Stoltenberg, Victor Fernández-Juárez, Mario Müller, Isabell Hentschel, Birgit Quack, Sandra Golde, Theresa Barthelmeß, Paula Eisnecker, Clara McKellar, Martha Gledhill, Laurenz van Bonn, Mats Jacobsen, Leon Schmidt, Hendrik Großelindemann, Jannis Usinger, Julia Mickenbecker, Hendrik Feil, Kira Lange, Dennis Booge, Sönke Rolfes, Tjark Andersch, Rena Czeschel and Leandro Nazzari.

2.2 Scientific Party

Name	Discipline	Institution
Bange, Hermann, Prof. Dr.	Trace gases / Chief Scientist	GEOMAR
Schmidt, Leon	Nutrients, O_2	Hereon
Usinger, Jannis	Nutrients, O_2	GEOMAR
Lange, Kira	Nutrients, O_2	GEOMAR
Czeschel, Rena, Dr.	CTD, microstructure, Argo float deployment, mooring deployment	GEOMAR
Müller, Mario	CTD, microstructure, Argo float deployment, mooring deployment	GEOMAR
Zhong, Qingwen	CTD, microstructure, Argo float deployment, mooring deployment	GEOMAR
Großelindemann, Hendrik	CTD, microstructure, Argo float deployment, mooring deployment	GEOMAR
Duerkop, Felix	CTD, microstructure, Argo float deployment, mooring deployment	GEOMAR
McKellar, Clara	CTD, microstructure, Argo float deployment, mooring deployment	GEOMAR
Stoltenberg, Ina, Dr.	N_2O, CH_4, NO	GEOMAR
Van Bonn, Laurenz	N_2O, CH_4	GEOMAR
Hentschel, Isabell	N_2O, CH_4	GEOMAR
Eisnecker, Paula	CO, N_2O, CH_4, N_2O/CO underway	GEOMAR
Sommer, Marcel	CO, N_2O, CH_4, N_2O/CO underway	GEOMAR
Ingeniero, Riel	NO	GEOMAR
Barthelmeß, Theresa, Dr.	POM, DOC, drifting sediment traps	GEOMAR
Golde, Sandra	POM, DOC, drifting sediment traps	GEOMAR
Roa, Jon	POM, DOC, drifting sediment traps	GEOMAR
Barbot, Antoine	POM, DOC, drifting sediment traps	GEOMAR
Gledhill, Martha, Dr.	Trace elements/metals	GEOMAR
Firus, Albert	Trace elements/metals	GEOMAR
Conventz, Anja	Trace elements/metals	GEOMAR
Quack, Birgit, Dr.	Halocarbons	GEOMAR
Ploschke, Jule	Halocarbons	GEOMAR
Mickenbecker, Julia	Halocarbons	GEOMAR
Booge, Dennis, Dr.	DMS, isoprene	GEOMAR
Feil, Hendrik	DMS, isoprene	GEOMAR
Rolfes, Sönke	DMS, isoprene, meta genomics	U. Oldenburg
Schulz, Gesa, Dr.	^{15}N isotopes, suspended mater	U. Hamburg
Andersch, Tjark	^{15}N isotopes, suspended matter	U. Hamburg
Nazzari, Leandro	^{15}N isotopes, suspended matter	U. Hamburg
Schlangen, Isabell	Microbial processes, meta genomics	SDU
Jacobsen, Mats	Microbial processes, meta genomics	SDU

Nielsen, Lubrina	Microbial processes, meta genomics	SDU
Fernández Juárez, Victor, Dr.	Microbial processes, meta genomics	SDU
Rabe, René	Aerosols, atm. trace gases	TROPOS
Babu Suja, Arun, Dr.	Aerosols, atm. trace gases	TROPOS
Deshmukh, Shravan	Aerosols, atm. trace gases	TROPOS

2.3 Participating Institutions

GEOMAR	Helmholtz-Zentrum für Ozeanforschung Kiel
Hereon	Helmholtz-Zentrum Geesthacht
SDU	University of Southern Denmark, Odense, Denmark
TROPOS	Leibniz-Institut für Troposphärenforschung, Leipzig
U. Hamburg	Universität Hamburg
U. Oldenburg	Universität Oldenburg

3 Research Program

3.1 Description of the Work Area

3.1.1 Bay of Bengal

The Bay of Bengal (BoB, located between 05°-23°N and 80°-95°E) forms the north-eastern basin of the Indian Ocean. The BoB is characterized by a unique environmental setting which shows a remarkable seasonality driven by the Asian monsoon system with a summer monsoon season (SW monsoon) from June-August and a winter monsoon season (NE monsoon) from December-February. The major physical drivers of the environmental setting of the BoB are summarized in Fig. 3.1. The Asian monsoon system leads to

(i) pronounced rainfall and river discharge with maximum freshwater inputs in September by the Ganges/Brahmaputra and Irrawaddy river systems in the northern BoB,
(ii) a seasonally reversing upper ocean circulation and
(iii) a severe atmospheric pollution (known as the ‘South Asian Brown Cloud’) which lasts over the BoB from November to May.

Moreover, the BoB hosts one of the world-wide most intense oxygen minimum zones (OMZ) with persistent minimum oxygen concentrations as low as 0.01 µM (Bristow et al., 2017).

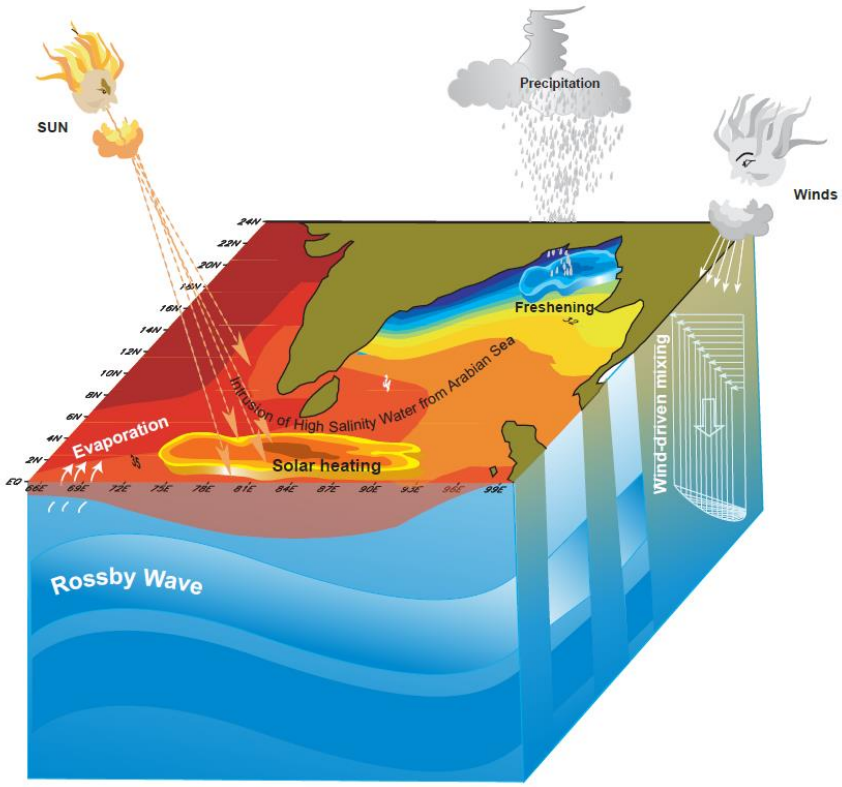

Fig. 3.1 Schematic representation of the local and remote physical forcings that influence the water column of the BoB. Colour shading depicts the climatological monthly mean salinity for August. Local forcing that affect the BoB are precipitation, river runoff, solar heating and mixing by monsoon winds. The remote forcing are the intrusions of high salinity waters from the Arabian Sea and propagation of Rossby waves. (Fig. is taken from Narvekar and Prasanna Kumar, 2014).

3.1.2 Eastern Equatorial Indian Ocean

The eastern part of the equatorial Indian Ocean is located at the southern boundary of the BoB between 05°N-10°S and 80-95°E and separates the BoB from the south-eastern Indian Ocean. The equatorial circulation of the Indian Ocean is characterized by annual mean winds that are westerly along the equator rather than easterly. These winds favour downwelling at the equator rather than upwelling as observed in the equatorial Pacific and Atlantic Oceans (Phillips et al., 2024). Moreover, seasonal reversals of the winds along the equator lead to strong semi-annual variability, with strong eastward currents, known as Wyrtki jets, dominating the upper 100 m during the transitions between the NE and SW monsoons (Phillips et al., 2024). There is no permanent equatorial undercurrent, i.e., no distinctive core of eastward flow in the thermocline. An undercurrent-like structure does appear in February-March near the end of the NE monsoon following a two-month period of sustained easterly winds along the equator, but this feature is transient and quickly disappears with the onset of westerly winds during the following monsoon transition season. A weaker and more variable undercurrent appears in August–September (Phillips et al., 2014).

3.2 Aims of the Cruise

The overarching goal of SO305 BIOCAT-IIOE2 was to quantify the key (micro)biological processes in the water column and ocean/atmosphere exchange fluxes in order to assess their impacts on the OMZ of the Bay of Bengal. The specific goals of the cruise were:

- To decipher the physical and biogeochemical setting of the water column,
- To identify the physical and biogeochemical/microbial processes which are crucial for the, development and maintenance of the OMZ,
- To assess the efficiency of the biological pump,
- To quantify the fluxes of climate-relevant trace gases across the ocean/atmosphere interface,
- To estimate the fluxes of trace metals and nutrients to the ocean from the ocean boundaries (i.e. atmosphere, continent and sediments) and
- To characterize the species and amount of natural and anthropogenic constituents (incl. trace gases and aerosols) in the marine boundary layer of the Asian outflow and their effects on the self-cleaning capacity (i.e. oxidizing efficiency) of the atmosphere.

3.3 Agenda of the Cruise

The regular, repetitive work at 38 stations included the use of the CTD/Rosette (CTD/Ro, from the water surface to the sea floor at a maximum water depth of 4500 m), microstructure measurements (with a free-falling microstructure probe up to 200 m water depth) and the use of GoFlo water samplers (up to a water depth of 500 m). At five 24h-stations, the regular station program was supplemented by zodiac deployments to sample the uppermost meter of the water column, the use of a submersible pump (up to a water depth of 150 m) and the deployment of drifting sediment traps (which were picked up again after 48 hours). In addition to the station work, continuous measurements were carried out in the atmosphere (trace gases, aerosols) and in the surface water (dissolved trace gases and sampling for trace metals with a Towed-fish). Moreover, we deployed a long-term deep-sea mooring at the equator and deployed two Argo floats in the southern and central BoB. The cruise track of SO305 BIOCAT-IIOE2 is shown in Fig. 3.2.

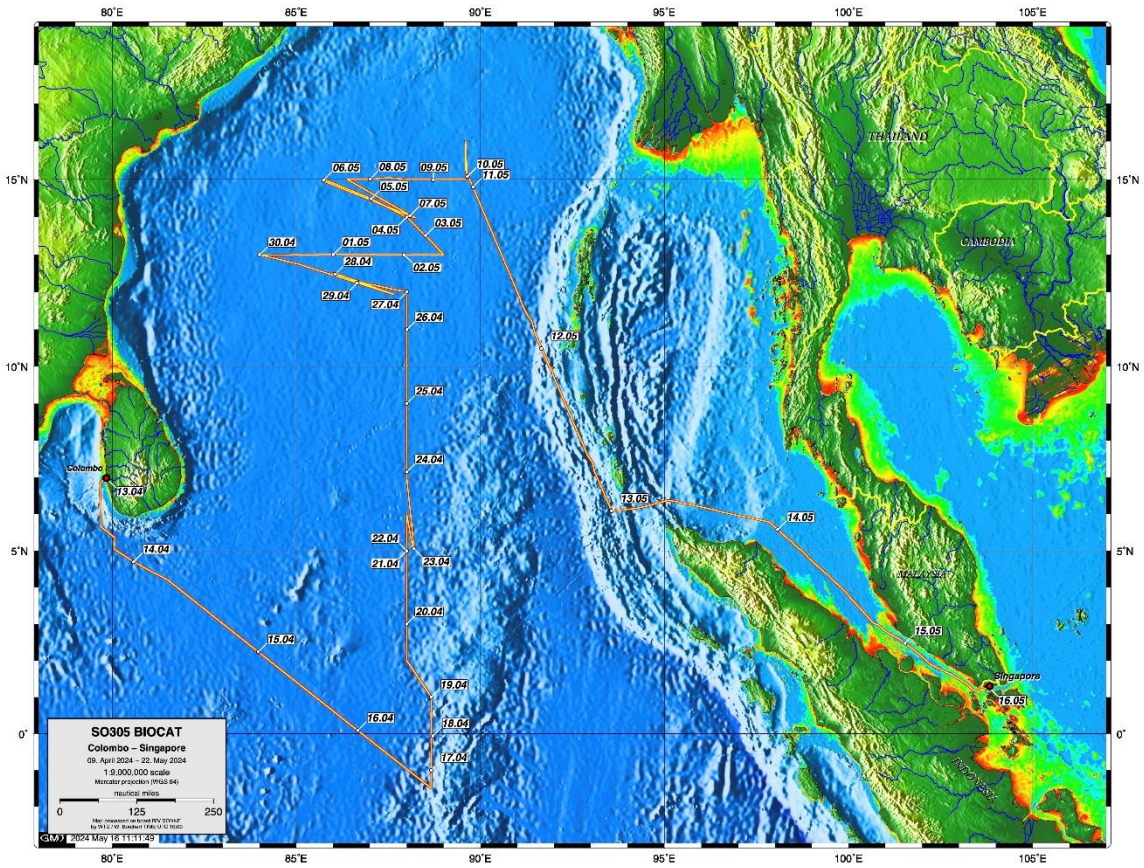

Fig. 3.2 Cruise track of RV SONNE Cruise SO305 BIOCAT-IIOE2.

3.3.1 Unforeseen Deviations from the Original Agenda of the Cruise

1) The cruise was originally planned to take place in spring 2021 but was shifted to April/May 2024 because of the Corona pandemic.
2) The originally planned stations in the EEZ of Bangladesh (i.e. on the shelf off Bangladesh) have been cancelled a few days prior to the departure from Colombo because an appropriate diplomatic permission was missing. The berth reserved for an observer from Bangladesh was, therefore, not occupied.
3) The national Bangladesh Contact Point for matters relating to the Nagoya Protocol never replied to our repeated requests for approval of collection of biological samples in the EEZ of Bangladesh.
4) We left the port of Colombo (Sri Lanka) with a delay of about 3.5 days because the six transport containers did not arrive in Colombo in time. One dangerous goods container is still in Singapore while writing this report (31 July 2024).
5) Due to a medical emergency caused by an accident at work, the cruise was terminated prematurely on 11 May. We arrived in Singapore on 16 May, six days earlier as originally planned.

3.3.2 Responsible Marine Research

Sampling and measurements (incl. hydroacoustic surveys) in both the water and in the atmosphere were carried outside the EEZs in international waters only. All drifting instruments (except for the

two Argo floats) were successfully recovered. The deep-sea mooring was deployed in international waters and will be recovered in the upcoming 2-3 years. No zoological material was collected. All data will be archived and will be published after 2 years after the end of the cruise.

4 Narrative of the Cruise

We left the port of Colombo (Sri Lanka) at 20:30 LT on 13 April with a delay of about 3.5 days because the delivery of our six transport containers was delayed. Underway measurements in the surface water and the atmosphere started after leaving the EEZ of Sir Lanka on 15 April at around 05:00 LT (= UTC + 5.5h). After a transit of 2.5 days we performed a test station (stat #01) close to the equator at 0°27.4'N 86°10.7'E on 16 April to test the CTD/Ro and to optimize seawater sampling from the Niskin bottles. The first regular station (stat #02) was performed at 1.5°S 88°40'E on 17 April. It was followed by a series of four stations (stat #03 - #06) on a south to north section crossing the equator along 88°40'E up to 1°N with a latitudinal spacing of 0.5°. At station #04, located at equator (0°N 88°40'E), a long-term deep-sea mooring (with ADCP, oxygen sensors and CTD devices) was deployed in about 4500 m water depth. We then steamed a little further west to 88°E, to the start of our main south to north section through the Bay of Bengal. Stations #07 to #10 were spaced 1° apart from 2°N to 5°N along 88°E. On 21 April we had the first 24h-station (stat #10 at 5°N 88°E). At this station we deployed a first set of drifting particle traps and an Argo float. We continued the section along 88°E with station #11 (sampled at 6°N 88°E on 23 April). After completing station #11 we steamed back south to pick up the drifting traps at 5°0.3'N 88°10.8'E (= stat #12 on 23 April I the afternoon). Between 24 April and 26 April, stations #13 (7°N) to #18 (12°N) located in 1° intervals along 88°E were sampled. At station #18, which was the second 24h-station, we deployed both a second set of drifting particle traps and an Argo float. After completing station #18 we followed a diagonal section to the northwest with stations #19 (12°12.3'N 87°1.5'E on 28 April in the morning) and 20# (12°30'N 86°0'E on 28 April in the afternoon). After station #20 we steamed back to pick up the drifting traps at 11°55.7'N 87°43.9'E (= stat #21). We completed the diagonal section with stations #22 (at 12°44.5'N 85°4.5'E on 30 April) and #23 (13°N 84°E on 30 April in the afternoon). This was followed by stations #24 (13°N 85°E on 01 May) to #28 (13°N 89°E on 03 May) which were located in 1° intervals along the west to east section at 13°N. A second diagonal section to the northwest was started with stations #29 (13°30.7'N 88°30.6'E) and #30 (at 14°N 88°E on 04 May). Station #30 was the third 24-station. At this station we deployed the third set of drifting particle traps. The diagonal section was completed with station #31 (14°30'N 87°E on 05 May) and #32 (15°N 85°45'E on 06 May). Station #32 was the fourth 24h-station. After station #32 we steamed back to pick up the drifting traps at 13°59.11'N 88°11.7'E on 07 May (= stat #33). This was followed by stations #34 (15°N 88°E on 08 May) to #37 (15°N 89°36'E on 09 May) which were located along a west to east section at 15°N. Station #37 was the fifth 24h-station. The last station (#38) was performed at 16°N 89°36'E on 11 May. Due to a medical emergency caused by an accident at work on 06 May, the cruise was terminated prematurely at 10h on 11 May after the station work at station #38 had been completed. All underway measurements in the atmosphere and in the water were stopped on 11 May at 14:00 LT (= UTC + 6h) with the entry into the EEZ of India. We arrived at the pier in Singapore at 11:00 LT (= UTC + 8h) on 16 May.

5 Preliminary Results

5.1 Hydrographic Observations

5.1.1 CTD System, Oxygen Measurements and Calibration

(R. Czeschel[1], F. Duerkop[1], H. Großelindemann[1], C. McKellar[1], M. Müller[!], Q. Zhong[1])

[1] GEOMAR

5.1.1.1 CTD Rosette System

During SO305 BIOCAT-IIOE2 a total of 114 CTD-profiles and 2357 water samples were collected. The rosette system was installed in a Seabird Rosette System frame for 24 bottles. All casts were made with 22 bottles installed. Depth profiles up to a maximum pressure of 4482 dbar were performed. On average, the full water column was sampled at every third stations. Data acquisition was done using Seabird Seasave software version 7.26.7. Pre-processing was done with SBE Data Processing 7.26.7. Some of the Niskin bottles did not close reliably, therefore the corresponding hooks of the water carousel have been replaced and the water carousel has been cleaned. At CTD Station #3 the pump did not work due to a defect conductivity sensor. After we replaced the conductivity sensor the CTD system worked fine at first. During the upcast of CTD Station #19, the pump did not work reliably. After we replaced the connection cable between CTD and conductivity sensor the CTD system worked fine throughout the cruise. Additional to all regular sensors (P, T, S, O) a Chl-fluorescence and turbidity sensor FLNTU manufactured by Wetlabs, a CDOM, and a PAR sensor were attached to the frame of the CTD-rosette system. The cable connection between turbidity sensor and CTD had to be changed after CTD cast #37. Afterwards the turbidity sensor as and all other sensors provided high quality data throughout the cruise. At CTD cast #83 the protecting cap of the turbidity sensor was not removed resulting in unrealistic high data.

The exact configuration of the CTD system can be found in Table 5.1. Additionally, a high precision oxygen sensor (MicroTail), two self-recording LADCPs, a self-recording, self-powered UVP5 (see section 5.6), and a self-recording nutrient sensor (OPUS #71F9) were attached to the water sampler. The spectrometer measure in situ the absorption of UV light by seawater. From comparison with the absorption of clear water and water with a known concentration of nitrate, the nitrate concentration in the seawater sample can be derived. A processing toolbox for OPUS spectrometers had been developed at GEOMAR. The NO_x (NO_2^- + NO_3^-) concentrations resulting from the processing still require a calibration comparable to that of the CTD's conductivity and oxygen sensors.

Processed preliminary CTD data, 5-dbar binned, was sent in near real time to the Coriolis Data Centre in Brest, France, (via email: codata@ifremer.fr) for integration in the databases to be used for operational oceanography applications and the WMO supported GTS/TESAC system.

Table 5.1 Summary of CTD system SBE #9 configuration and during SO305.

	CTD system SBE#9
Pressure sensor	# 0410
T primary	# 5806
T secondary	# 5807
C primary #1	# 3300 (profile 1-3)
C primary #2	# 2512 (profile 4-114)
C secondary	# 4062
O_2 primary	SBE 43 # 0631
O_2 secondary	SBE 43 # 2600
PAR Sensor	# 70714
Altimeter	# 42299
Fluorometer/Turbidity sensor	FLNTURTD-2928
CDOM	FLCDRTD-2687

5.1.1.2 CTD Conductivity Calibration

Overall, 158 calibration points were obtained by sampling for salinity. Due to the change of the primary conductivity sensor after profile #3, only 154 calibration points were used for the calibration of the second primary conductivity sensor. Salinity samples were taken by the CTD watch in 'Flensburger' bottles, which have been proven to be ideal for storing salt samples. The measurements with one of GEOMAR's OPTIMARE Precision Salinometers (OPS) are described in section 5.1.2. A simple outlier removal method was applied that discarded the 33% samples with the largest deviations between CTD and bottle samples prior to calibration. The projection of data taken during the bottle stops of the upcast to the data from the downcast was done using the WOCE recommendations by searching within a 30-dbar pressure interval for similar potential temperatures. The conductivity calibration of the downcast data was performed using a 1st order linear fit with respect to temperature, pressure and conductivity (Table 5.2). The calibration results in a salinity RMS-misfit for the downcast of order 0.002145 psu for the second primary and 0.00211 psu for the secondary sensor. The up-cast calibration surpasses these values with a RMS-misfit of 0.001969 psu for the primary and 0.002082 psu for the secondary sensor.

Table 5.2 End of cruise salinity and pressure summary of downcast calibration information for the two CTD systems used during SO305.

	CTD system SBE 911	CTD system SBE 911
Sensor pair	Cond. Primary #2512	Cond. Secondary #4062
RMS misfit after calibration - salinity	0.0021447	0.0020858
Polynomial coefficients - conductivity	Offset: 0.046616 P1: 9.027e-07 T1: 0.0016065 C1: -0.016658	Offset: 0.020858 P1: 3.4209e-07 T1: 0.00067976 C1: -0.0073755

5.1.1.3 Oxygen Calibration

The CTD oxygen downcast for CTD systems is calibrated by using the best 66% of the joint data pairs between downcast CTD sensor value and Winkler-titrated oxygen. For the calibration a correction polynomial depending on pressure, temperature, oxygen and the product of pressure and oxygen was fitted (Table 5.3). A total of 295 oxygen samples were taken. In the end, 196 different oxygen data points were used, which resulted in an RMS-misfit for the downcast of 0.8024 µmol kg^{-1} for the primary SBE43 and 0.781234 µmol kg^{-1} for the secondary SBE43.

Table 5.3 End of cruise downcast oxygen summary of calibration information for the CTD system used during SO305.

	Oxygen Sensor #631	Oxygen Sensor #2600
Sensor pair	primary	secondary
RMS misfit after calibration - oxygen	0.8024	0.78123
Polynomial coefficients - oxygen	Offset: 3.88 P1: -0.00037329 T1: -0.10493 O1: -0.078256 P*O: 1.2599e-5	Offset: 3.3656 P1: -0.00053824 T1: -0.072756 O1: -0.08279 P*O: 1.1036e-5

5.1.2 Conductivity Measurements

(H. Großelindemann[1], C. McKellar[1])

[1] GEOMAR

In order to calibrate the conductivity sensors of the CTD system, the conductivity of 158 water samples was measured using the GEOMAR OPTIMARE Precision Salinometer (OPS) SN 020. Prior to measuring the conductivity with the OPS, the bottle samples have to be degassed to remove gas micro-bubbles as the OPS is sensitive to gas bubbles in probes. Salinity samples were taken with ‘Flensburger' bottles from the CTD. Once a box of bottles was full, the bottles were taken into a warm water pool of about 40°C for an hour. Then the bottles were shortly opened to degas. Afterwards the sample bottles were brought to the salinity lab where their conductivity could be measured after 24 hours of cooling down to the lab temperature. The measurement procedure always started by rinsing with old substandard seawater and a test measurement, in order to figure out whether the measurements were stable. This was then followed by the actual standardization with the IAPSO Standard Seawater and a new substandard measurement. Afterwards the measurements of the samples were started. After every tenth sample bottle another substandard was measured. This was done to test whether the instrument is drifting. Mostly the substandard measurements yielded reasonable results. The ending of a measurement series was again followed by another substandard and finalized by re-measuring the remaining Standard Seawater from the standardization in the beginning, which was expected to be slightly higher (0.001-0.002) than the original standard measurement.

In addition to the salinity samples from the CTD, 44 samples from the thermosalinograph (TSG, see section 5.1.3) were also measured. These were used for the calibration of the TSG. Furthermore, a couple of samples were measured for other groups (GoFlo and sediment traps), because they needed precise salinity values for their own investigations.

5.1.3 Thermosalinograph

(H. Goßelindemann[1], C. McKellar[1])

[1] GEOMAR

Underway measurements of sea surface temperature (SST) and sea surface salinity (SSS) were continuously done by the ship's dual thermosalinograph. One inlet is located at the portside (TSG1) while the other thermosalinograph's inlet is at the starboard side (TSG2). The parallel system worked well throughout SO305. Due to the switch off of scientific measurements in the EEZ of Sri Lanka and before entering the EEZ of India for the transit to Singapore there are no measurements for these areas either. A total of 44 salinity samples were taken during the cruise and measured during the transit with the GEOMAR OPTIMARE Precision Salinometer (OPS) SN 020 for calibration.

5.1.4 Underway CTD (uCTD)

(R. Czeschel[1], F. Duerkop[1], H. Großelindemann[1], C. McKellar[1], M. Müller[1], Q. Zhong[1])

[1] GEOMAR

The Underway CTD (uCTD) of Oceanscience was used for underway profiling of upper ocean temperature, salinity, and pressure. The system consisted of a Sea-Bird CTD instrument with embedded data acquisition. The sensor is contained within a streamlined pressure case with an integrated line spool. The winch holds 1400 m of Spectra line for profiles to over 400 m depth. The tail rewinder loads the tail spool with the Spectra line. The uCTD was installed on the back of the working deck. The nominal operating depth of the uCTD depends on the vessel speed. We used the uCTD while steaming with ~8kn. The profile depth was up to 250 m depth. We used the uCTD to measure between our CTD stations between 5°N and 7°N while we were crossing an eddy. In total, 15 profiles were recorded with the uCTD (see Table 11.1 in the Appendix). After two profiles the laser of the Rewinder displayed an error. After cleaning the light barrier, the uCTD worked again. After another profile, a pin which was used to lock the tail in the rewinder when winding up the Spectra line on the tail got stuck. The pin was then replaced by a screw. From then on, the uCTD worked well without any problems and another 12 profiles were recorded. We stopped recording after we had crossed the eddy.

5.2 Current Observations

5.2.1 Vessel-Mounted ADCP

(R. Czeschel[1])

[1] GEOMAR

Underway-current measurements of the upper ocean were performed continuously throughout the entire cruise (except in the territorial waters of Sri Lanka, India, Myanmar and Singapore) using two vessel-mounted Acoustic Doppler Current Profilers (vmADCP): a 75kHz RDI Ocean

Surveyor (OS75) and a 38kHz RDI Ocean Surveyor (OS38) both mounted in the ship's hull. Measurements started at 2.9°N, 83.11°E on 15 April 2024, 02:38 UTC. We stopped the record of both vmADCP at the EEZ of India at 15.17°N, 89.63°E on 11 May 2024, 08:00 UTC. Due to the test of the hydrophone for the mooring deployment we stopped recording of vmADCP data on 17 April from 07:49 to 08:59 UTC. The 75 kHz ADCP broke down twice after stop/start recording. Therefore, the following files are corrupt:

1) so305os75004_000000.ENX, *ENR, *LOG, *N2R, *N3R, *NMS, *VMO so305os75005_000000. ENX, *ENR, *LOG, *N2R, *N3R, *NMS, *VMO
2) so305os75013_000000.ENX, *ENR, *LOG, *N2R, *N3R, *NMS, *VMO

After the vmADCP was restarted, the data was accidently saved under the file name of the previous cruise. Therefore, following files should be renamed:

1) so304_os75_304_00000* -> so305os75005_00000*
2) so304_os75_305_00000* -> so305os75006_00000*

The OS75 and the OS38 are aligned to zero degrees (relative to the ship's center line). Both instruments ran in narrowband mode. The OS75 instrument was configured with 100 bins of 8 m and a blanking distance of 4 m, pinging 24 times per minute and reaching a range of 600 m to 700 m. The OS38 used 55 bins of 32 m and a blanking distance of 16 m, pinging 19 times per minute and reaching a range between 1200 m and 1500 m. During the entire cruise, the SEAPATH navigation data was of high quality. No interference with the 12kHz echosounder EM122 that delivered high quality bathymetry data was detected. Post processing of the data was carried out separately for each instrument. The applied mean misalignment angles and amplitude factors with the associated standard deviation are summarized in Table 5.4.

Table 5.4 Vessel-mounted ADCP calibration.

OS	Mode	Misalignment angle ± std	Amplitude factor ± std
75	NB	-0.1181° ± 0.5368°	1.0007 ± 0.0094
38	NB	-0.2790° ± 0.6262°	1.0049 ± 0.0136

5.2.2 Lowered ADCP

(R. Czeschel[1], F. Duerkop[1], H. Großelindemann[1], C. McKellar[1], M. Müller[1], Q. Zhong[1])

[1] GEOMAR

During the whole cruise the CTD/Rosette system was equipped with a lowered ADCP setup based on two Teledyne RDI ADCPs. The setup consisted of an upward looking and a downward looking 300-kHz instrument. These two instruments were mounted inside the CTD rosette with specially manufactured frames protecting the instruments and allowing zero obstruction of the acoustic beams. The LADCP system worked without trouble with SN #11461 as downward-looking master instrument and #11436 as upward-looking slave during the whole cruise. During the cruise we used a software, which controlled the start, stop, download, and erase of the cycles of the two LADCP systems (ladcp_tool_1.9.3 developed at GEOMAR). An energy supply system that draws energy for the ADCPs from the CTD system using rechargeable capacitor (10.000uF / 100V)

worked well throughout the cruise. The start as well as the download signal for the LADCP system was conducted via Bluetooth. The distance between the LADCP instruments and the Bluetooth transmitter was reduced by installing the transmitter at a tension belt that was stretched in the hangar next to the CTD to minimize communication problems. Therefore, the communication with the LADCPs via Bluetooth worked well throughout the cruise. Data processing took place during the cruise using the GEOMAR LADCP processing software V10.22, which includes both shear and inversion methods to derive an absolute velocity profile. As additional data are necessary for the processing, the corresponding pre-processed CTD files were used containing pressure, temperature and salinity profiles as well as time and navigation data. The instruments of Teledyne RDI instruments delivered very good deep-ocean velocity profiles when processed in conjunction with the observations of the vmADCP and when coming close enough to the seafloor to obtain TRDI bottom track data.

5.3 Floats

(M. Müller[1], R. Czeschel[1])

[1] GEOMAR

During SO305, two NKE floats (= Argo floats) were deployed (Table 5.5). These profiling floats are measuring temperature, salinity, oxygen and pressure of the upper 2000 m of the ocean. The Argo floats were tested, activated and then deployed by hand.

Table 5.5 Float deployments during SO305.

Float serial number	WMO	Latitude	Longitude	Deployment Date (UTC)
AI2600-22DE009	6904212	11˚20.222’S	012˚14.944’E	26-Apr-2022 01:26
AI2600-22DE008	6904213	11˚10.467’S	011° 13.183’E	26-Apr-2022 14:41

5.4 Mooring

5.4.1 Mooring Operations

(M. Müller[1], R. Czeschel[1], F. Duerkop[1])

[1] GEOMAR

Mooring work during SO305 BIOCAT-IIOE2 consisted of the deployment of a long-term mooring at the equator at 89°E (Table 5.6). This mooring consists of a WH-ADCP (up-looking) and a Signature-ADCP (down-looking) measuring the strength of the upper currents as well as oxygen (Optodes), temperature and salinity (MicroCats), McLane moored profiler (849 – 3324m) and single point current meters (Aquadops) just below the ADCP to analyse water mass variability.

Table 5.6 Mooring operations during SO305.

Mooring Deployment					**Notes:**	**KPO_1234**
Vessel:	Sonne	SO305				
Deployed:	18-April	2024	12:46 UTC			
Vessel:						
Recovered:						
Latitude:		00°	01.461’	S		
Longitude:		88°	40.076’	E		
Water depth:		4513	Mag Var:	2.2		
ID	**Designed Depth**	**Instr. Type**	**s/n**	**Start-up**	**Remarks**	
KPO_1234_01	100	XEOS-XMA Argos	214435	**ready**		
KPO_1234_02	100	Float	Ani 4			
KPO_1234_03	100	WH ADCP 300kHz	2379	**x**		
KPO_1234_04	100	Signature ADCP	200065	**x**		
KPO_1234_05	199	Microcat	3196	**x**		
KPO_1234_06	199	O2 Logger (ind. Opt.)	054	**x**		
KPO_1234_07	303	Microcat	8947	**x**		
KPO_1234_08	303	O2 Logger (ind. Opt.)	101	**x**		
KPO_1234_09	503	Microcat /p	6855	**x**		
KPO_1234_10	503	O2 Logger (ind. Opt.)	078	**x**		
KPO_1234_11	849					
	3324	MMP	14754	**x**		
KPO_1234_13	3631	Aquadopp down /p	16454	**x**		
KPO_1234_14	3942	Aquadopp down /p	16453	**x**		
KPO_1234_15	4252	Aquadopp down /p	16456	**x**		
KPO_1234_16	4368	Microcat /p	6859	**x**		
KPO_1234_17	4504	Release AR661	642	Mode: A	Enable: 4A83 / Release: 4A84	
KPO_1234_18	4504	Release AR861	1645	Mode: B	Enable: 0A8A / Release: 0A55	

5.4.2 Calibration of Moored Instruments

(M. Müller[1], F. Duerkop[1], R. Czeschel[1])

[1] GEOMAR

CTD/O_2 cast calibrations were performed for all MicroCATs, Optode loggers and Aquadops as pre-deployment calibration (CTD casts 2 and 4) by attaching the instruments to the CTD frame. During the upcast, 5 and 3 calibration stops were done over the whole profile range (depths chosen at low gradient-regimes for the respective parameters). Each stop had a duration of at least 6 min in order to ensure fully adjusted measurements at the calibration points. Additionally, releaser tests were performed at CTD cast 2. Lab calibrations at GEOMAR were conducted for all O_2 loggers in water-filled beakers of 0% and 100% O_2-saturated water at two different temperatures (~6°C and ~21°C) following the Aanderaa Optode manual.

5.5 Shipboard Microstructure Measurements

(R. Czeschel[1], F. Duerkop[1], H. Großelindemann[1], C. McKellar[1], M. Müller[1], Q. Zhong[1])

[1] GEOMAR

A microstructure (MSS90) profiler (#028) of Sea and Sun Technology was used to infer turbulent dissipation rate and diapycnal diffusivity, aimed at calculating turbulent fluxes of oxygen, heat, momentum, nutrients, and nitrous oxide (N_2O). The loosely tethered profilers are equipped with 2 airfoil shear sensors (#121, #122) and a fast thermistor, as well as some common CTD sensors: pressure, conductivity, temperature and turbidity sensor. In total, 120 profiles were recorded on 42 MSS stations to a maximum depth of 320 m. Most stations consisted of 3 microstructure profiles between 2 CTD casts. A list of all MSS profiles is given in Table 11.2 in the Appendix.

The MSS worked fine in the beginning of the cruise. However, at profile #55 the MSS started to have some data dropouts. In the following stations the dropouts got more. The analyse with the time domain reflectometer (TDR) didn't show any clear hints of a problem with the underwater cable. Since the most likely problem should have been in the first few meters of the cable, the cable was shortened about 10 m before profile #81. The following profiles still had some severe data dropouts that's why the whole underwater cable was exchanged before profile #85. Again, there was not much improvement in the following profiles. Before profile #101 the MSS itself was opened to look for any water within the device. No signs of water were found but two dry bags were added to prevent condensation water. The IC of the RS485 interface was exchanged. Also, all connectors have been thoroughly cleaned and visually checked. An insulation measurement of the cable didn't show any problems. In the following profiles the data dropouts were less, but still not completely gone. Often the first profile had the most dropouts and the data dropouts of the following profiles decreased for some reason. The dropouts appeared to come up randomly, sometimes on the up- and sometimes on the down cast. They also came up at different depth. The brushes of the slip rings might be worn out, but that couldn't be verified on board due to the high risk of losing some parts while doing that.

The fall rate of the profilers was 0.55 m/s in the beginning. Before profile #101 additional weight (2 thin rings) was added in the hope to bring the high noise level (~1 10^{-8} m^2/s^3) down. That increased the fall rate to about 0.85 m/s. As the noise level was still high, but now the fall rate too high the weight was reduced by each one 1 thin ring before profile #104 (#112, #118) leading to a fall rate of 0.8 m/s (0.7 m/s, 0.55 m/s).

5.6 Underwater Vision Profiler

(M. Müller[1], R. Kiko[1])

[1] GEOMAR

During all regular CTD casts, an Underwater Vision Profiler 5 HD (UVP5 HD; serial number 28) was operated on the CTD rosette. The instrument consists of one down-facing HD camera in a 6000 dbar pressure-proof case and two red LED lights which illuminate a 1.24 L water volume. During the downcast, the UVP5 takes 20 pictures of the illuminated field per second. For each picture, the number and size of particles are counted and stored for later data analysis. Furthermore,

images of particles with a size > 500 µm are saved as a separate “Vignettes” - small cut-outs of the original picture – which allow for later, computer-assisted identification of these particles and their grouping into different particle, phyto- and zooplankton classes. Since the UVP5 was integrated in the CTD rosette and interfaced with the CTD sensors, fine-scale vertical distribution of particles and major planktonic groups can be related to environmental data. In total 90 UVP5 profiles could be obtained. At each station with a water depth < 6000 m a full-depth profile was obtained. Further, computer-assisted analysis of the approximately 700,000 images taken with the UVP5 will be done in the home laboratory in order to reveal fine-scale distribution patterns of particles and zooplankton.

5.7 Dissolved Nutrients and Dissolved Oxygen

(L. Schmidt[1], J. Usinger[2], K. Lange[2], H. Bange[2])

[1] Hereon, [2] GEOMAR

5.7.1 Methods

Dissolved inorganic nutrients (nitrate, nitrite, silicate and phosphate) were measured with a continuous flow analyser (CFA) according to the photometric methods described in Grasshoff et al. (1999): The right amount of reagent is added to the sample and mixed to form a colour complex. Its concentration is quantified by the build-in photometer. In contrast to the other nutrients, nitrate is determined by reducing the nitrate to nitrite with cadmium. The nitrate concentration is calculated by subtracting the nitrate-derived nitrite concentration from the total concentrations of nitrite. The CFA works automatically and needs less than 2 mL of sample for the determination of all four nutrients. Approximately 50 samples per hour can be measured.

Dissolved ammonium was analysed with the ortho-phthalaldehyde (OPA) fluorometric method following Holmes et al. (1999). The working reagent containing OPA is forming a fluorescent complex with ammonium. It can be measured within 12 to 24 hours. The efficiency of the OPA is dependent of the matrix of the sample. Therefore, low nutrient sea water from a recent station is used for the calibration using the method of standard addition.

The Winkler method was used to determine dissolved oxygen. The sample was taken air free for all stations. Then manganese chloride and alkaline sodium iodide were simultaneously added to the sample. Manganese is oxidized by the dissolved oxygen and forms a precipitate. By adding sulfuric acid, the oxidized manganese dissolved and converted iodide to iodine which resulted in a yellow colour. Then, iodine was titrated with sodium thiosulfate until the solution almost lost its colour. Zinc iodide starch solution was added and coloured the solution in purple. The titration continued until the solution reached transparency. The titrated volume was used to calculate the oxygen concentration via: O_2 (µmol/L) = a * f * 5000 / (b-2), with a representing the titrated volume (in mL), b the volume of the sampling flask and f the factor of the sodium thiosulfate solution.

Reusing the lids of the sampling vials would result in too high nitrate concentrations if they were not rinsed properly while sampling. As the ammonium concentrations were very low, avoiding contamination and achieving good replicates was difficult.

Bubbles were only present in oxygen samples in near-surface waters. Near-surface waters are more than 10 °C warmer than the room temperature. While cooling down, the shrinking volume might have caused the bottle to suck in air from outside. These bubbles might have influenced the measurements. The lids of the glass bottles are prone to slipping out easily, so it is advised to use clippers to prevent accidentally opening the bottle.

All measurements and quality control were finished during the cruise. No samples will be transported to GEOMAR, and all data is already processed.

5.7.2 Sampling

All dissolved nutrients and dissolved oxygen were sampled from every CTD station. Furthermore, the CFA measured nutrients were sampled and measured for the underway system, the GoFlo bottle sampling, and the Towed-fish. Besides samples of the two on-board running incubations were taken and nutrients were analysed. Sampling from the underway system was organized by Dennis Booge, GEOMAR. Nutrient triplicates were taken every three hours. The underway system is sampling surface water from 5 m water depth. The GoFlo and towed-fish sampling was under the responsibility of Martha Gledhill, GEOMAR. Dennis Booge and the participants from the SDU were running and sampling their incubations.

At the first CTD station, the nutrients were sampled as triplicates to check the standard deviation and necessity of taking triplicates. The following CTD casts were sampled as single sample. Ammonium was always sampled separately as triplicates. At the first stations, one replicate was taken for every depth. After further evaluation, triplicates were taken at two specific depths to determine the accuracy of the measurement. The chosen depths were at the oxygen minimum and maximum. From station 5 onwards, the sampling procedure was changed to sampling triplicates at previously specified depths including bottom, oxygen maximum, oxygen minimum, chlorophyll maximum, and salinity minimum. This reduced the number of samples which needed to be measured and increased the accuracy of the calibration for the O_2 sensor of the CTD. It was avoided to sample too close to the surface. As the oxygen concentration strongly changes close to the chlorophyll maximum and, thus, provides unreliable data for calibrating the O_2 sensor of the CTD, sampling this depth was discarded later on.

5.7.3 Preliminary Results

At 0°59.969’ S and 88°40.209’E (Station 2), the oxygen minimum zone was not yet reached. Below the fully oxygenated surface, the oxygen concentrations declined to approximately 50 µmol/L in the depth range below the euphotic zone till 1000 m including a secondary oxygen maximum in 430 m with 78.44 µmol/L. Below 1000 m, oxygen concentrations were increasing with depth. Nitrite was only present between 50 and 100 m with concentrations lower than 0.96 µmol/L. Ammonium concentrations fluctuated between 0.04 and 0.20 µmol/L. All other nutrients were depleted in the surface and increased with depth. At depth, the nutrients showed maximal concentrations of approximately, 36.83 µmol/L for nitrate, 2.43 µmol/L for phosphate and 134.36 µmol/L for silicate (Figure 5.1).

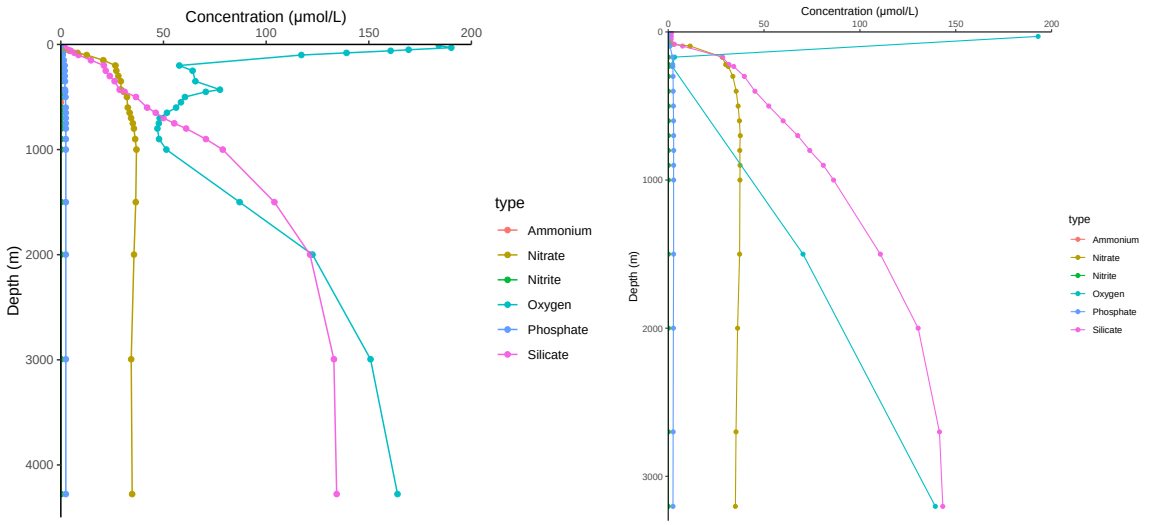

Fig 5.1 Depth profiles of ammonium, nitrate, nitrite, oxygen, phosphate, and silicate concentrations (in µmol/L) outside the oxygen minimum zone (figure left: station 2) and in the oxygen minimum zone (figure, right: station 24)

At 13°00.097’ N and 85°00.062’E (station 24), low oxygen concentrations were found. The surface was fully oxygenated. Minimal oxygen concentrations of 2.08 µmol/L were reached at 233 m depth. Below the oxygen minimum zone, oxygen concentrations were increasing with depth. Nitrite was only present between 50 and 100 m and at maximum depth with a maximum concentration of 0.41 µmol/L in 83 m. Ammonium concentrations fluctuated between 0.03 and 0.05 µmol/L. All other nutrients were depleted in the surface and increased with depth. At depth, the nutrients showed maximal concentrations of approximately, 37.59 µmol/L for nitrate, 2.86 µmol/L for phosphate and 143.23 µmol/L for silicate (Figure 5.1).

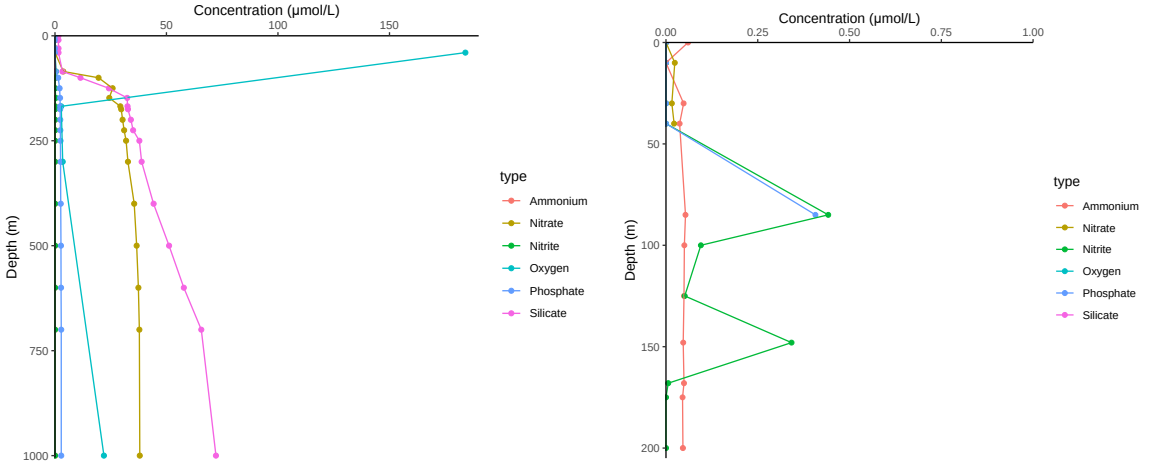

Fig 5.2 Depth profiles of ammonium, nitrate, nitrite, oxygen, phosphate, and silicate concentrations (µmol/L) in the oxygen minimum zone at Station 32 showing a secondary nitrite peak (figure right).

At 14°58.149’ N and 85°43.914’E (station 32, cast 88 and 91), the lowest oxygen concentration was 2.80 µmol/L in 168 m. Again, the surface was fully oxygenated, and oxygen concentrations were increasing with depth below the oxygen minimum zone. Nitrite showed a regular maximum at 85 m with 0.44 µmol/L and a secondary nitrite peak at 148 m with 0.34 µmol/L. Ammonium concentrations fluctuated between 0.04 and 0.06 µmol/L. All other nutrients were depleted in the

surface and increased with depth. At depth, the nutrients showed maximal concentrations of approximately, 38.04 µmol/L for nitrate, 2.82 µmol/L for phosphate and 72.19 µmol/L for silicate within the first 1000 m (Figure 5.2, data referring to station 32, cast 91).

5.8 Nitrous oxide and Methane

(I. Hentschel[1], L. van Bonn[1], I. Stoltenberg[1], H. Bange[1])

[1] GEOMAR

5.8.1 Introduction

The major goal of the working group nitrous oxide and methane during the SO305 BIOCAT-IIOE2 cruise was the determination of dissolved nitrous oxide (N_2O) and methane (CH_4) throughout the water column in the Bay of Bengal. Both gases are microbially produced in the water column and represent the second and first most important greenhouse gases, respectively. The global warming potential (GWP100) of methane equals 27.9. Thus, one methane molecule has the same radiation force as 28 molecules of CO_2 (Pachauri et al., 2014). The GWP100 for nitrous oxide is about 298. Most of the atmospheric methane is formed via biological production called methanogenesis. It is typically believed that the major formation of methane is performed under strictly anoxic conditions, however, several processes have been suggested to produce CH_4 under oxic conditions as well (Bange et al., 2024). Nitrous oxide is formed dominantly as a byproduct via nitrification under oxic/suboxic conditions in the water column. Its formation increases under suboxic/anoxic conditions as an intermediate product of denitrification. Under anoxic conditions N_2O is consumed via denitrification. Therefore, the enrichment of nitrous oxide in the water column depends on the oxygen concentration (Bakker et al., 2014). In view of the ongoing climate change, it is essential to understand the global natural and anthropogenic pathways of the two greenhouse gases.

5.8.2 Methods

Samples for methane and nitrous oxide were collected with special focus on the oxygen minimum zone and the surface water. Nitrous oxide samples were measured on board using static headspace analysis. For this, brown 20 mL vials were filled air bubble-free directly from the Niskin bottles at the CTD/RO and sealed with rubber stoppers (Butylgummihohlstopfen, Chromatographiehandel Müller, Fridolfing, Germany) and aluminium caps (Bördelkappe R20-oA, Chromatographiehandel Müller, Fridolfing, Germany). All the samples were immediately poisoned with 50 µL of saturated aqueous mercury chloride ($HgCl_2$) solution. Afterwards, a headspace of 10 mL Helium (He 5.0, Air Liquide GmbH, Düsseldorf) was injected into the sample vial with a gas-tight syringe (Series A-2 Syringe 10 mL, VICI Precision Sampling, Baton Rouge, LA, USA). An empty 20 mL syringe (20mL BD PlastikpakTM, BD Heidelberg, Germany) was injected through the rubber stopper of the sample vial beforehand for pressure compensation. This method was applied to every sample taken. The samples were vortexed for 30 seconds using a vortex shaker (Vortex Genie 2, Scientific Industries Inc., New York, USA) and then stored for at least two hours. A solubility equilibrium develops between the liquid phase and the gas phase (= headspace), as the dissolved gas from the sample diffuses into the overlying gas phase. After two

hours the equilibrium state is reached, and the samples can be measured. For this, 9 mL of the headspace was transferred to a 10 mL gas-tight syringe. Any anomalies that may have occurred up to this point, such as inconsistencies in the amount of compensation fluid or residual liquid when extracting the headspace, were recorded in the measurement protocol. The sample was injected into the gas chromatograph (Hewlett Packard HP 5890 Series II, Agilent Technologies, Santa Clara, California, USA) via a two-position valve (Valco Valve, VICI International, Schenkon, Switzerland). It passes through a dry trap filled with phosphorus pentoxide (P_2O_5, Sicapent®, Merck, Darmstadt, Germany) before entering the sample loop. By switching the valve, 2 mL aliquot were injected onto the column together with the carrier gas (argon/methane gas mixture 95/5, AirLiquide GmbH, Düsseldorf, Germany). The column used is a 6' 1/8" stainless steel column packed with a 5 Å molecular sieve (Grace GmbH & Co. KG, Worms, Germany), which effectively separates nitrous oxide. The GC is equipped with an electron capture detector (ECD) which was operated at 350°C. The GC temperature was set to 190°C. The argon/methane was set to a flow rate of 30 mL min^{-1}. Samples were run every 2.40 minutes and every 9.40 minutes. Before sampling, the GC was calibrated daily. Therefore, two standard gas mixtures with different dilutions were injected in triplicates and a calibration curve with a quadratic fit was applied. A correlation coefficient of R^2>0.95 had to be met. The two standard gases had calibrated concentrations of 330 ppb to 990 ppb of N_2O (Deuste Steiniger GmbH, Mülheim, Germany). By diluting the standard with Helium at atmospheric pressure, a 66% dilution of the 990 ppb standard gas and a 44% dilution of the 330 ppb standard gas mixture was used. In some cases, the sample concentrations exceeded the range of the calibration, then the linear fit was applied. The signals measured at the ECD were further processed with the ChromStar software (ChromStar Version 6.3, Software für Chromatographie und Prozessanalytik GmbH, Wehye-Leeste, Germany). N_2O peaks were integrated manually and transferred to a Microsoft Excel spreadsheet, calculating the final concentrations and standard deviation. During the measurements two dry traps broke due to mechanical pressure, which was then prevented by adjusting the setup at the GC and an additional dry trap was lost due to an excess amount of sample water that had entered the syringe. The calibrations of specific stations vary from the remaining calibrations due to presumably leaking septa at the helium outlet and GC injection port. Upon identifying the source of the error, these were replaced and thereafter renewed every other day.

The methane samples were only poisoned and then stored for measurement in the lab. This will be done by using a purge and trap unit. The purge and trap method relies on continuously passing a carrier gas through the sample, causing the volatile gases in the sample to be released with the carrier gas and collected in a trap stored in liquid nitrogen.

Since the measurement of nitrous oxide data was already completed during the cruise and the data could be collected, the evaluation of these will likely take place a few months after the cruise ends. Predicting the evaluation of methane is difficult, as ongoing issues with the purge and trap unit can lead to time delays, and the method is generally time-consuming. Results can be expected at the earliest during the next year.

5.8.3 Overview Sampling and Measurements

During the SO305 BIOCAT-IIOE2 cruise, we took water samples for methane and nitrous gas from every second station except stations 37 and 38, where we sampled both due to the premature

termination of the cruise. At the 24h-stations, only one depth profile was sampled (stations 10, 18, 30, 32, 37). Additionally, a gradient pump system was applied during sampling from the Zodiac to achieve high-resolution measurements in 0.25 m steps from the sea surface down to a water depth of 2 m. We collected data from the Zodiac for all 24h-stations except station 32 due to bad weather conditions. From regular CTD/Ro profiles, we collected trace gas water samples from the ocean bottom to 1000 m in 1000 m steps. At water depth <1000m, the sampling was continued in 100 m steps for nitrous oxide and 200 m steps for methane. An extra set of samples (triplicates) for both gases was taken if there was a chlorophyll maximum (or two), and oxygen minimum or maximum. Thus, at water depths <100 m we usually had up to 4 samples (e.g. 60 m, 30 m, 10 m, and surface) depending on the CTD profile. All nitrous oxide water samples were measured on board (around 1000 samples). Methane samples will be measured at the GEOMAR in Kiel after the cruise.

5.8.4 Preliminary results

The primary results of the measurement show a correlation between oxygen concentrations in the water column and nitrous oxide concentrations. As we descended deeper into the oxygen minimum zone, and oxygen levels more and more decreased, the N_2O concentrations simultaneously increased. They reached their maximum at station 30 with 133.2 µmol/L. Particularly notable was the observation of the decline in N_2O levels at the depth of the oxygen minimum at station 32, which may be attributable to denitrification processes.

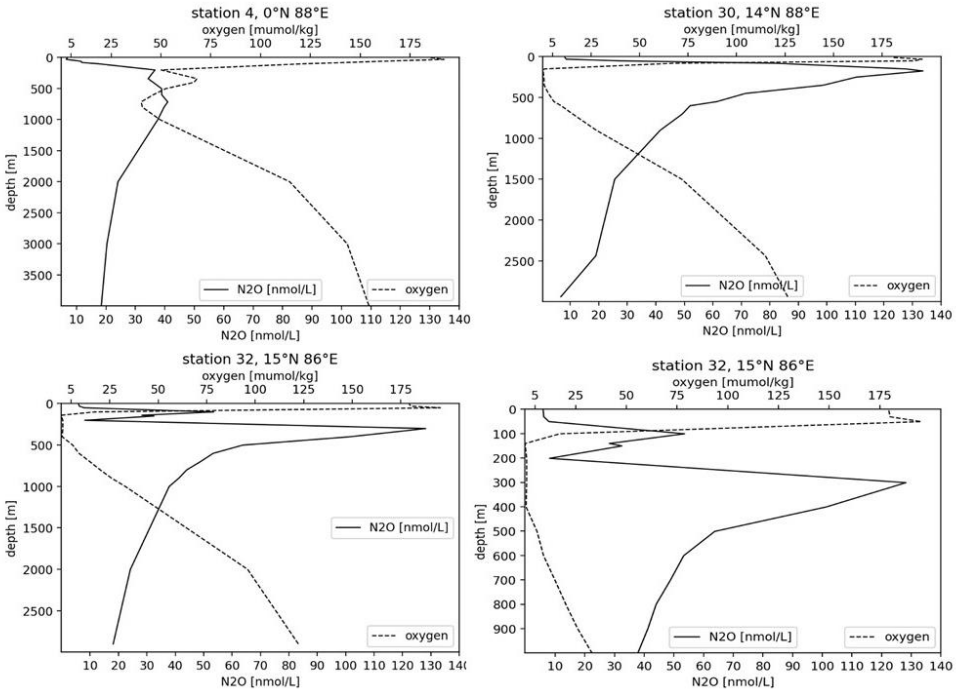

Fig 5.3 Depth profiles of N_2O (in nmol/L and oxygen (in µmol/L) concentrations on the equator (upper left) and at 14°N (upper right) on the 88°E transect and a possible denitrification peak at 15°N 86°E on a full depth profile (lower left) and for the first 1000 m (lower right).

5.9 Underway Trace Gas Measurements

(P. Eisnecker[1], M. Sommer[1], D. Arévalo-Martínez[1,2], H. Bange[1])

[1] GEOMAR, [2] Radboud Univ., Nijmegen, NL

Continuous measurements of dissolved N_2O, CO_2, CO, and CH_4 in seawater were carried out during SO305 BIOCAT-IIOE2 by means of an autonomous equilibrator headspace setup coupled to an off-axis integrated cavity output spectroscopy analyser (LGR; N_2O and CO) and a cavity ringdown spectroscopy analyser (PICARRO; CO_2 and CH_4) (Arévalo-Martínez et al., 2013). Water was drawn into the system at ~ 6 L min^{-1} by a LOWARA submersible pump installed in the ship's moonpool (~ 6 m depth). Ambient air measurements were carried out every six hours by drawing air into the system from an air inlet located at deck 10 about 32 m above sea level. Control measurements were performed every 6 hours by means of three standard gas mixtures (DEUSTE STEININGER GmbH) bracketing the expected concentrations in this area. These gas mixtures were calibrated against primary NOAA standards at the Chemical Oceanography Department of GEOMAR Helmholtz Centre for Ocean Research, Kiel.

5.10 Carbon Monoxide

(P. Eisnecker[1], M. Sommer[1], H. Bange[1])

[1] GEOMAR

The air-sea exchange and oceanic cycling of climate forcers (or greenhouse gases, GHG), including the indirect GHG carbon monoxide (CO) are fundamental in controlling the evolution of the Earth's atmospheric chemistry and climate. Hence, the investigation of their distribution and sea-air fluxes is pivotal for better understanding potential responses of the ocean and the overlying atmosphere to environmental changes such as warming and deoxygenation. It is well-established now that the ocean under the current conditions is a minor source for CO. However, oceanic emission estimates are still associated with a high degree of uncertainty and there are still large knowledge gaps in the processes controlling the production, distribution, and reduction of CO in the ocean (Bange et al., 2024).

Water samples from CTD/Ro stations have partly been taken from different CTD casts, with the primary cast taking deep water samples and the following cast taking mid-depth and shallow water samples. Aimed sampling depths are 100 m, 70 m, 50 m, 30 m, 10 m, surface. Focus depths are adapted or added for peaks in oxygen concentration and the primary chlorophyll α maximum. Triplicates have been taken from each depth. CO concentrations in the samples have been measured immediately on board with a CO analyser (ta3000R SP, Gas Monitor CO in Headspace, AMETEK). Discrete CTD samples from selected CTD stations including the 24h-stations (marked with x) are listed in Table 5.7. Carbon monoxide samples from the surface gradient pump system were taken at 200 cm, 175 cm, 150 cm, 125 cm, 100 cm, 75 cm, 50 cm, and 25 cm water depth while sampling with the Zodiac.

Tab. 5.7 Station number and sampled depths for carbon monoxide measurements.

DShip Station ID	24h-Station	Sampled depths [m]
SO305_2_5	-	200, 100, 80, 60, 50, 30, 10
SO305_4_2	-	200, 150, 100, 80, 60, 50
SO305_4_3	-	30, 10
SO305_6_3	-	200, 170, 100, 70, 50, 30, 10
SO305_8_3	-	215, 100, 80, 55, 30, 5
SO305_10_5	x	90, 70, 43, 30, 10, 2
SO305_10_8	x	100, 70, 60, 50, 30, 10, 2
SO305_10_12	x	100, 85, 70, 50, 30, 10, 2
SO305_10_16	x	100, 85, 70, 55, 30, 2
SO305_13_4	-	150, 100, 75, 60, 50, 30, 10, 2
SO305_15_3	-	100, 80, 65, 50, 30, 10, 2
SO305_18_4	x	100, 80, 73, 50, 30, 10, 2
SO305_18_9	x	100, 80, 70, 50, 30, 10, 2
SO305_18_13	x	100, 80, 70, 50, 30, 10, 2
SO305_18_16	x	100, 80, 70, 50, 30, 10, 2
SO305_20_3	-	100, 80, 50, 30, 10, 2
SO305_23_3	-	90, 80, 55, 30, 10, 2
SO305_25_3	-	100, 80, 70, 50, 30, 10, 2
SO305_28_2	-	100, 80, 50, 30, 10, 2
SO305_30_3	x	100, 75, 50, 30, 10, 2
SO305_30_5	x	100, 75, 50, 30, 10, 2
SO305_30_8	x	100, 80, 50, 30, 10, 2
SO305_30_10	x	100, 75, 50, 30, 10, 2
SO305_32_5	x	100, 90, 50, 30, 10, 2
SO305_32_6	x	100, 85, 45, 30, 10, 2
SO305_32_14	x	100, 85, 40, 30, 10, 5
SO305_35_4	-	100, 85, 55, 30, 10, 5
SO305_37_3	x	100, 70, 40, 30, 10, 3
SO305_37_8	x	100, 60, 50, 30, 10, 2
SO305_37_12	x	100, 80, 50, 45, 10, 2

5.11 Nitric Oxide (NO) Measurements

(R. Ingeniero[1], H. Bange[1])

[1] GEOMAR

5.11.1 Introduction

Nitric oxide (NO) is a short-lived climate forcer that indirectly contributes to greenhouse gas effects by interacting with other compounds to form ozone, methane, and nitrate aerosols, leading to negative radiative forcing (IPCC, 2021). The determination of dissolved NO concentration is challenging because of its reactivity, which results in a very short lifetime in (sea)water, ranging from 3 to 100 s. Until now, little is known about the distribution as well as the production and consumption processes of NO in the marine environment. Despite these challenges, there has been a growing interest in dissolved NO measurements in different aquatic systems, including open seas, coastal waters, and rivers, over the past decade. Most of the studies have indicated that the marine environment is a source of atmospheric NO. NO is a short-lived intermediate in the

microbial nitrogen cycle (Kuypers et al., 2018), particularly in nitrification, denitrification, and anammox. To this end, this study has two main objectives:

1) To estimate the sources and sinks of NO in the ocean/atmosphere. To achieve this, we measured the NO concentration in the near-surface water along the cruise track. Furthermore, using the atmospheric NO concentration measured by the Leibniz Institute for Tropospheric Research (TROPOS), we will estimate the seawater-atmosphere flux densities.
2) To determine NO concentration/distribution along the water column in selected stations. Given that the Bay of Bengal is also known as an oceanic region with a pronounced minimum zone, we aim to understand how deoxygenation influences nitrogen cycling processes and, ultimately, how it could influence NO distribution.

5.11.2 Methods

5.11.2.1 Sampling and measurement of NO from the underway and submersible pump

Triplicate bubble-free water samples from approximately 6 m depth were collected from the vessel's underway pump every 6 hours along the cruise track. At the 24h-stations, a submersible sampling pump with a depth sensor was deployed up to approximately 140 meters depth to collect water samples. Approximately >300 samples were measured on board. To ensure that the water samples are taken at and representative of the desired sampling depth, sampling was done 10 minutes after reaching the determined depth. A portable NO calibration source (2BTech Model 714 NO_2/NO/O_3 Calibration Source™) was used to calibrate the NO detector (Birks et al., 2020). The resulting gas output from the calibrator covered the detection range of the NO detector from 0 to 1000 ppb NO. NO signal outputs by the NO detector were recorded using PuTTY 0.78, a free and open-source client application for Windows. To determine NO mole fractions, the Rieman integrals of the signal peaks were calculated using the MATLAB (2022b) trapezoidal numerical integration function trapz. Since stripping measurement time was logged manually, it will take some time to process and analyse all the data obtained from the SO305 cruise. This will be done back at GEOMAR and may take approximately 2 to 3 months.

5.11.2.2 Incubation Experiments

A conceptual experiment was conducted to investigate the influence of nitrite concentration on dissolved nitric oxide concentration in seawater. Surface seawater samples were collected using a CTD/Ro sampler and transferred into 50 mL glass vials under bubble-free conditions. The samples were divided into control and treatment groups, with the latter spiked with varying concentrations of nitrite. These samples were incubated under alternating light/dark cycles and complete darkness for 24 and 48 hours. Dissolved NO concentrations were subsequently measured, providing insights into the interaction between nitrite levels and NO production in marine environments.

5.11.3 Preliminary Results

Shown below are profiles of dissolved NO and oxygen concentrations (Fig. 5.4). The NO concentration seems to increase in the area with low oxygen concentration, probably due to microbial NO production from the denitrification process.

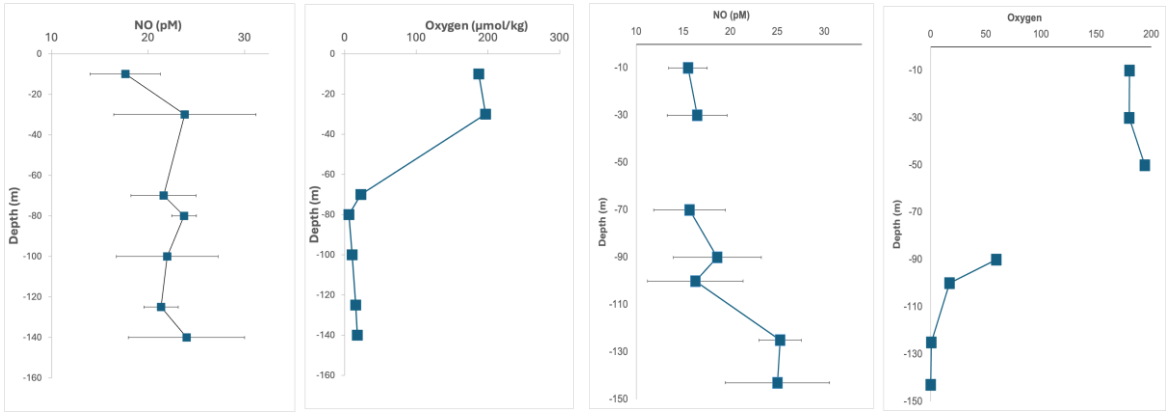

Fig 5.4 Depth profiles of NO (pM) and oxygen (µmol kg^{-1}) concentrations at the 24h-station on 27 April 2024 (figure left) and 6 May 2024 (figure right).

5.12 DMS, OCS, CS_2 and Isoprene

(D. Booge[1], H. Feil[1], C. Marandino[1], S. Rolfes[2], B. Engelen[2])

[1] GEOMAR, [2] Univ. Oldenburg

5.12.1 Introduction

The goal of our project was to understand the impact of anthropogenic inputs on microbial processes and the subsequent effects on the cycling of climate-active trace gases between the ocean and atmosphere. By investigating the aerosols on land and over the ocean (in cooperation with TROPOS), in conjunction with atmospheric trajectories, microbial mediated transformations (in cooperation with WG Engel), trace gas distributions in the ocean and in the atmosphere (in cooperation with WG Quack), we cover the full feedback cycle. The analysis of microbial communities in natural Bay of Bengal water will help to understand the influence of the anthropogenic inputs on the sulphur cycle, specifically the production of the climate-active gas DMS, as well as other biogenically produced and consumed volatile gases such as isoprene, OCS and CS_2, which are measured in the surface ocean (underway) but also in different waters depth during stations (CTD/rosette). Comparing microbial communities from areas with high anthropogenic inputs (northern area of the cruise track) with areas of low inputs (southern area of the cruise track) will give information about the influence of these factors on key organisms involved in the production and degradation of the volatiles. Further, identification of key genes within respective metagenomes will allow us to follow metabolic pathways for the conversion of e.g. organic sulphur compounds. Additionally, we perform incubation experiments on board SO305, in which natural water samples will be spiked with collected atmospheric aerosols from filters or scrubber water from ships. These experiments will allow us to specifically target

processes and microorganisms that are involved in trace gas cycling under anthropogenic influences.

5.12.2 Methods

Surface water from the underway pump, located at about 6 m depth in the ship's moonpool, was sampled every 1 to 3 hours, in order to investigate the spatial distribution of DMS, isoprene and CS_2 in the surface waters along the cruise track. Chromophoric dissolved organic matter (CDOM) samples were taken every 3 hours. Besides surface measurements, discrete samples from different depths (surface to bottom) were collected to resolve trace and CDOM concentration variations also in a vertical resolution. The water for the depth profiles were sampled using Niskin bottles attached to the CTD. During each shallow CTD shallow cast, 6 - 7 different depths were sampled. 1 - 2 different depths were sampled from the deep CTD cast. During 4 stations, 5 to 6 different depths were additionally sampled for flowcytometry and DNA/RNA analysis.

Continuous measurements (LGR OCS Analyzer) for OCS/CO_2/CO were carried out in the air (air inlet in front of the bridge) and in the surface water using the ship's underway pump. The one hourly time interval was set to 50 min of water measurements and 10 min of air measurements.
Daily integrated aerosol filter measurements were performed from the ship's monkey bridge and were/will be used for incubation experiments on board and back in Germany.

In addition to oceanic and atmospheric samplings, two incubation experiments were performed during SO305. 63 polycarbonate bottles (2 L volume) were filled with surface water from 5 m depth. 21 bottles were spiked with 1% and 2% of scrubber water and with 1% scrubber water and aerosol filter leachate at the beginning of the first and second experiment, respectively. The other 21 bottles were used as controls. The bottles were placed in a water bath at current ocean surface temperature and were exposed to a natural day/night light cycle to a maximum time of six days. Triplicate sample bottles for each treatment (treatment and control) were taken once a day at the same time in order to be analysed for following different parameters: CS_2, isoprene, DMS/DMSP/DMSO, nutrients, DNA, RNA, bacteria and phytoplankton counts, CDOM and trace metals.

All trace gas samples were directly measured on board, within two hours after sampling, using a purge and trap system coupled to a gas chromatograph attached with a mass spectrometer (P&T-GC-MS). After the analysis, samples were prepared to be brought back to GEOMAR home lab for further analysis of DMSP and DMSO concentrations. Besides nutrient measurements, which were performed on board, all other samples will be analysed after the cruise in the home labs of GEOMAR and Univ. Oldenburg.

Originally, a third incubation experiment was planned for the last week of the cruise. Due to the prematurely termination of the cruise we were not able to perform the experiment. Measurements of samples back in the home labs and further data analyses will be finalized within one and a half year after the cruise until end of October 2025.

5.12.3 List of samples/measurements

OCS/CO/CO_2: Continuous measurements; April 17th – May 11th; 50 min water (from UW pump at ~5 m depth), 10 min air (from atmospheric line; inlet above bridge)
Aerosols: 24h integrated PM10 aerosol filter sampling; April 17th – May 10th
DMS, isoprene and CS_2: Surface water from the underway pump, sampled every 1 to 3 hours

Besides surface measurements, discrete samples from different depths (surface to bottom) were collected for trace gases During each shallow CTD shallow cast, 6 - 7 different depths were sampled. 1 - 2 different depths were sampled from the deep CTD cast.
CDOM: samples were taken every 3 hours from the underway pump system.

Table 5.8 Sampling for DNA/RNA and flowcytometry

Gear	Station	Bedford No.	depth [m]	lat	lon	date
CTD	8_1	30510263	4191.3	3.00	88.00	20.04.2024
CTD	8_1	30510273	759	3.00	88.00	20.04.2024
CTD	8_1	30510284	340	3.00	88.00	20.04.2024
CTD	8_3	30510288	229.1	3.00	88.00	20.04.2024
CTD	8_3	30510297	55.1	3.00	88.00	20.04.2024
CTD	8_3	30510303	2.4	3.00	88.00	20.04.2024
CTD	20_1	30511008	3216.8	12.30	86.00	28.04.2024
CTD	20_4	30511015	1000	12.30	86.00	28.04.2024
CTD	20_4	30511055	240	12.30	86.00	28.04.2024
CTD	20_4	30511058	170	12.30	86.00	28.04.2024
CTD	20_4	30511066	80	12.30	86.00	28.04.2024
CTD	20_4	30511068	1	12.30	86.00	28.04.2024
CTD	25_1	30511254	3167.3	13.00	86.00	01.05.2024
CTD	25_1	30511263	1000	13.00	86.00	01.05.2024
CTD	25_3	30511286	121.4	13.00	86.00	01.05.2024
CTD	25_3	30511289	69.9	13.00	86.00	01.05.2024
CTD	25_3	30511293	1.9	13.00	86.00	01.05.2024
CTD	38_2	30512306	2523.4	16.00	89.60	10.05.2024
CTD	38_4	30512329	200	16.00	89.60	10.05.2024
CTD	38_4	30512335	139.3	16.00	89.60	11.05.2024
CTD	38_4	30512340	36	16.00	89.60	11.05.2024
CTD	38_4	30512346	4.2	16.00	89.60	11.05.2024

5.12.4 Preliminary results

First preliminary results show contrasting variabilities of different trace gases in the surface ocean as shown in Figure 5.5. Isoprene, directly produced by phytoplankton, shows slightly elevated concentrations between 6°N and 10°N. Further northwest, values are very low and close to the detection limit indicating very low isoprene production in this area. DMS, a secondary product of microbial production, has highest concentrations at the equator, which could be due to equatorial upwelling of nutrients. Further north, DMS variability follows a similar pattern as isoprene concentrations. CS_2 concentrations are generally low and do not show much variability, except higher concentrations south of the equator. Overall low concentrations of CS_2 indicate low concentrations of CDOM, which is a precursor of photochemical production of CS_2.

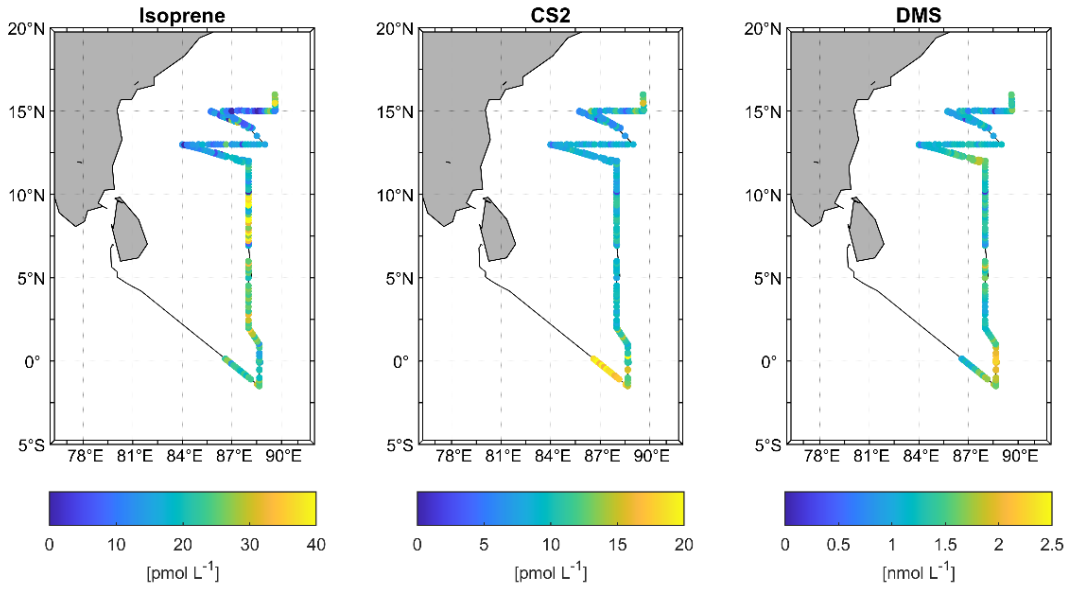

Fig. 5.5 Surface concentrations of isoprene (left), CS_2 (middle) and DMS (right) during SO305.

First insights into the results of one incubation experiment indicate a significant influence of aerosol filter and scrubber water addition on the production of DMS and isoprene (Figure 5.6). Isoprene concentrations decrease over the course of the incubation in the experiment in the control and in the scrubber water treatment. However, after day 3, isoprene concentrations increase in the aerosol filter treatment, which is most likely due to an induced phytoplankton bloom triggered by nitrate addition from the aerosol filters. DMS concentrations show a distinct different picture in the incubation experiment. DMS concentrations increase after day 3 in all three treatments. However, the increase is much lower and higher in the scrubber and aerosol filter treatment, respectively. Increasing concentrations in the aerosol filter treatment are due to increased nitrate concentrations. Lower concentrations in the scrubber water treatment indicate a potential toxic effect of scrubber water constituents on the microbial community and the subsequent biogenic production of DMS.

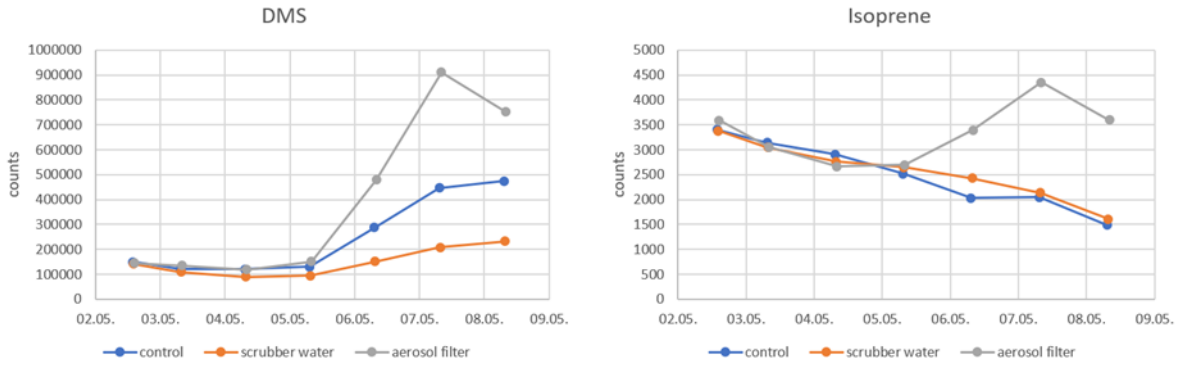

Fig. 5.6 DMS (left) and isoprene (right) values over the course of one experiment using scrubber water and aerosol filter leachate.

5.13 Halogenated Methanes

(J. Mickenbecker[1], J. Ploschke[1], B. Quack[1], E. Atlas[2])

[1] GEOMAR, [2] RSMA, Miami, FL, USA

5.13.1 Introduction

The greenhouse gas ozone acts as an important UV radiation-protector in the stratosphere for life on earth. It is rapidly destroyed by radical reactions of halogens, e.g. chlorine from long-lived fluorochlorocarbons, which were banned by the Montreal protocol in the 1990s. Ozone is recovering in the global upper stratosphere, while it is still declining in the lower stratosphere of the tropics. Surface ozone, on the other hand, is increasing due to air pollution, especially when fossil fuel is combusted. Over the oceans an active halogen chemistry caused by natural halogenated volatile substances and aerosols destroys ozone effectively. These substances, such as bromoform ($CHBr_3$), the largest organic bromine source for the atmosphere, dibromomethane (CH_2Br_2) and methyl iodide (CH_3I) are formed in the oceans and contribute to ozone depletion in the troposphere and stratosphere. Despite their short lifetimes, very short-lived substances (VSLS) can be rapidly lifted to the stratosphere by tropical deep convection. Shipboard observations have shown that emissions are often higher near the coast and in upwelling areas than in the open ocean, due to natural sources as phytoplankton and macroalgae. Meanwhile coastal anthropogenic sources must also be taken into account (Mehlmann et al., 2020), as e.g. $CHBr_3$ is produced in large quantities during the disinfection of seawater and transported to the upper troposphere (Jia et al., 2023). Chlorinated very short-lived substances (VSLS) are identified as present major ozone-depleting VSLS due to increasing anthropogenic emissions (Villamayor et al., 2023). Dichloromethane (CH_2Cl_2) is the most abundant, with the fastest increasing emissions at present, especially from Asia, and emissions of chloroform ($CHCl_3$) have also grown. Measurements of VSLS in and above the world's oceans are sparse and data show great variability. Little is known about the emission strengths or the uptake into the seawater and biogeochemical cycling of VSLS from the Indian Ocean. A single measurement campaign in the Bay of Bengal (Yamamoto et al., 2001) suggests that the Bay of Bengal might be a significant source of bromine and iodine to the atmosphere, as concentrations of the compounds were generally higher than data reported for other open ocean regions at mid- and high-latitudes (Ziska et al., 2013). During SO305, we measured the above compounds in water and air, in order to understand their source strengths and learn about their biogeochemical cycling in the oxygen minimum zone of the Bay of Bengal.

5.13.2 Methods

Sampling of the halocarbons in seawater was done with 250 ml amber glass bottles from the CTD-rosette bottles and from the underway supply by the submersible pump in six to twelve-hour intervals, which were filled bubble free and closed with Teflon lids. Surface water samples were stored in the lab, deep water samples in a ~7°C refrigerator until they were measured with a purge and trap system attached to a gas chromatograph (Agilent 6890N) with mass spectrometric detection (Agilent Technologies 5975 inert XL MSD) (GC-MS), within 1-12 hours after the sampling. Prior to analysis, the samples were warmed to room temperature (~20°C) to ensure purge efficiency and consistency. The bottles were attached to a manifold, which pressurizes the

top of the sample with helium and fills the purge-chamber with 30 ml of the seawater through a second submerged outlet, so that a pure sample can by transferred. Halocarbon concentrations were measured by purging 38 ml of sample water from ambient to 65°C in a long glass chamber for 45 min with a stream of helium at around 52 ml min-1, resulting in a purge efficiency of > 98%. A Nafion dryer (Ansyco GmbH, TT-050) was installed for the desiccation of the purge flow, using a counter-flow of 120 ml min-1 of N2. The volatilized trace gases were trapped between -150 and -170 °C above liquid nitrogen in a coil of deactivated stainless-steel tubing. After purging, the compounds were desorbed from the trap and injected into the GC-MS by heating the trap electronically to 180°C within 1.5 min. The sample was then separated on a 60 m by 0.38 mm Rtx-624 capillary column (film thickness = 1.8 µm) and finally detected by the MS in single ion mode. The concentrations were quantified with external standards, which were volumetrically prepared in methanol. The calibration curves were prepared with 1-4 µl of standards containing 0.02, 0.3 and 3 pmol of compound per µl. During transport of the standards, contamination occurred within the standard flasks and they will be recalibrated in Kiel. One calibration standard was repeatedly run in triplicate for sample quantitation, to account for sensitivity changes of the mass spectrometer during the cruise. The seawater measurements generally have a reproducibility of 2 to 10% for methyl iodide (CH_3I), dichloromethane (CH_2Cl_2), chloroform ($CHCl_3$), carbon tetrachloride (CCl_4), dibromomethane (CH_2Br_2), chloroiodomethane (CH_2ClI), trichloroethene ($CHCl_3$), tetrachloroethene (C_2Cl_4), dichlorobromomethane ($CHCl_2Br$), dibromochloromethane ($CHBr_2Cl$), bromoform ($CHBr_3$), diiodomethane (CH_2I_2).

Underway air samples of SO305 were taken at the bow in 2 L stainless steel canisters with a metal bellows pump. Air samples will be analysed for halocarbons at the National Center for Atmospheric Research (NCAR) in Boulder by Elliot Atlas (RSMAS, Miami) using GC/MS. The samples were taken simultaneously with underway seawater samples or with a delay of up to two hours to the corresponding water samples. Air samples were taken in parallel to the NCAR-samples in order to intercalibrate between air and water measurements and those samples will be analysed in Kiel on the onboard GC/MS.

Air-sea fluxes of the compounds will be calculated using air-sea exchange parameterizations. Compound specific transfer coefficients (k_w) will be derived from the transfer coefficient k_{CO2} of CO_2 by Schmidt number corrections (Sc).

All data will be available in winter 2024/2025.

5.13.3 Phytoplankton Pigments

Water samples taken from 6 surface depth (0-200 m) of the CTD deployments and regularly from 6h intervals from the underway sampling have been filtered for phytoplankton pigment analysis by HPLC for later biomass and algal taxonomic group analysis. Flow cytometry subsamples (850 µL) have been taken from the individual water samples and where added to Glutaraldehyde in 1 mL vials. After 30 minutes at 4°C the samples were frozen in liquid nitrogen and then stored at -80°C for later analysis in the Biological Oceanography at GEOMAR. 2 L of water samples were immediately filtered through GF/F-Filters, at an under pressure of maximum 200 mbar and the filters stored at -80°C until later analysis in the Biological Oceanography at GEOMAR.

5.13.4 List of Samples

382 seawater samples from depth profiles (see Table 11.3 in the Appendix) and 89 surface seawater samples were taken (see Table 11.4 in the Appendix) and analysed on board. 80 air sample canisters for Elliot Atlas (RSMAS, Miami, FL, USA) to be measured at NCAR, Boulder and 20 air samples for intercalibration in Kiel were taken during the cruise (see Table 11.5 in the Appendix). A list of samples for phytoplankton pigment analysis is given in Table 11.6. in the Appendix.

5.13.5 Preliminary Results

Varying distributions of the 12 halocarbons in surface and deep waters of the Bay of Bengal, reveal patterns of the compounds, related to biology, water masses and air-sea gas exchange. The following plots (Fig. 5.7 – 5.10) show some results of a few halocarbons in the upper 600 m of the water column.

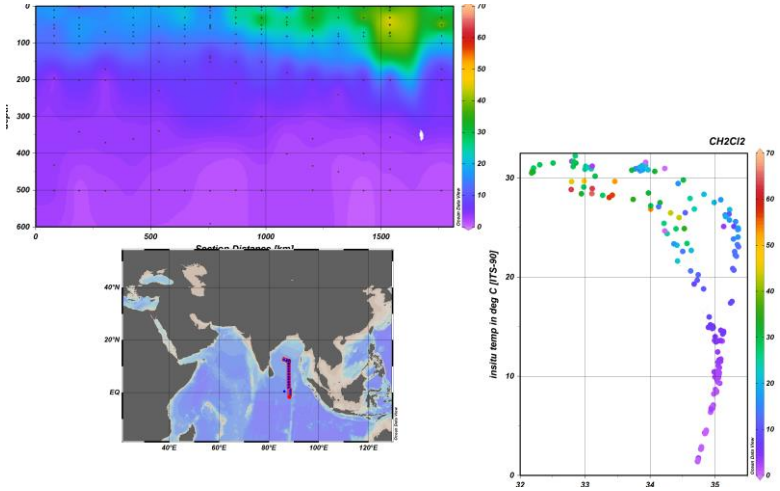

Fig. 5.7 Dichloromethane (CH_2Cl_2) is an anthropogenic compound, with increasing concentrations in the atmosphere. It increases in less saltier waters towards the northern Bay of Bengal.

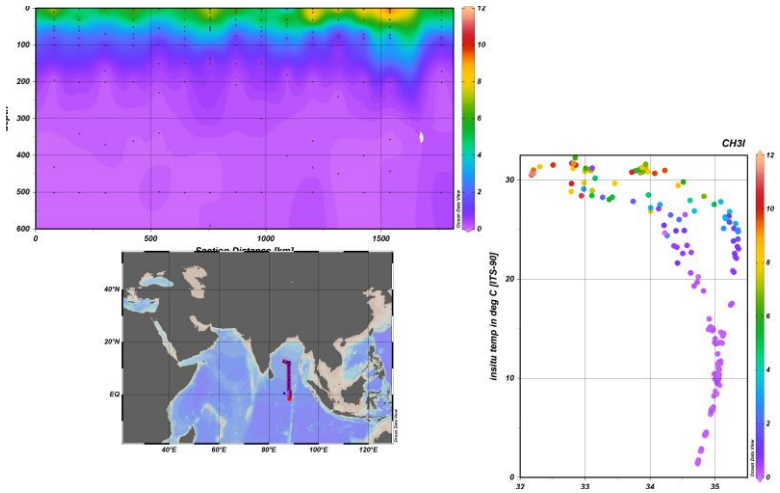

Fig. 5.8 Methyl iodide (CH_3I) is produced in sunlit reactions with DOM. Its concentrations are higher during the day in surface waters and appear to also increase in less saline surface waters.

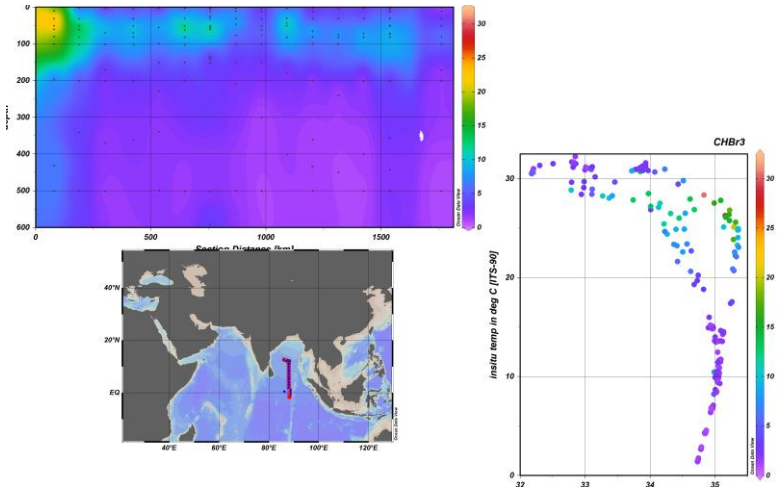

Fig. 5.9 Bromoform ($CHBr_3$) is produced in the chlorophyll maximum of the entire oceans. It appears to have higher concentrations in the equatorial region.

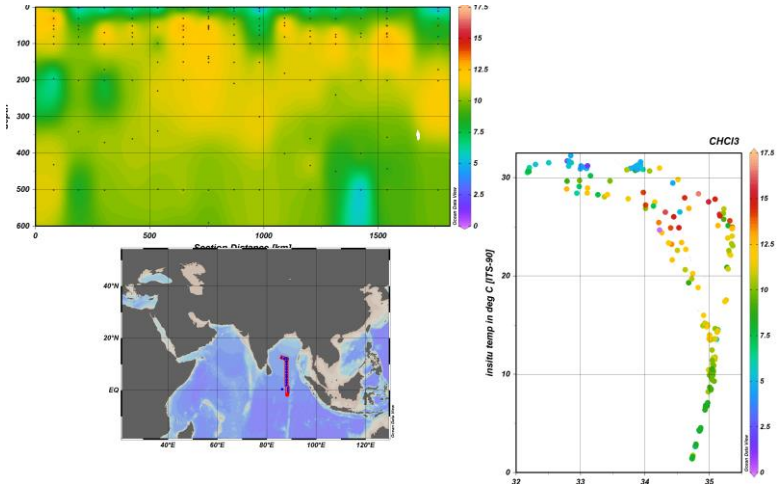

Fig. 5.10 Chloroform ($CHCl_3$) is both a natural and anthropogenic compound. It appeared to be elevated in a certain water mass, below the mixed layer.

5.14 Nitrogen Cycle - Isotopes

(G. Schulz[1], L. Nazzari[1], T. Sanders[1], K. Dähnke[2], N. Lahajnar[1], B. Gaye[1])

[1] Univ. Hamburg, [2] Hereon

5.14.1 Introduction

The SO305 BIOCAT-IIOE2 project aims to decipherer nitrogen sources as well as turnover processes to contribute to a better understanding of the emergence and spreading of the oxygen minimum zone in the Bay of Bengal. The working groups of Biogeochemistry in the Earth System from the University of Hamburg and Aquatic Nutrient Cycles from the Helmholtz Centre Hereon contribute to this goal using a two-fold approach by (1) sampling natural abundance isotopes of reactive nitrogen in the water column and (2) conducting process rate studies for nitrification and nitrogen and carbon uptake.

Accurate rate measurements are rare in oxygen minimum zones, and the understanding of the oxygen threshold values of different nitrogen turnover processes is constantly evolving. This also

applies to the understanding of nitrification, which can occur in niches with very low oxygen concentrations, partially inhibited by oxygen, and is therefore not realistically reproduced in models (Sun et al., 2021). Changes in nitrate stable isotopes have been used frequently to track sources and sinks of reactive nitrogen (e.g. nitrification, N_2 fixation, assimilation, and denitrification) in the open ocean (e.g. Sigman et al., 2005; Gaye et al., 2013; Marconi et al., 2015; Harms et al., 2019). Biological turnover processes favour lighter isotopes, leading to an enrichment in the remaining nitrogen pool (Granger et al., 2004; Dähnke et al., 2010; Sigman and Fripat, 2019). Thus, elevated nitrate isotope ratios in the photic upper layers are a possible sign for assimilation and can indicate consumption via denitrification and/or anammox in the oxygen minimum zone (e.g. Granger et al., 2004; Sigman and Fripat, 2019).

5.14.2 Sampling Strategy

For natural abundance isotopes, water samples were filtered (CN/GF, MINISART, 0.45 µm) and stored frozen for later nitrate analysis in the home lab. For nitrite isotope analysis, 1000 µL of 1M KOH was added to one sample replicate and kept cool to minimize oxygen isotope exchange (Böhlke et al., 2007). To quantify nitrification, we used a parallel setup of the ammonium tracer method (Ward, 2011) and the isotope dilution method (Norton and Stark, 2011; Sanders et al., 2018). Both methods are based on nitrate stable isotope measurements, whereas the ammonium tracer method tracks the turnover of ^{15}N-labelled ammonium to nitrate and the dilution method the isotopic dilution of a ^{15}N-labelled nitrate pool by freshly formed ^{14}N-nitrate. Incubation time was 24 hours and up to 10 days for the ammonium method and isotope dilution method, respectively. Subsamples at different time steps were filtered (CN/GF, MINISART, 0.45 µm) and stored frozen for later nutrient and nitrate isotope analysis.

Water samples for uptake incubations were spiked with $NaH^{13}CO_3$ and either ^{15}N-nitrate or ^{15}N-ammonium. After an incubation time of 2 and 4 hours for ammonium and nitrate uptake, respectively, at in situ light and temperature conditions, triplicate water samples were filtered over pre-combusted GF/F filters (450 °C, overnight). Filters were dried (40 °C, 48 hours) and stored in the dark for later analysis of ^{15}N and ^{13}C of the suspended particulate matter. Samples will be measured and data finalized in the following two years.

5.14.3 List of Samples

In total, natural abundance stable isotope samples were taken at 21 stations (Tab. 5.9) from 39 CTD casts with a high resolution of 25 - 50 m in water depths with low oxygen concentrations. Incubation experiments to determine nitrification rates in the water column were done at 6 stations at five to six distinct water depths chosen based on oxygen and fluorescence profiles. Nitrogen and carbon uptake experiments were done at 5 stations in two water depths.

Table 5.9 Overview of natural abundance isotopes (NA), nitrification potential (NP) and uptake rates (UR) sampling depths.

Gear	Station	Date	Latitude	Longitude	Samples		
					NA	NP	UR
CTD	2	17.04.2024	0.6°S	88.4°E	25		
CTD	4	18.04.2024	0.0°S	88.4°E	27	5	
CTD	6	19.04.2024	1.0°N	88.4°E	22		
CTD	8	20.04.2024	2.6°N	87.6°E	23		
CTD	10	22.04.2024	4.6°N	87.6°E	24	6	2
CTD	11	22.04.2024	5.6°N	88.0°E	23		
CTD	15	25.04.2024	9.0°N	88.0°E	21		
CTD	18	26.04.2024	12.0°N	88.0°E	23	6	2
CTD	20	28.04.2024	12.3°N	85.6°E	22		
CTD	23	30.04.2024	13.0°N	84.0°E	25		
CTD	24	30.04.2024	13.0°N	85.0°E	6		
CTD	25	01.05.2024	13.0°N	86.0°E	9		
CTD	26	01.05.2024	13.0°N	87.0°E	6		
CTD	27	02.05.2024	12.6°N	88.0°E	24		
CTD	28	03.05.2024	12.6°N	89.0°E	6		
CTD	30	04.05.2024	13.6°N	88.0°E	24	6	2
CTD	32	06.05.2024	14.6°N	85.4°E	26	6	2
CTD	34	08.05.2024	15.0°N	86.6°E	25		
CTD	35	08.05.2024	15.0°N	87.6°E	6		
CTD	37	09.05.2024	15.0°N	89.4°E	25	6	2
CTD	38	10.05.2024	15.6°N	89.4°E	24		

5.14.4 Preliminary Results

The isotopic composition of natural abundance samples and process rates results will only be available after analysis in the home lab. However, nutrient data shows accumulation of nitrate concentration in most sampled depths, which will allow isotopic determination. The dual stable isotope approach comparing $\delta^{15}N$ and $\delta^{18}O$ of nitrate will help to identify nitrate assimilation in the photic upper layer as well as nitrate consumption (denitrification and/or anammox) in the regions with low oxygen concentrations (e.g. Granger et al., 2004; Sigman and Fripat, 2019). Within the primary oxygen minimum zone, a portion of the samples exhibited nitrite accumulation. Conducting separate nitrite isotope analysis will help in disentangle the processes accountable for nitrite accumulation in these samples. Additional interpretation and process rate calculations will be feasible following isotopic determination.

5.15 Suspended Matter

(G. Schulz[1], T. Andersch[1], N. Lahajnar[1], B. Gaye[1])

[1] Univ. Hamburg

5.15.1 Introduction

The objective of the SO305 BIOCAT-IIOE2 project is to investigate the sources and degradability of particulate organic matter, with the goal of enhancing our comprehension of the development and expansion of the oxygen minimum zone in the Bay of Bengal. The working group Biogeochemistry in the Earth System from the University of Hamburg contribute to the project by collecting suspended matter samples.

Suspended particulate matter samples help to assess the composition of non-sinking particulate matter and advance our understanding of biogeochemical element cycles. Since suspended matter is too small and insufficiently dense to sink, it primarily disperses into deeper waters through the subduction of surface waters (Resplandy et al., 2019) and is passively transported by the ocean conveyor belt (Silver et al., 1998; McCave, 1984). Consequently, suspended matter sampling allows to trace the biogeochemical processes of source water masses and thereby decipher water mass transport mechanisms in the research area.

5.15.2 Methods

Suspended particulate matter was sampled via large-volume filtration of water samples collected at selected depths using the CTD/rosette with 24 10 L bottles. Water samples were filtered using a self-made filtration unit (Universität Hamburg) and combusted (450 °C, overnight), pre-weighed GF/F filters (WHATMAN, ~0.7 µm, 47 mm diameter). Following filtration, the suspended matter samples were rinsed with MILLI-Q water to remove sea salt. Afterwards, filters were dried at 40 °C for 48 hours in the ship's dry oven and stored in a dark. In the home lab, suspended particulate matter composition will be analysed starting with suspended particulate matter load followed by analyses of total nitrogen, total carbon, organic carbon, amino acid composition and stable isotope ratios of nitrogen. Samples will be measured and data finalized in the following two years.

5.15.3 List of Samples

In total, suspended particulate matter samples were taken at 23 stations leading to 165 filters (Table 5.10). Samples were taken at distinct depths depending on the CTD profile ranging between five and nine depths per station.

Table 5.10 Overview of suspended matter sampling.

Gear	Station	Date	Latitude	Longitude	Depths
CTD	2	17.04.2024	0.6°S	88.4°E	5
CTD	4	18.04.2024	0.0°S	88.4°E	5
CTD	6	19.04.2024	1.0°N	88.4°E	5
CTD	8	20.04.2024	2.6°N	87.6°E	5
CTD	10	22.04.2024	4.6°N	87.6°E	5
CTD	11	22.04.2024	5.6°N	88.0°E	5
CTD	13	24.04.2024	7.0°N	88.0°E	5
CTD	15	25.04.2024	9.0°N	88.0°E	5
CTD	18	26.04.2024	12.0°N	88.0°E	8
CTD	20	28.04.2024	12.3°N	85.6°E	5
CTD	23	30.04.2024	13.0°N	84.0°E	9
CTD	24	30.04.2024	13.0°N	85.0°E	7
CTD	25	01.05.2024	13.0°N	86.0°E	9
CTD	26	01.05.2024	13.0°N	87.0°E	7
CTD	27	02.05.2024	12.6°N	88.0°E	9
CTD	28	03.05.2024	12.6°N	89.0°E	7
CTD	30	04.05.2024	13.6°N	88.0°E	9
CTD	32	06.05.2024	14.6°N	85.4°E	8
CTD	34	08.05.2024	15.0°N	86.6°E	6
CTD	35	08.05.2024	15.0°N	87.6°E	7
CTD	36	09.05.2024	14.6°N	88.4°E	6
CTD	37	09.05.2024	15.0°N	89.4°E	9
CTD	38	10.05.2024	15.6°N	89.4°E	4

5.15.4 Preliminary Results

The composition of the suspended particulate matter will only be available after analysis in the home lab. Visual inspection of loaded filters showed generally higher loaded filters in the shallower water depths. The filters from the fluorescence maximum had the highest loads with a greenish colour.

5.16 Nitrogen Cycle - Microbial Processes

(I. Schlangen[1], M. Jacobsen[1], V. Fernández-Juárez[1], L. Nielsen[1], B. Thamdrup[1], L. Bristow[2], C. Löscher[1])

[1] SDU, [2] Univ. Gothenburg, DK

5.16.1 Introduction

During the SO305 BIOCAT-IIOE2 cruise, water was collected for on board incubations using various ^{15}N-nitrogen species combined with water filtrations for posterior molecular analysis in order to elucidate potential rates of microbial nitrogen transformation processes, and the key players involved in such processes. While other oxygen minimum zones (OMZ) in regions such

as the East Pacific and the Arabian Sea experience an annual estimated net loss of nitrogen to the atmosphere (14 Tg N yr^{-1}), the Bay of Bengal (BoB) exhibits a significantly lower net loss (7 Tg N yr^{-1}) compared to other systems. This lower loss can be attributed to the unique characteristics of the Bay of Bengal, which may account for the trace amounts of oxygen found in the area. Therefore, our study aims to gain a deeper understanding of the processes controlling nitrogen cycling in the BoB.

5.16.2 Methods

On board the RV SONNE, incubations were carried out in deck-based tanks as well as in the climate lab using stable isotope tracing. The deck-based incubations contained water sampled at the surface, chl-max and O_2 gradient. The sampled water was amended with $^{15}N_2$ gas to quantify the potential rate of nitrogen fixation over a period of 24 hours in addition to ^{13}C-bicarbonate to determine the potential rate of carbon fixation.

Concurrently, experiments were carried out in the temperature-controlled lab using ^{15}N-nitrogen species quantifying processes responsible for the loss of nitrogen through denitrification ($^{15}NO_2^-$, $^{15}NO_3^-$, and $^{15}N_2O$) and anammox ($^{15}NH_4^+$ and $^{15}NO_2^-$) or cycling of nitrogen through oxidation processes ($^{15}NH_4^+$ and $^{15}NO_2^-$). Kinetic experiments using either ^{15}N-nitrogen species or oxygen were also carried to determine the role these environmental factors for microbial nitrogen cycling in the BoB.

Additional water was collected from incubation depths and filtered for DNA and RNA extraction and will be used for metagenomic and transcriptomic analysis. In addition to this, water was also collected and filtered for Fluorescence in Situ Hybridization (FISH) analysis. The collected samples will be processed at SDU using techniques such as GC-IRMS and elemental analyser/MS for N-cycling experiments. Molecular work will involve FISH, DNA and RNA sequencing, as well as flow cytometry.

Unfortunately, the temperature lab did not work optimally with temperature fluctuating between 8°C to 18°C (target temperature 12°C). This was a problem for the in-lab incubations. It will take approx. 1 year to get all data from the experiments conducted in the climate lab.

5.16.3 List of Samples

Water was collected from the CTD and the underway pump. All 24h-stations were targeted for incubations, while additional stations were sampled occasionally for both incubation work and molecular samples. Molecular samples were collected across the cruise track, while incubation experiments started from 5°N (station 10). The primary focus for the incubation experiments were on the northern most stations where the OMZ was located. In each CTD, samples were collected from surface, chlorophyll max, and several depths between 100 and 400 covering the OMZ for incubation and molecular analyses.

Table 5.11- Stations sampled for N- and C-fixation (on-deck experiments) and molecular work.

Station	Molecular	N_2-fixation	N-cycling	Date
4	X			18/04/2024
6	X			19/04/2024
8	X			20/04/2024
10	X	X	X	21/04/2024
13	X	X	X	24/04/2024
15	X			25/04/2024
16	X		X	26/04/2024
18	X	X	X	27/04/2024
20			X	28/04/2024
22	X			29/04/2024
23	X	X	X	30/04/2024
26	X		X	02/04/2024
28	X			03/04/2024
30	X	X	X	04/04/2024
32	X	X	X	07/04/2024
34	X			08/04/2024
35	X		X	09/04/2024
37	X	X	X	10/04/2024

Stations sampled for N cycling and N loss (temperature lab experiments): 10, 13, 16, 18, 20, 23, 26, 30, 32, 35, and 37. Number of samples generated: For the recycling vs. loss of fix nitrogen analyses we generated a total of 876 samples. For FISH samples, we generated a total of 72 samples. For N_2O analysis we generated xxx samples. For N_2 fixation we generated a total of xxx samples.

5.16.4 Preliminary Results

Since all the samples collected have to be processed at SDU, we cannot not show any preliminary result.

5.17 Drifting Sediment Traps

(T. Barthelmeß[1], J. Roa[1], S. Golde[1], A. Barbot[1], B. Pontiller[1], K. Becker[1], A. Engel[1])

[1] GEOMAR

5.17.1 Introduction

The Bay of Bengal in the Indian Ocean is an oligotroph system, which is defined by complex eddies, currents, and divergent water mass stratification in which a deep Chlorophyll a maximum evolves between 50 and 100 m depth (Fig. 5.11a). At the northern stations of the cruise track of SO305, the surface waters are expected to be influenced by the enormous freshwater inflow of the Brahmaputra and Ganges delta. The Bay of Bengal is furthermore characterized by an expanded oxygen minimum zone (OMZ) below a varying depth of 100 to 200 m (Fig. 5.11b). Depending on

the stations, it expands towards more than 600 m depth. OMZs are thought to evolve due to the degradation of organic matter via respiration of organisms, i.e. the consumption of oxygen, and poor physical ventilation. Although primary production in the surface waters was shown to be rather low during the last decades, the export of organic carbon towards depth is larger than expected in the Bay of Bengal (Unger and Jennerjahn, 2009; Rixen et al., 2009). Hypothetically, riverine organic matter and inflow of lithogenic material may 1) enhance particle formation, and 2) accelerate particle sedimentation by ballasting (Ray et al., 2015). Additionally, 3) polluted air masses have been recently shown to form a large cloud which may transport minerals, nutrients, and pollutants off the coast (Ramanathan et al., 2017). Pollutants may deposit at the ocean surface and are considered as a further factor influencing surface biogeochemistry and particle export. In general, data are scarce which assess particle export and export efficiency. They are yet insufficient to fully comprehend the evolution of OMZ and their influence on long-term carbon storage (Engel et al., 2023).

To assess biogenic particle export dynamics out of the surface mixed layer into the OMZ, we deployed drifting sediment traps along a S/N transect at 88°E from 5°N to 15°N. The drifting sediment traps resolve the sedimentation flux at high resolution in the surface ocean (every 50 m) until a depth of 200 m and at lower resolution (every 100 m) down to a depth of 600 m (Fig. 5.11c). The drifting buoys at the surface hold the sediment traps in place which are further ballasted by a ground weight (Fig. 5.11d-f). The most important components of the traps are the eight rosettes equipped with twelve sedimentation tubes. Above a formaldehyde-brine at the bottom, the tubes are filled with filtered seawater (Fig. 5.11e). The brine conserves the captured, sinking particles. The sediment traps deployments lasted between 48 and 69 hours. To define particle export dynamics, we have collected samples for the analysis of e.g., particulate organic carbon (POC) and its molecular components including lipids, amino acids, and carbohydrates. Samples for biogenic silica (BSi) and total particle mass were also collected, enabling us to deduce the contribution of lithogenic material. The contribution of different organisms to particle formation and degradation along its sedimentation pathway is complemented by enzyme activity measurements, meta-genome, and -transcriptome analysis. To assess the surrounding water column and its potential POC budget driving sedimentation fluxes, additional CTD casts were sampled at the beginning and end of each sediment trap deployment and at in total nine different depths (additionally including 5 m depth sample).

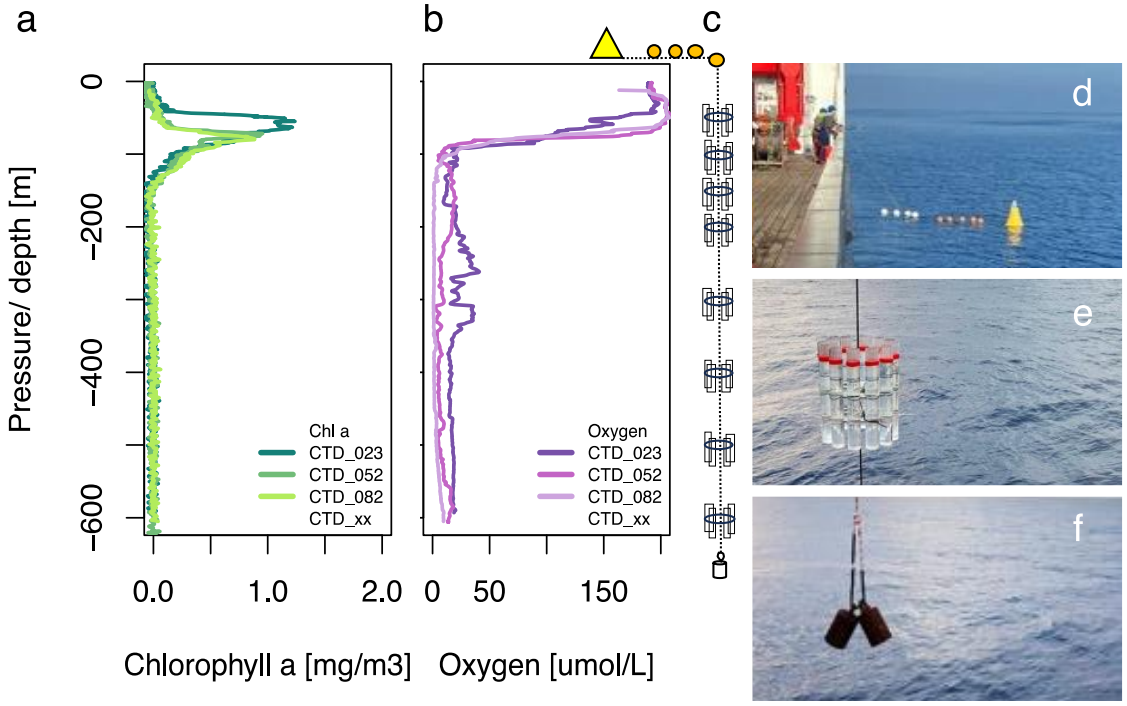

Fig. 5.11 The drifting sediment traps were deployed three times along a S/N transect during SO305 in the Bay of Bengal. a) Chlorophyll a maxima were located between a depth of 50 to 100 m. b) From S to N oxygen was depleted beyond a depth of 100 to 200 m and reduced to concentrations <10 µM. c) The rosettes of the drifting sediment traps collected sinking particles at eight depths, with a higher resolution until 200 m and a lower resolution until 600 m. The sediment traps are composed of three basic modules including d) the drifting surface buoys equipped with a GPS tracker, e) the eight rosettes in which 12 sedimentation tubes were mounted, and f) the ground weight.

5.17.2 Methods

We collected mainly particulate organic matter (POM) larger than 0.7 µm in size, exceptions are mentioned in the paragraph below. The material collected in the sedimentation tubes was pooled, well-mixed and distributed for triplicate filtration. Samples for POC, particulate organic nitrogen (POC), total particulate carbon (TPC), particulate amino acids (PAA), particulate carbohydrates (PCHO), Chlorophyll a (Chl a), and particulate organic phosphorus (POP) were filtered onto GFF filters (Whatman, 0.7 µm), while samples for particulate lipids were filtered onto PVDF membranes (Millipore, 0.2 µm), biogenic silica (BSi) on cellulose acetate filters (Sartorius, 0.8 µm), and total particle mass, transparent exopolymer particles (TEP), and Coomassie stainable particles (CSP) were filtered onto polycarbonate membranes (Whatman, 0.45 µm pore size) applying a vacuum of ~200 mbar. Leftover sample volume was filled into glass bottles for the analysis of microplastics. In order to asses meta-transcriptomics (meta-t, based on RNA) and -genomics (meta-g, based on DNA), two size fractions were distinguished and filtered onto Sterivex (0.22 µm) and PVDF membranes (Millipore, 3 µm) for selected depths (50, 300 and 600 m). Extracellular enzyme activity (EEA) was assessed for the same selected depths from CTD casts and trap deployments. Selected sedimentation tubes were further prepped to collect sinking particles in a gel-matrix for microscopical analysis (conserved in polyacrylamide, Lundsgaard,

1995; Engel et al., 2022). Flow cytometry samples were collected for the analysis of phytoplankton cell abundance, bacterial cell counts, and virus particles in addition to POM from corresponding CTD casts.

In brief, POC, PON, and TPC is analysed using a Euro EA elemental analyser (Sharp, 1974). PAA and PCHO will be determined by high-performance liquid chromatography (HPLC) and anion exchange chromatography (HPAEC), equipped with a fluorescence and pulsed amperometric detector (PAD), respectively (Lindroth and Mopper, 1979; Engel and Händel, 2011). In total, 13 amino acids and 12 carbohydrate monomers can be discriminated including neutral and acidic compounds. Lipids and pigments will be analysed on a HPLC coupled to a Orbitrap high resolution mass spectrometer (MS) according to Becker et al. (2018). Chl a will be assessed via photometry (Turner Design, USA) after the modified protocol of Evans et al. (1987). After digestion and dissolution, POP and BSi will be analysed in our central nutrient lab using photometry (QuAAtro, Seal Analytical; Grasshoff et al., 1999). Total particle mass will be assessed by high-precision weight. TEP and CSP were stained with Alcian and Coomassie Blue after filtration, which enables the distinction of carbohydrate-like and protein-like particles via photometry (Passow and Alldredge, 1995; Cisternas-Nova et al., 2014). Microplastics will be analysed by digestion (Cole et al., 2014; Mintening et al., 2016), followed by pyrolysis and coupled to gas chromatography and MS (GC-MS) (Fischer et al., 2019). Meta-g and meta-t analysis will follow the methodology as outlined by Fontanez et al., (2015). EEA produced by the overall microbial community was assessed on board by spectrofluorometric measurements of fluorogenic substrates. Following the methodology outlined by Hoppe (1983), the hydrolysis rates of five distinct enzymes were determined, including e.g., peptidase and glucosidase activity (Baltar et al., 2010). Flow cytometer samples are fixed in glutaraldehyde and flow cytometry (FACSCalibur) will allow the distinction of five different phytoplankton classes via their cell size distribution (0.2-20 µm) and phytopigments (phycoerythrin and Chl a). To count bacteria and virus particles, samples will be stained with SYBR Green (following standard procedure of our lab, e.g., Engel and Galgani, 2016).

We applied a new sediment trap design during SO305 BIOCAT-IIOE2. After the first deployment (23.04.2024), we lost in total nine out of 96 tubes. During the process of recovery, the sediment traps started spinning due to tension and internal coiling of the rope. The new rosette holders of the tubes could not withstand the centrifugal forces which unravelled. In order to avoid further losses, we implemented three measures, i.e. cutting the rope and integrating vertebra to avoid the internal progression of spin, fixing the tubes to a further rosette holder, and tightening them with cable ties instead of bungee ropes. Our measures were successful.

We also installed an optical fluorescent dissolved organic matter (FDOM) sensor at the CTD frame, however, had to change its orientation from horizontal to vertical (pointing towards depth) as we noticed that scattering of the data was significantly reduced (29.03.2024, 10:43 UTC).
All data measurements will be finalized within two years and selected data are made available on request to interested colleagues. We highly welcome potential collaborations and common publications. After publication in a scientific journal, data will be published in an open-access online repository such as PANGAEA.

5.17.3 List of Samples

The list of samples from the drifting sediment trap deployments is given in Table 11.7 in the Appendix.

5.18 Microbial Activity and Community Composition

(A. Barbot[1], A. Engel[1])

[1] GEOMAR

5.18.1 Methods

The activity of extracellular enzymes (EEA) produced by the overall microbial community was assessed on board by spectrofluorometric measurements of fluorogenic substrates. Following the methodology outlined by Hoppe (1983), the hydrolysis rates of five distinct enzymes were determined, as detailed in the studies conducted by Baltar et al. (2010). To assess the microbial community composition and diversity, filtrations was conducted on two size fraction filters, 0.22 µm and 0.3 µm. Metagenomic and meta-transcriptomic analysis will be done within one year following the methodology outlined by Fontanez et al. (2015).

Potential hydrolytic rates of L-Leucin-7-amido-4-methylcoumarin-hydrochlorid (LAPase), 4-Methylumbelliferyl-α-D-glucopyranosid (AGase), 4-Methylumbelliferyl-β-D-glucopyranosid (BGase), 4-Methylumbelliferyl-N-acetyl-β-D-glucosaminid (NAG), 4-Methylumbelliferyl-phosphat (APase) were determined with fluorescent substrate analogs (Hoppe, 1983). 10 µL of the following standards, L-leucine-7-amido-4-methylcoumarin (Sigma Aldrich) and 4-methylumbelliferone (Sigma Aldrich) were added with final concentrations of 1.25, 2.5, 10, 50, 100, 500 and 1000 nmol L^{-1} in black 96 well plates (Costar) and kept frozen for at most one day until replicates of 290 µL water sample were added. These concentrations were previously determined as saturating substrate concentrations (Baltar et al, 2010). The final substrate concentration of 30 µmol L^{-1} was used to measure Agase, BGase and NAG activities, 100 µmol L^{-1} for APase, and 500 µmol L^{-1} for LAPase. Individual depths corresponding plats were incubated in the dark, close to in situ temperature. After 0, 3, 6 and 12 h of incubation, fluorescence was measured with a plate reader fluorometer (FLUOstar Optima, BMG Labtech, excitation: 355 nm; emission: 460 nm).

Enzyme activities were measured onboard immediately after sampling using L-leucine-4-methylcoumarinyl-7-amide (MCA) hydrochloride and 4-methylumbelliferone (MUF) β-D-glucopyranoside (Sigma-Aldrich) as substrate proxies for Lpase (hereafter referred to as peptidase), AGase and BGase activities (hereafter referred to as glucosidase), respectively (Hoppe, 1983). Enzymatic hydrolysis of MCA- and MUF-substrate proxies can be measured with short-term (several hour) incubations and is generally considered to reflect activities of the in situ microbial community. Fluorescence changes were calibrated using MUF and MCA standard solutions in seawater and used to calculate hydrolysis rates.

5.18.3 List of Samples

Table 5.12 Extracellular enzymatic activity and metagenomic samples.

SO305_Extracellular enzymatic activity and metagenomics samples									
Date (UTC)	Time [UTC]	Lat (N)	Long (W)	Station	CTD/TRAP cast	Niskin bottle #1	Niskin bottle #2	depth_m	Comments
23/04/2024	8:06:00 AM	5° 03.344 N	88° 11.796 E	SO305/12-1	TRAP_1			50	Only 0.22 µm filters
23/04/2024	8:36:00 AM	5° 03.344 N	88° 11.796 E	SO305/12-1	TRAP_1			300	
23/04/2024	8:47:00 AM	5° 03.344 N	88° 11.796 E	SO305/12-1	TRAP_1			600	
29/04/2024	1:58:24 AM	11° 56.548 N	87° 38.265 E	SO305/21-1	TRAP_2			50	
29/04/2024	2:25:52 AM	11° 56.548 N	87° 38.265 E	SO305/21-1	TRAP_2			300	
29/04/2024	2:49:23 AM	11° 56.548 N	87° 38.265 E	SO305/21-1	TRAP_2			600	
07/05/2024	11:28:09 AM	13° 58,912' N	088° 13,463' E	SO305/33-1	TRAP_3			50	
07/05/2024	12:03:44 PM	13° 59,019' N	088° 13,649' E	SO305/33-1	TRAP_3			300	
07/05/2024	12:32:52 PM	13° 59,241' N	088° 13,741' E	SO305/33-1	TRAP_3			600	
23/04/2024	8:06:00 AM	5° 03.344 N	88° 11.796 E	SO305/12-1	TRAP_1			50	
23/04/2024		5° 03.344 N	88° 11.796 E	SO305/12-1	TRAP_1			300	
23/04/2024	8:47:00 AM	5° 03.344 N	88° 11.796 E	SO305/12-1	TRAP_1			600	
29/04/2024	1:58:24 AM	11° 56.548 N	87° 38.265 E	SO305/21-1	TRAP_2			50	
29/04/2024	2:25:52 AM	11° 56.548 N	87° 38.265 E	SO305/21-1	TRAP_2			300	
29/04/2024	2:49:23 AM	11° 56.548 N	87° 38.265 E	SO305/21-1	TRAP_2			600	
07/05/2024	11:28:09 AM	13° 58,912' N	088° 13,463' E	SO305/33-1	TRAP_3			50	
07/05/2024	12:03:44 PM	13° 59,019' N	088° 13,649' E	SO305/33-1	TRAP_3			300	
07/05/2024	12:32:52 PM	13° 59,241' N	088° 13,741' E	SO305/33-1	TRAP_3			600	
22/04/2024	5:10:00 AM	4° 59.926 N	87° 59.774 E	SO305/10-13	CTD 10-13	SO305_1_455		50	Deployment CTDs
22/04/2024	5:10:00 AM	4° 59.926 N	87° 59.774 E	SO305/10-13	CTD 10-13	SO305_1_444		300	
22/04/2024	5:10:00 AM	4° 59.926 N	87° 59.774 E	SO305/10-13	CTD 10-13	SO305_1_338	SO305_1_339	600	
27/04/2024	7:40:00 AM	12° 00.139 N	87° 59.933E	SO305/18-8	CTD 18-8	SO305_1_851		50	
27/04/2024	7:40:00 AM	12° 00.139 N	87° 59.933E	SO305/18-8	CTD 18-8	SO305_1_842		300	
27/04/2024	7:40:00 AM	12° 00.139 N	87° 59.933E	SO305/18-8	CTD 18-8	SO305_1_834	SO305_1_835	600	
05/05/2024	12:05:00 AM	13° 59.653 N	87° 59.119 E	SO305/30-12	CTD 30-12	SO305_1_1709		50	
05/05/2024	12:05:00 AM	13° 59.653 N	87° 59.119 E	SO305/30-12	CTD 30-12	SO305_1_1710		300	
05/05/2024	12:05:00 AM	13° 59.653 N	87° 59.119 E	SO305/30-12	CTD 30-12	SO305_1_1092	SO305_1_1093	600	
23/04/2024	9:31:00 AM	5° 03.345 N	88° 11.797 E	SO305/12-2	CTD 12-2	SO305_1_543		50	Recovery CTDs
23/04/2024	9:31:00 AM	5° 03.345 N	88° 11.797 E	SO305/12-2	CTD 12-2	SO305_1_534		300	
23/04/2024	9:31:00 AM	5° 03.345 N	88° 11.797 E	SO305/12-2	CTD 12-2	SO305_1_526	SO305_1_527	600	
29/04/2024	4:00:00 AM	11° 56.730 N	87° 37.442 E	SO305/21-2	CTD 21-2	SO305_1_1093		50	
29/04/2024	4:00:00 AM	11° 56.730 N	87° 37.442 E	SO305/21-2	CTD 21-2	SO305_1_1084		300	
29/04/2024	4:00:00 AM	11° 56.730 N	87° 37.442 E	SO305/21-2	CTD 21-2	SO305_1_1075		600	
05/05/2024	12:44:00 AM	13° 59,650' N	87° 59,129' E	SO305_33_2	CTD32-2	SO305_1_1951		50	
05/05/2024	12:44:00 AM	13° 59,650' N	87° 59,129' E	SO305_33_2	CTD32-2	SO305_1_1942		300	
05/05/2024	12:44:00 AM	13° 59,650' N	87° 59,129' E	SO305_33_2	CTD32-2	SO305_1_1934	SO305_1_1935	600	
27/04/2024	2:42:00 AM	12° 00,137' N	087° 59,938' E	SO305_18_6	Underway				
10/05/2024	2:14:00 AM	15° 00,140' N	089° 36,124' E	SO305_37_6	Underway				
27/04/2024	2:42:00 AM	12° 00,137' N	087° 59,938' E	SO305_18_6	Zodiac				
10/05/2024	2:14:00 AM	15° 00,140' N	089° 36,124' E	SO305_37_6	Zodiac				
01/05/2024	12:07:00 AM	13° 00,098' N	085° 00,065' E	SO305/24_3	CTD 24-3	SO305_1_1243		50	13° N West - East
01/05/2024	12:07:00 AM	13° 00,098' N	085° 00,065' E	SO305/24_1	CTD 24-1	SO305_1_1226		300	Transect
01/05/2024	12:07:00 AM	13° 00,098' N	085° 00,065' E	SO305/24_1	CTD 24-1	SO305_1_1223		600	
01/05/2024	11:30:00 AM	13° 00,072' N	086° 00,010' E	SO305/25_3	CTD 25-3	SO305_1_1290		50	
01/05/2024	11:30:00 AM	13° 00,072' N	086° 00,010' E	SO305/25_3	CTD 25-3	SO305_1_1280		300	
01/05/2024	11:30:00 AM	13° 00,072' N	086° 00,010' E	SO305/25_1	CTD 25-1	SO305_1_1270		600	
02/05/2024	3:00:00 PM	12° 59,585' N	087° 59,851' E	SO305/27_4	CTD 27-4	SO305_1_1422		50	
02/05/2024	3:00:00 PM	12° 59,585' N	087° 59,851' E	SO305/27_4	CTD 27-4	SO305_1_1414		300	
02/05/2024	3:00:00 PM	12° 59,585' N	087° 59,851' E	SO305/27_2	CTD 27-2	SO305_1_1402		600	
03/05/2024	2:44:10 AM	12° 59,992' N	089° 00,094' E	SO305/28_2	CTD 28-2	SO305_1_1485		50	
03/05/2024	2:44:10 AM	12° 59,992' N	089° 00,094' E	SO305/28_2	CTD 28-2	SO305_1_1472		300	
03/05/2024	2:44:10 AM	12° 59,992' N	089° 00,094' E	SO305/28_1	CTD 28-1	SO305_1_1465		600	
05/05/2024	11:50:00 PM	15° 00.007 N	85° 45.003 E	SO305/32-2	CTD 32-2	SO305_1_1775		50	Extra CTD
05/05/2024	11:50:00 PM	15° 00.007 N	85° 45.003 E	SO305/32-2	CTD 32-2	SO305_1_1766		300	
05/05/2024	11:50:00 PM	15° 00.007 N	85° 45.003 E	SO305/32-2	CTD 32-2	SO305_1_1758	SO305_1_1759	600	
11/05/2024	3:01:00 AM	16° 00,009' N	089° 36,003' E	SO305/38_6				50	
11/05/2024	3:01:00 AM	16° 00,009' N	089° 36,003' E	SO305/38_6				300	
11/05/2024	3:01:00 AM	16° 00,009' N	089° 36,003' E	SO305/38_6				600	

5.19 Trace Elements, Trace Element Speciation, Major Ions, Dissolved Organic Carbon and pH

(M. Gledhill[1], A. Firus[1], A. Conventz[1])

[1] GEOMAR

5.19.1 Introduction

Trace elements are essential micronutrients in the ocean, and provide information on material sources and water mass provenance. Many steps in the marine nitrogen cycle, a key focus of SO305, are catalysed by enzymes incorporating trace elements such as iron (Fe), molybdenum (Mo) and copper (Cu). Furthermore, the pronounced oxygen minimum zone in the region can be expected to impact redox sensitive trace elements such as Fe (Moffett et al., 2007; Zhu et al., 2021). Oxygen minimum zones are also characterised by low pH, which influences the chemical equilibria that determines the chemical forms of trace elements present in the water column (chemical speciation) and the binding of trace metals to marine dissolved organic matter (DOM) (Turner et al., 2024).

Rivers and atmospheric deposition are sources of many trace elements to the ocean. The Bay of Bengal receives inputs from the Ganges-Brahmaputra River, which results in a surface low salinity layer and a strongly stratified water column. Furthermore, atmospheric deposition is also significant in the region, with the Bay of Bengal predicted to receive more than 50 µmol m^{-2} yr^{-1} (Hamilton et al., 2020). The impact of the material sources on the distributions of trace elements in the Bay of Bengal have not been thoroughly studied.

We therefore aimed to characterise the distribution and chemical speciation of the trace elements Fe, Cu, nickel (Ni), zinc (Zn), lead (Pb), cadmium (Cd), manganese (Mn) and cobalt (Co) in the surface waters of the Bay of Bengal. Our aim is to identify the impact of fresh water inputs, atmospheric deposition, physical mixing and internal biogeochemical cycling on trace element distributions in the region.

Despite being among the most abundant elements present in the global ocean, the concentration and distribution of some dissolved major elements (Ca, Sr, Li) are not well studied. Although typically considered conservative, the salinity-normalised concentrations of these major ions do vary by measurable quantities as result of material sources (Steiner et al., 2020). A particular focus of study in this region will be the major ion concentrations in the surface low salinity waters that cap the Bay of Bengal.

5.19.2 Method Description

5.19.2.1 Sample Collection

Near surface water (nominal depth 2.0 ± 0.5 m) was sampled using a trace metal clean towed-fish positioned aft on the starboard side of the ship. Water was pumped directly from the towed-fish through polyethylene tubing into a clean tent supplied with filtered air (MAX 10L HEPA filter) constructed in a laboratory on the SONNE. The towed-fish supply was sampled for dissolved trace metals (DTMs, <0.2 µm), particulate trace metals (PTMs, >0.2 µm), nutrients (nitrate, nitrite, phosphate, silicate), major ions (Ca, Sr, Li and F), pH and dissolved organic carbon (DOC). A

total of 74 towed-fish samples were collected at approximately 3 hourly intervals whilst the ship was underway.

Six depths up to 500 m were sampled from 27 stations using contamination free GoFlo water samplers (General Oceanics) deployed on a Kevlar wire. A mini conductivity-temperature-depth logger (Star-Oddi) was attached to the deepest water sampler. The water samplers were transferred to the clean tent prior to sampling for DTMs, PTMs, dissolved organic trace metals (D-orgTMs), particulate organic trace metals (P-orgTMs), major ions, nutrients (nitrate, nitrite, phosphate, silicate), pH and DOC.

5.19.2.2 Methods

Nutrients: Nutrients were sampled directly (unfiltered) into 15 mL nutrient vials for analysis on board (see section 5.7 above).

pH: pH samples were collected without filtration into 15 mL vials and analysed directly on board via spectrophotometry with the indicator meta-cresol purple using a SAMI-pH logger (Sunburst Sensors). Samples were analysed on the total pH scale at room temperature assuming a salinity of 35. At station 30 the SAMI pH logger developed a technical fault which could not be resolved. pH values will be corrected to in-situ temperature, salinity and pressure post-cruise using the Sunburst Sensor QC-pH routine. pH of surface waters was also logged continuously using a pH logger (Alphox, Pyroscience) deployed in the laboratory at the towed-fish outflow. Data will be available in December 2024.

Major ions: Samples for analysis of major ions were filtered (0.8/0.2 µm, AcroPak 500, Pall) into acid washed 15 mL polypropylene centrifuge tubes and acidified to pH 1.8 with hydrochloric acid. Concentrations of Ca, Sr and Li will be determined at GEOMAR by inductively coupled plasma optical emission spectroscopy (Varian). Data will be available in June 2026.

Dissolved trace metals: Sample for DTMs were filtered (0.8/0.2 µm, AcroPak 500, Pall) into acid washed 125 mL low density polyethylene bottles following GEOTRACES protocols (Cutter et al., 2014). Samples were acidified to pH 1.8 with ultra-high purity hydrochloric acid (Optima, Fisher). Concentrations of iron, manganese, cobalt, copper, cadmium, nickel, lead and zinc will be determined at GEOMAR after preconcentration (SeaFAST, ESI) by high resolution inductively coupled plasma mass spectrometry (Element-XR, Thermo) (Rapp et al., 2017). Data will be available in June 2025.

Dissolved organic carbon: Samples (25 mL) for DOC were filtered (0.8/0.2 µm, AcroPak 500, Pall) into acid washed and pre-combusted (450 °C, 4 hours) 30 mL glass vials sealed with fluorinated ethylene propylene (FEP) septa. Samples were acidified to pH 2 with hydrochloric acid. Dissolved organic carbon and nitrogen will determine at GEOMAR after catalytic oxidation (TOCN-L, Shimadzu). Data will be available in June 2025.

Dissolved and particulate organic trace metals: Samples (ca. 2 L) for D-orgTMs and P-orgTMs were transferred to flexible polyethylene media bags (Flexboy, Sartorius). Water from the bags was passed through a 0.2 µm polyvinylidene fluoride (PVDF) cartridge filter (Sterivax, Millipore) and then over polystyrene divinyl benzene solid phase extraction (SPE) cartridge (500 mg, ENV+, Agilent) using a peristaltic pump at a flow rate of ca. 10 mL/min. Filter and cartridge had been precleaned with methanol (10 mL) and 0.01 M hydrochloric acid (20 mL). Filter cartridges were frozen at -80°C for analysis of the P-orgTM fraction while SPE cartridges were frozen at -20°C

for analysis of D-orgTM fractions. Organic trace metal fractions will be analysed at GEOMAR after extraction from the filter and cartridge by size exclusion and reversed phase high performance liquid chromatography – electrospray ionisation/inductively coupled plasma - mass spectrometry (Thermo) (Gledhill et al., 2022). Data will be available in June 2026.

Particulate trace metals (PTMs): Particulate trace metals were collected on 0.2 µm acid washed polyethylene sulfone filters (25 mm, PALL) placed in an acid-cleaned polyethylene filter holder and directly attached to the GoFlo bottle tap. GoFlo bottles were pressurized with nitrogen for PTM filtration. For PTM samples collected from the towed-fish, an FEP vacuum unit was connected to the polyethylene filter holder and water was supplied using a flexible media bag (Flexboy, Sartorius). Between 2 and 4 L of seawater was filtered from four depths on each cast. Filters were carefully folded in half, placed into small ziplock bags and frozen at -20°C for transportation back to the laboratory at GEOMAR. Particulate trace metals will be determined after digestion of filters according to GEOTRACES protocols (Al-Hashem et al., 2022; Cutter et al., 2014). Data will be available in June 2026.

5.19.3 List of Samples

Table 5.13 List of samples

Parameter	Number of GoFlo samples	Number of towed-fish samples
Nutrients	157	71
pH	157	73
Major ions	157	73
DTMs	157	73
DOC	157	71
D-orgTMs	119	
P-orgTMs	119	
PTMs	95	48

5.19.4 Preliminary Results

Only preliminary pH data are available at the time of writing as most of the analysis of this WP must be undertaken in the laboratory at GEOMAR. A preliminary pH section plot is shown for the latitudinal transect to 14°N (Fig. 5.12). Oxygen distributions (data: CTD, see section 5.1) are shown for context. pH decreased in the oxygen minimum zone and, in surface waters, towards the north of the transect as the water freshened. The strong relationship between pH and oxygen suggests remineralisation processes made a contribution to decreases in pH in subsurface waters in the Bay of Bengal, although increased CO_2 solubility as a result of lower temperatures can also be expected to be important.

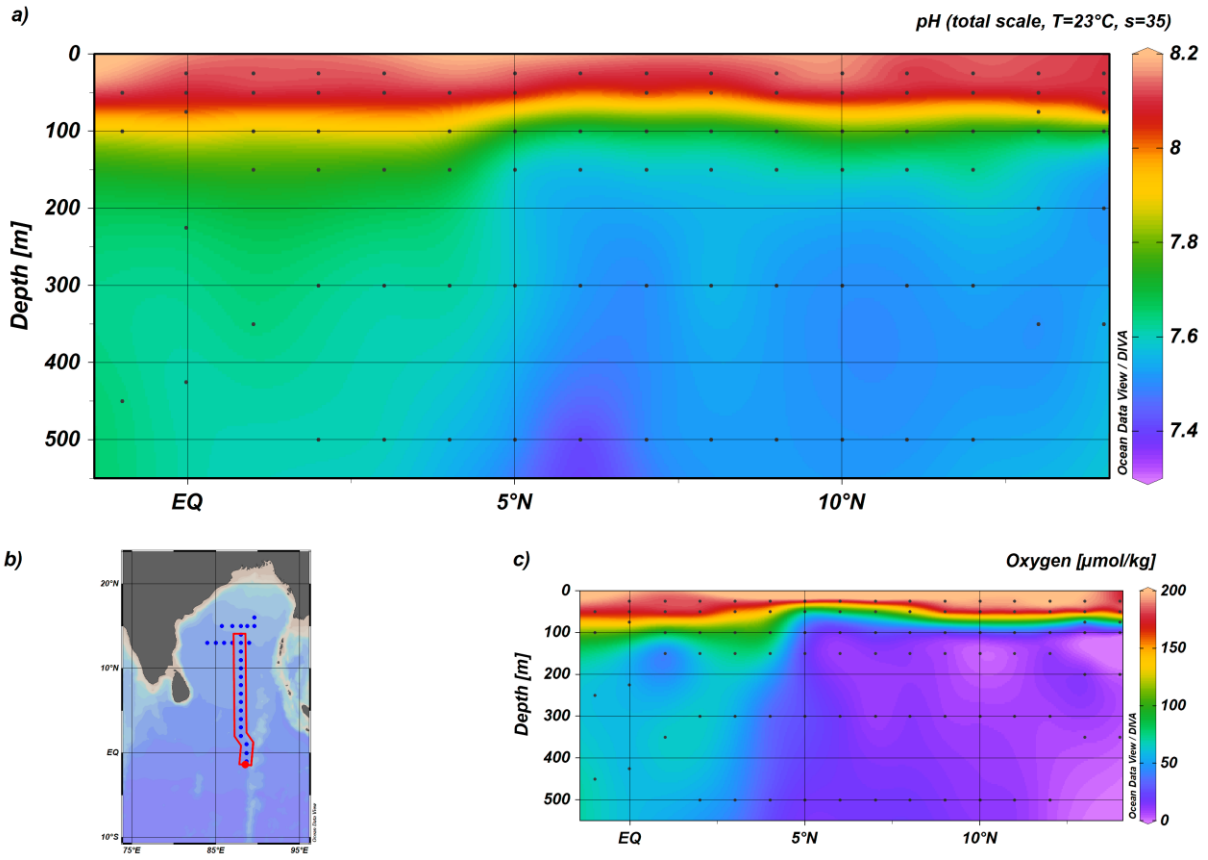

Fig. 5.12 a) Interpolated distribution of pH along a latitudinal transect (1°S, 14°N) at 88°E in the Bay of Bengal. b) Map showing positions of GoFlo deployment. c) Interpolate oxygen distribution between 1°S and 14 °N at 88°E.

5.20 Nd and REE Isotopes

(A. Conventz[1], M. Gledhill[1], A. Firus[1], E. Hathorne[1], M. Frank[1])

[1] GEOMAR

5.20.1 Introduction

The Bay of Bengal (BoB) is a critical area for studying rare earth elements (REEs) and neodymium (Nd) isotopes due to its unique geochemical and hydrological characteristics. The REE concentrations in the BoB, particularly at various depths, are among the highest in the Indian Ocean (Nozaki et al., 2002). This high concentration is primarily driven by the substantial influx of sediments and freshwater from major rivers, such as the Ganges-Brahmaputra and the Irrawaddy, which collectively contribute a significant amount of terrestrial debris and dissolved materials into the northern part of the Bay (Nozaki et al., 2002).

Nd in these waters reflects the type and age of the rocks in the drainage basins, imparting a distinct geochemical signature to the rivers and seawater through weathering processes (e.g., Goldstein and Jacobsen, 1987; Frank, 2002). The BoB has a thin, low-salinity mixed layer that persists year-round, influenced by substantial freshwater inputs (Sengupta et al., 2006). The massive Bengal and Nicobar fan, the largest submarine fan system on Earth (Curray et al., 2002), also impacts sediment distribution and REE cycling in the region (Hathorne et al., 2020).

Studies have shown elevated REE concentrations in the BoB and Andaman Sea surface waters compared to the rest of the Indian Ocean, with a distinctive REE pattern and unradiogenic Nd isotopes likely resulting from South Asian weathering inputs (Amakawa et al., 2000). These concentrations vary seasonally, correlating with monsoon-induced river discharge (Hathorne et al., 2020).

The enrichment of REEs in the BoB is not solely due to dissolved riverine inputs. The underlying fan sediments act as a sink for dissolved REEs (Nozaki et al., 2002), while the partial dissolution of detrital particles significantly contributes to the dissolved REE pool (Hathorne et al., 2020). These particles are transported by rivers and surface currents, settling through the water column and releasing REEs in the process.

Nd concentration in the BoB surface waters decreases from north to south, influenced by the mixing of radiogenic Indonesian Throughflow waters with less radiogenic BoB waters (Singh et al., 2012). The seasonal monsoon cycle further affects REE distribution, with higher concentrations in surface waters during periods of increased river discharge (Hathorne et al., 2020).

Balancing the Nd budget in the BoB suggests that additional sources, such as release from particulate phases supplied by the Ganges-Brahmaputra river system, are necessary to explain observed distributions. The substantial labile particulate pool, originating from massive river sediment fluxes, plays a crucial role in these seasonal and spatial variations in REE concentrations. Yttrium and REE data also indicate that freshwater input into the BoB can be traced using specific ratios, providing valuable geochemical tracers for monsoon-related freshwater inputs (Yu et al., 2017).

5.20.2 Sample Collection

40 near surface water samples were collected from a towed-fish (nominal depth 2.0 ± 0.5 m) that was positioned on the starboard side of the ship. Through polyethylene tubing the water was pumped into a clean tent constructed in a laboratory on the RV SONNE. In the laboratory, water was filtered (0.8/0.2 µm, AcroPak 500, Pall) into acid cleaned cubitainers (10 L volume) or acid cleaned bottles (125 mL bottles). For later Nd and REE measurements 29 filtered 10 L water samples were collected, including 5 pairs of filtered and unfiltered waters. To increase the resolution additionally 1 L filtered samples with a volume of 125 mL were taken, including one filtered-unfiltered pair, for REE analysis.

From 10 stations 28 samples were collected from GoFlo bottles from at least two depths per station up to 500 m. These 125 mL bottles are again for an increased resolution of REE measurements.

From 3 stations between 8°N and 16°N depth profiles were sampled from a CTD with 10 samples throughout the water column per station. The water was sampled into stable canisters with a volume of 10 L and taken into the clean laboratory. There the samples were filtered with a peristaltic pump over a 142 mm diameter membrane filter within a couple of hours into cubitainers. The membrane filters were folded and saved in plastic bags. Additionally, at a fourth CTD station smaller samples (125 mL) were filtered through AcroPak into small bottles.

All samples were acidified on board with 1 mL concentrated HCl per litre of sample (0.1 %). All further sample preparation for Nd and REE measurements will take place at GEOMAR in Kiel

starting in November this year, so measurements will be finished, and data finalized in late summer 2025.

It was planned to take more samples at high resolution in the northern part of the BoB until 18°N, but this was not possible due to an earlier end of the cruise because of a medical emergency.

5.20.3 List of Samples

Table 5.14 Sampling at stations (except underway towed-fish sampling between 8°N and 16°N)

Station	Longitude	Latitude	Devices
14	087° 59.962' E	07° 59.971' N	CTD/Ro
15	088° 00.042' E	09° 00.076' N	GoFlo
18	088° 00.283' E	12° 00.239' N	GoFlo
22	085° 04.503' E	12° 44.537' N	GoFlo
23	083° 59.845' E	12° 59.035' N	GoFlo
25	085° 59.889' E	13° 00.025' N	GoFlo
26	086° 59.735' E	12° 59.772' N	GoFlo
27	087° 59.852' E	12° 59.579' N	GoFlo
28	089° 00.094' E	12° 59.988' N	GoFlo
30	087° 59.121' E	13° 59.654' N	GoFlo
32	085° 43.913' E	14° 58.152' N	GoFlo
34	086° 59.932' E	15° 00.115' N	GoFlo
35	087° 59.846' E	15° 00.018' N	GoFlo
36	088° 43.412' E	14° 59.091' N	CTD/Ro
37	089° 38.855' E	15°04.352' N	CTD/Ro
38	089° 35.998' E	15° 59.999' N	CTD/Ro

5.21 Aerosols and Atmospheric Trace Gases

(A. Babu Suja[1], S. Deshmukh[1], R. Rabe[1], M. van Pinxteren[1], T. Müller[1], L. Poulain[1], S. Henning[1], M. Pohlker[1], H. Herrmann[1])

[1] TROPOS

5.21.1 Introduction

Aerosol particles are important climate drivers as they scatter and absorb solar radiation (direct aerosol effect) and impact the formation and characteristics of clouds (indirect aerosol effect) (Kanakidou et al., 2005). To better understand the diverse climatic effects of aerosol particles, a proper understanding of their sources and transformation/processing is required. However, especially in non-remote marine areas, aerosol particles over the ocean constitute a complex mixture of local marine sources and of non-marine sources with anthropogenic origin (ship emissions) and long-range transported aerosol form continents, which are again a complex mixture of biogenic and anthropogenic sources (Hawkins et al., 2010). In this context, the northern part of the Indian Ocean and in particular the Bay of Bengal (BoB) is the only place in the world where an intense source of continental anthropogenic trace species (and their reaction products) originating from the Northern Hemisphere are directly connected to the pristine air of the Southern Hemisphere by a cross-equatorial monsoonal flow into the Intertropical Convergence Zone (Crutzen and Ramanathan, 2001). Moreover, continental influence is not only driven by

anthropogenic emissions but it can also contain an important fraction of dust. Due to the large content of Iron and Phosphorus on the dust and anthropogenic aerosols, dust deposition can act as fertilizer for the marine biological activities. The strength of continental and anthropogenic emissions on the aerosol particles over the ocean in general, and over northern part of the Indian Ocean in particular, is, however, little understood and poorly-quantified, causing strong uncertainties in the estimation of the climate effect of marine aerosols (Liss and Johnson, 2014).

Despite several research activities carried out in the BoB, detailed knowledge of the atmospheric aerosol chemical composition, sources and processing, especially on the organic fraction and trace metal content of aerosol particles over this region are still very limited. Chemical investigations of aerosol particles were mainly based on offline measurements, which provide no information on the variability of aerosol chemical properties regarding their temporal and spatial resolution as well as information on their mixing state. Altogether, the results from previous campaigns showed that future studies involving a more comprehensive chemical characterization of different aerosol particle sources are essential to better understand the interaction between marine aerosols and long-range transported anthropogenic aerosols and therefore allowing for a proper assessments of Asia's pollution impact on regional and global scales (Balasubramanian et al., 2013; Guazzotti et al., 2003). A scientific understanding of how mixing state affects climate relevant aerosol properties, such as cloud condensation and ice nucleating particle concentrations and aerosol optical properties is still missing over BoB. Consequently, to better understand the sources and the impact to the ocean of the marine boundary aerosol over the BoB, a three-part work approach is deployed in order to better understand: 1) the emissions of primary and secondary aerosol from the marine surface microlayer (SML), 2) the bio-relevance of trace metal on the atmospheric aerosol and their impact on the ocean, and 3) the contribution and mixing state of the different aerosol sources (primary, secondary biogenic or anthropogenic) to the total composition and their impact on climate relevant aerosol properties.

5.21.2 Work at Sea

The atmospheric aerosol measurements were carried out from 16th April 2024 to 11th May 2024 during the expedition. This includes continuous aerosol sampling and measurement activities as well as additional sampling of the SML (sampled from the Zodiac) and sampling from the continuous underway seawater supply. For continuous measurements of physical and chemical aerosol parameters, a laboratory container (Aerosol-Container) equipped with instrumentation was placed on the ninth deck of the ship. Continuous Aerosol-Container measurements include particle number size distributions from 2 nm to 10 µm using a combination of NAIS, SMPS (Scanning Mobility Particle Sizer) and APS (Aerodynamic Particle Sizer), Optical properties, such as absorption and scattering coefficients, were continuously measured by MAAP (Multiangle Absorption Photometer), Aethalometer (AE33), and Nephelometer (Table 5.15). The near real-time measurements of the mixing state and size distribution of airborne BC (black carbon)-containing particles were carried out using the Single Particle Soot Photometer (SP2). Further to understand the CCN (cloud condensation nuclei) characteristics, a CCN counter was operated during the cruise. CCN was operational only up to 29th of April. In addition, a standalone CPC was measuring the total aerosol number concentration in 2s time resolution. Together with this, a high-volume filter sampler (PM10) and a Berner impactor (size segregated sampling) was installed

on the roof of the container to collect aerosol particles at a sampling regime of 24 hours during the cruise to provide information on the total particle mass concentration and the chemical composition of the aerosol particles (organic and elemental carbon, OC/EC, water-soluble ions, trace metals etc.). A total of ~26 days of filter sampling were carried out during the expedition. During this period, 36 PM10 samples and 24 size segregated sampling was carried out. Together with this several field blanks were also collected to understand the background handling contaminations. A halfback sampler was used to collect the aerosols in the nucleopore filters for the INP (ice nucleating particle) analysis to provide general coverage of INP concentrations throughout the whole cruise. 43 samples were collected during the cruise for the offline INP analysis. Sea water samples were taken regularly throughout the cruise from the onboard underwater pipeline for the analysis of black carbon and INP in the ocean water. All filters and water samples were stored frozen at -20 degrees on the ship for offline analysis at TROPOS after the expedition. Further, an O_3, NO_X, SO_2 analysers were also operated during the cruise to have the concentrations of these gases. Table 5.15 gives an overview of the instrumentation/measurements during the SO305 BIOCAT-IIOE2 campaign.

Table 5.15 Overview of the aerosol instrumentation and parameters measured during the SO305 campaign.

Instrumentation	Purpose/derived parameters
Digitel DHS-80 with PM10 inlet	Sampling aerosol particles smaller 10 µm
Five stage Berner impactor	Size segregated sampling of aerosol particles with upper cut-off diameters of 0.05, 0.14, 0.42, 1.2, 3.5 and 10 µm
Particle sampler (Halfbac)	Sampling aerosol particles for the measurements of INP concentration
HR-SP-AMS	Non-refractory aerosol chemical composition (organics, nitrate, sulphate, ammonium, chloride) and soot
NAIS/MPSS/APS	Particle number size distribution (PNSD) from 2 nm to 10 µm.
SP2	Refractory black carbon concentration (rBC), rBC mass size distribution, coating thickness on rBC cores.
MAAP	Light absorption coefficient at wavelength 635 nm.
Aethalometer	Light absorption coefficients at wavelengths 350, 450, 590, 660, 880, and 960 nm.
Nephelometer	Light scattering coefficients at wavelength 450, 525 and 635 nm.
CCN counter	CCN concentration
Gas sensors	Ozone, NO_X, SO_2

A highly advanced high-resolution soot particle aerosol mass spectrometer (HR-SP-AMS) that is a combination of a high-resolution AMS and a single-particle soot photometer (SP2) laser (Onasch et al., 2012; Avery et al., 2020) was deployed during the cruise to study the quantitative chemical information of near PM1 size and mass concentration. This will represent important information to properly apportion the different aerosol particle sources and their physical properties. The HR-SP-AMS is equipped with an intracavity Nd:YAG laser (1064 nm), allowing aerosol particle vaporization of black carbon together with metal (Onasch et al., 2012) together with the determination of the aerosol chemical composition, including total organic matter nitrate, sulphate, ammonium and chloride. With such an instrument, it is possible to perform source apportionment analysis not only on the organic aerosol fraction but also on the refractory black carbon (Bibi et al., 2021; Farley et al., 2022), which will strongly help us to better understand the sources of

aerosol over the Bay of Bengal. From the organic matter, MSA mass concentration will be extracted from the AMS data following the method developed by Huang et al. (2018). Source apportionment Advance receptor models will be performed on the dataset by Positive Matrix Factorization (PMF) later. The PMF is a factor analytical method to decompose a matrix of observation (chemical species identified on the filter samples or mass spectra from the AMS) into a set of factor profiles defined by a specific fingerprint and factor contribution (i.e. source contribution to the observed explanatory variable, like total PM mass for the filter samples or organic mass for the AMS). For this purpose, the advanced multilinear engine (Paatero, 1999) approach associated with the source finder program SoFi (Canonaco et al., 2013) will be used. Since our measurements constitutes online and offline aerosol chemical composition, we will take advantage of both the high time resolution provided by the AMS and the comprehensive chemical composition of the offline on a combined source apportionment analysis (Srivastava et al., 2019). Compared to classical source apportionment analysis based on the AMS data, combining online and offline measurements on the same analysis will allow providing chemical information on the AMS PMF factor, which was missing up to now. Parallel to this chemical source apportionment analysis, the PMF approach will also be applied to the MPSS dataset (Ogulei et al., 2007), providing a size-resolved factor.

The originality of our approach is that we applied a broad combination of online and offline aerosol measurements and detailed chemical characterisations associated to seawater and SML chemical studies. Our study will deliver a unique aerosol data set and finally contribute to an advanced understanding of ocean-atmosphere interactions in general and the role of aerosol particles over the BoB in particular. The expected results will be extremely valuable for better modelling particle transport over BoB and the oceans and then improve our prediction on their climate effects.

5.21.3 Preliminary Results

Figure 5.13 shows the aerosol particle size distribution measured with SMPS during SO305 BIOCAT IIOE2. We observed the lowest particle concentration during the initial phase of the cruise. These periods were mostly influenced by the precipitation. The aerosol particle size distribution showed bi-modal size distribution with first mode in the Aitken mode (~50 nm) and the second mode in the accumulation mode region (~ 200 nm) during the cruise. Most of the period during the cruise, the accumulation mode was present with higher number concentrations. The total aerosol number shows some periods with very high concentrations. These episodes indicate extra aerosol particles emitted from the exhaust of the research vessel, blown in the direction of the Inlet. These periods will be carefully checked and marked in the final data.

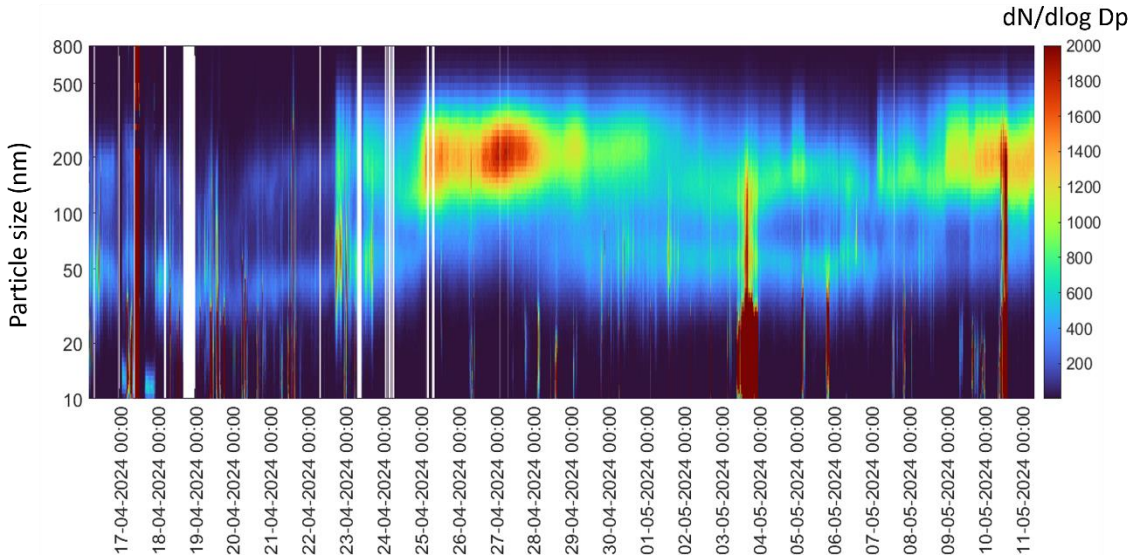

Fig. 5.13 Aerosol particle size distribution measured during the cruise.

Figure 5.14 shows the mass concentrations of different chemical species measured using SP-AMS during the cruise period as well as the daily average concentration of sulphate and ammonium. The sulphate concentration increases as the cruise approaches to the northern most stations. The increased pollutant concentrations mostly refer to transported airmass either from the lands or the sea spray, depending on the wind direction and speed. DMS and sea spray are the main sources of sulphate over the ocean surface.

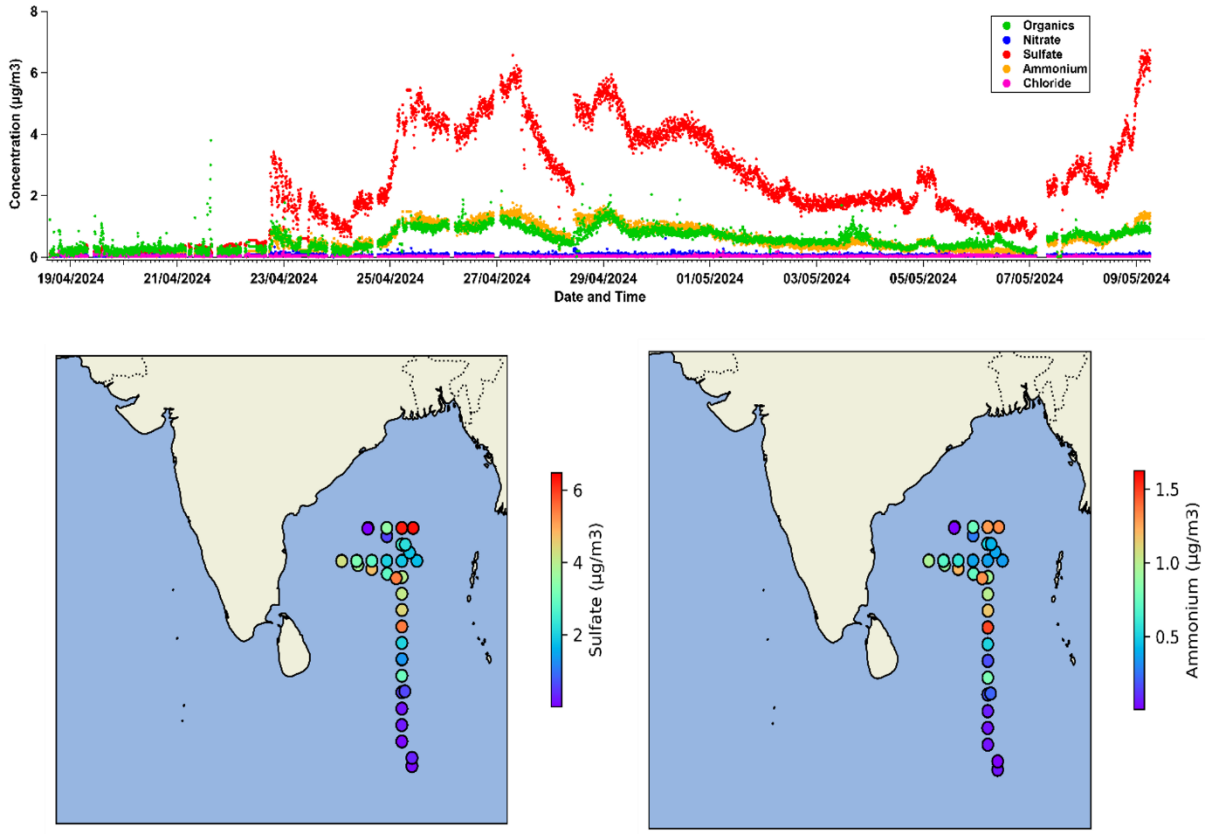

Fig. 5.14 a) Mass concentrations of different chemical species measured during the cruise period, (b-c) shows the daily average concentration of sulphate and ammonium.

6 Station List SO305

6.1 Overall Station List

Station	Device	Date & Time, UTC	Latitude	Longitude	Depth, m
SO305_0_Underway-4	VMADCP_75kHz	2024/04/15 02:30:00	03° 02,115' N	082° 58,218' E	0.0
SO305_0_Underway-5	PS	2024/04/15 02:30:00	03° 02,115' N	082° 58,218' E	0.0
SO305_0_Underway-3	VMADCP_38kHz	2024/04/15 02:30:00	03° 02,115' N	082° 58,218' E	0.0
SO305_0_Underway-6	FBOX	2024/04/15 02:30:00	03° 02,115' N	082° 58,218' E	0.0
SO305_0_Underway-2	EM122	2024/04/15 02:30:00	03° 02,115' N	082° 58,218' E	0.0
SO305_1-1	CTD	2024/04/16 02:59:39	00° 25,947' N	086° 13,861' E	4495.3
SO305_1-2	TMF	2024/04/16 06:28:07	00° 25,946' N	086° 13,890' E	4494.6
SO305_2-1	CTD	2024/04/17 04:22:43	00° 59,971' S	088° 40,211' E	4311.8
SO305_2-2	MSS	2024/04/17 08:26:25	00° 59,992' S	088° 40,211' E	4334.9
SO305_2-3	CTD	2024/04/17 09:25:18	00° 59,932' S	088° 40,217' E	4308.8
SO305_2-5	WS	2024/04/17 11:10:02	00° 59,933' S	088° 40,214' E	4307.8
SO305_2-6	CTD	2024/04/17 13:47:13	00° 59,935' S	088° 40,209' E	4307.2
SO305_3-1	CTD	2024/04/17 18:43:35	00° 30,001' S	088° 40,195' E	4486.8
SO305_4-1	CTD	2024/04/18 00:51:03	00° 01,531' S	088° 40,214' E	4515.8
SO305_4-2	CTD	2024/04/18 04:47:25	00° 01,543' S	088° 40,184' E	4517.7
SO305_4-3	CTD	2024/04/18 05:47:15	00° 01,537' S	088° 40,193' E	4516.5
SO305_4-4	MOOR	2024/04/18 07:22:57	00° 01,458' S	088° 39,926' E	4521.5
SO305_4-5	WS	2024/04/18 15:00:44	00° 00,463' S	088° 39,997' E	4518.4
SO305_4-6	TMF	2024/04/18 16:20:59	00° 00,445' S	088° 40,154' E	4517.9
SO305_5-1	CTD	2024/04/18 19:53:03	00° 29,996' N	088° 40,210' E	4835.7
SO305_5-2	MSS	2024/04/18 23:16:41	00° 30,030' N	088° 40,193' E	4479.4
SO305_6-1	CTD	2024/04/19 04:22:10	01° 00,066' N	088° 40,313' E	4384.7
SO305_6-2	MSS	2024/04/19 07:22:48	01° 00,075' N	088° 40,326' E	4382.0
SO305_6-3	CTD	2024/04/19 08:18:58	00° 59,877' N	088° 39,737' E	4380.6
SO305_6-4	CTD	2024/04/19 09:33:41	00° 59,875' N	088° 39,736' E	4381.2
SO305_6-5	WS	2024/04/19 10:49:07	00° 59,869' N	088° 39,742' E	4380.5
SO305_7-1	CTD	2024/04/19 19:22:07	02° 00,004' N	088° 00,004' E	4281.7
SO305_7-2	MSS	2024/04/19 22:24:02	02° 00,002' N	088° 00,006' E	4279.7
SO305_7-3	WS	2024/04/19 23:17:29	02° 00,025' N	087° 59,891' E	4282.2
SO305_8-1	CTD	2024/04/20 06:45:48	02° 59,998' N	088° 00,002' E	4221.3
SO305_8-2	MSS	2024/04/20 09:46:09	02° 59,999' N	087° 59,998' E	4223.1
SO305_8-3	CTD	2024/04/20 10:34:57	02° 59,782' N	087° 59,736' E	4222.0
SO305_8-4	WS	2024/04/20 11:50:01	02° 59,780' N	087° 59,737' E	4222.8
SO305_9-1	CTD	2024/04/20 19:14:54	03° 59,998' N	088° 00,003' E	4008.8
SO305_9-2	MSS	2024/04/20 22:03:17	03° 59,994' N	087° 59,994' E	4010.7
SO305_9-3	WS	2024/04/20 22:51:14	03° 59,926' N	087° 59,921' E	4007.9
SO305_10-1	CTD	2024/04/21 06:21:51	04° 59,977' N	088° 00,159' E	3976.5
SO305_10-2	DF	2024/04/21 06:43:46	04° 59,974' N	088° 00,157' E	3976.3
SO305_10-3	CTD	2024/04/21 08:45:42	04° 59,996' N	087° 59,998' E	3976.5
SO305_10-4	MSS	2024/04/21 11:32:27	05° 00,000' N	087° 59,999' E	3979.4
SO305_10-5	CTD	2024/04/21 12:35:49	04° 59,996' N	087° 59,914' E	3977.9
SO305_10-6	CTD	2024/04/21 13:54:40	04° 59,987' N	087° 59,915' E	3975.9

SO305_10-7	WS	2024/04/21 16:01:19	04° 59,990' N	087° 59,921' E	3976.5
SO305_10-8	CTD	2024/04/21 18:35:47	04° 59,985' N	087° 59,918' E	3977.2
SO305_10-9	MSS	2024/04/21 19:46:12	04° 59,995' N	087° 59,919' E	3978.3
SO305_10-10	BOAT	2024/04/22 00:26:36	04° 59,997' N	087° 59,911' E	3976.6
SO305_10-11	MSS	2024/04/22 01:37:45	05° 00,271' N	088° 00,130' E	3977.7
SO305_10-12	CTD	2024/04/22 03:01:29	04° 59,927' N	087° 59,779' E	3979.4
SO305_10-13	CTD	2024/04/22 04:31:47	04° 59,926' N	087° 59,774' E	3976.4
SO305_10-14	PUMP	2024/04/22 05:41:25	04° 59,807' N	087° 59,990' E	3976.7
SO305_10-15	MSS	2024/04/22 08:46:06	04° 59,803' N	087° 59,992' E	3977.9
SO305_10-16	CTD	2024/04/22 09:40:38	04° 59,804' N	087° 59,992' E	3978.1
SO305_10-17	FLOAT	2024/04/22 10:49:18	04° 59,804' N	087° 59,995' E	3976.4
SO305_10-18	TMF	2024/04/22 11:01:53	05° 00,184' N	087° 59,835' E	3976.8
SO305_0_Underway-8	uCTD	2024/04/22 12:43:54	05° 14,277' N	087° 59,995' E	3958.9
SO305_11-2	CTD	2024/04/22 18:28:59	05° 59,990' N	088° 00,002' E	3898.3
SO305_11-3	MSS	2024/04/22 21:18:55	05° 59,995' N	087° 59,998' E	3899.3
SO305_11-4	CTD	2024/04/22 22:13:57	05° 59,987' N	088° 00,007' E	3902.4
SO305_11-5	WS	2024/04/22 23:18:42	05° 59,989' N	088° 00,002' E	3898.2
SO305_12-1	DF	2024/04/23 07:11:07	05° 02,717' N	088° 11,104' E	3965.3
SO305_12-2	CTD	2024/04/23 09:30:37	05° 03,350' N	088° 11,803' E	3967.9
SO305_12-3	TMF	2024/04/23 10:22:33	05° 04,287' N	088° 11,712' E	3965.5
SO305_0_Underway-9	uCTD	2024/04/23 11:00:24	05° 07,777' N	088° 11,347' E	3960.0
SO305_13-1	CTD	2024/04/24 01:02:36	07° 00,031' N	087° 59,973' E	3761.9
SO305_13-2	MSS	2024/04/24 01:55:02	07° 00,031' N	087° 59,978' E	3769.2
SO305_13-3	CTD	2024/04/24 02:49:04	07° 00,605' N	088° 00,398' E	3770.1
SO305_13-4	CTD	2024/04/24 06:19:20	07° 00,602' N	088° 00,400' E	3788.7
SO305_13-5	WS	2024/04/24 07:39:34	07° 00,606' N	088° 00,398' E	3775.2
SO305_14-1	CTD	2024/04/24 15:14:50	07° 59,972' N	087° 59,959' E	3658.4
SO305_14-2	MSS	2024/04/24 17:57:09	07° 59,965' N	087° 59,963' E	3657.3
SO305_14-3	CTD	2024/04/24 18:59:05	07° 59,964' N	087° 59,960' E	3656.6
SO305_14-4	WS	2024/04/24 20:18:18	07° 59,971' N	087° 59,958' E	3657.9
SO305_15-1	CTD	2024/04/25 03:36:19	09° 00,075' N	088° 00,043' E	3531.6
SO305_15-2	MSS	2024/04/25 06:23:28	09° 00,072' N	088° 00,048' E	3535.2
SO305_15-3	CTD	2024/04/25 07:27:00	09° 00,077' N	088° 00,043' E	3538.0
SO305_15-4	CTD	2024/04/25 08:49:27	09° 00,075' N	088° 00,047' E	3534.9
SO305_15-5	WS	2024/04/25 10:00:40	09° 00,075' N	088° 00,038' E	3532.3
SO305_16-1	CTD	2024/04/25 17:16:03	10° 00,077' N	088° 00,040' E	3423.3
SO305_16-2	MSS	2024/04/25 19:49:15	10° 00,102' N	088° 00,060' E	3421.5
SO305_16-3	CTD	2024/04/25 20:39:54	10° 00,536' N	088° 00,534' E	3423.5
SO305_16-4	WS	2024/04/25 21:32:37	10° 00,537' N	088° 00,534' E	3422.1
SO305_17-1	MSS	2024/04/26 04:44:37	10° 59,957' N	088° 00,033' E	3332.0
SO305_17-2	CTD	2024/04/26 05:31:02	10° 59,439' N	088° 00,034' E	3335.6
SO305_17-3	WS	2024/04/26 09:27:10	10° 59,477' N	088° 00,046' E	3330.7
SO305_18-1	DF	2024/04/26 16:18:51	11° 58,949' N	087° 59,991' E	3229.7
SO305_18-2	CTD	2024/04/26 18:49:36	11° 59,983' N	087° 59,983' E	3226.7
SO305_18-3	MSS	2024/04/26 21:11:47	11° 59,984' N	087° 59,991' E	3226.4
SO305_18-4	CTD	2024/04/26 21:55:29	12° 00,241' N	088° 00,283' E	3227.5
SO305_18-5	WS	2024/04/26 23:18:52	12° 00,241' N	088° 00,285' E	3224.4

SO305_18-6	BOAT	2024/04/27 00:32:23	12° 00,146' N	087° 59,934' E	3224.3
SO305_18-7	PUMP	2024/04/27 02:50:10	12° 00,144' N	087° 59,939' E	3226.2
SO305_18-8	CTD	2024/04/27 06:32:29	12° 00,143' N	087° 59,937' E	3224.0
SO305_18-9	CTD	2024/04/27 07:40:33	12° 00,139' N	087° 59,933' E	3224.3
SO305_18-10	MSS	2024/04/27 08:51:35	12° 00,188' N	087° 59,977' E	3227.2
SO305_18-11	CTD	2024/04/27 09:43:49	12° 00,501' N	088° 00,220' E	3224.1
SO305_18-12	CTD	2024/04/27 11:49:11	12° 00,501' N	088° 00,210' E	3223.9
SO305_18-13	CTD	2024/04/27 13:00:47	12° 00,502' N	088° 00,215' E	3224.0
SO305_18-14	MSS	2024/04/27 14:04:10	12° 00,558' N	088° 00,190' E	3223.8
SO305_18-15	CTD	2024/04/27 15:13:37	12° 00,838' N	088° 01,101' E	3192.6
SO305_18-16	CTD	2024/04/27 16:35:49	12° 00,834' N	088° 01,100' E	3225.5
SO305_18-17	MSS	2024/04/27 17:47:36	12° 00,836' N	088° 01,106' E	3221.4
SO305_18-18	FLOAT	2024/04/27 18:40:24	12° 00,919' N	088° 01,502' E	3224.2
SO305_18-19	TMF	2024/04/27 18:42:45	12° 00,933' N	088° 01,531' E	3223.6
SO305_19-1	CTD	2024/04/28 00:55:16	12° 12,330' N	087° 01,567' E	3234.5
SO305_19-2	MSS	2024/04/28 03:28:31	12° 12,322' N	087° 01,556' E	3232.6
SO305_20-1	CTD	2024/04/28 10:28:32	12° 30,009' N	085° 59,988' E	3249.3
SO305_20-2	MSS	2024/04/28 12:49:32	12° 30,008' N	085° 59,990' E	3249.0
SO305_20-3	CTD	2024/04/28 13:40:34	12° 30,153' N	085° 59,579' E	3248.8
SO305_20-4	CTD	2024/04/28 14:54:37	12° 30,154' N	085° 59,583' E	3248.8
SO305_21-1	DF	2024/04/29 01:10:28	11° 56,823' N	087° 37,324' E	3227.7
SO305_21-2	CTD	2024/04/29 03:05:40	11° 56,730' N	087° 37,442' E	3228.2
SO305_21-3	TMF	2024/04/29 04:01:36	11° 56,728' N	087° 37,441' E	3227.6
SO305_22-1	CTD	2024/04/29 19:43:07	12° 44,521' N	085° 04,508' E	3255.9
SO305_22-2	MSS	2024/04/29 22:11:32	12° 44,535' N	085° 04,503' E	3255.3
SO305_22-3	WS	2024/04/29 23:18:50	12° 44,535' N	085° 04,502' E	3255.9
SO305_23-1	CTD	2024/04/30 07:09:03	13° 00,016' N	084° 00,010' E	3304.8
SO305_23-2	MSS	2024/04/30 09:50:52	12° 59,999' N	084° 00,003' E	3304.1
SO305_23-3	CTD	2024/04/30 10:53:09	12° 59,037' N	083° 59,847' E	3308.3
SO305_23-4	CTD	2024/04/30 12:24:00	12° 59,031' N	083° 59,841' E	3306.5
SO305_23-5	CTD	2024/04/30 13:24:37	12° 59,036' N	083° 59,848' E	3306.8
SO305_23-6	WS	2024/04/30 14:25:52	12° 59,035' N	083° 59,845' E	3307.7
SO305_24-1	CTD	2024/04/30 21:45:42	13° 00,097' N	085° 00,062' E	3238.6
SO305_24-2	MSS	2024/05/01 00:16:53	13° 00,088' N	085° 00,058' E	3238.9
SO305_24-3	CTD	2024/05/01 01:13:24	12° 59,461' N	084° 59,479' E	3238.7
SO305_24-4	CTD	2024/05/01 02:25:07	12° 59,459' N	084° 59,478' E	3240.5
SO305_25-1	CTD	2024/05/01 09:07:44	13° 00,077' N	086° 00,015' E	3199.4
SO305_25-2	MSS	2024/05/01 11:27:23	13° 00,072' N	086° 00,012' E	3200.0
SO305_25-3	CTD	2024/05/01 12:20:51	13° 00,025' N	085° 59,890' E	3199.4
SO305_25-4	CTD	2024/05/01 13:41:53	13° 00,019' N	085° 59,886' E	3198.0
SO305_25-5	WS	2024/05/01 14:30:43	13° 00,025' N	085° 59,889' E	3199.3
SO305_26-1	CTD	2024/05/01 21:38:48	13° 00,097' N	087° 00,002' E	3141.4
SO305_26-2	MSS	2024/05/02 00:05:07	13° 00,094' N	086° 59,996' E	3138.6
SO305_26-3	CTD	2024/05/02 01:04:37	12° 59,776' N	086° 59,729' E	3140.2
SO305_26-4	CTD	2024/05/02 02:08:49	12° 59,775' N	086° 59,738' E	3140.7
SO305_26-5	WS	2024/05/02 03:33:10	12° 59,775' N	086° 59,733' E	3138.3
SO305_27-1	CTD	2024/05/02 10:31:51	13° 00,006' N	088° 00,056' E	3083.6

SO305_27-2	CTD	2024/05/02 10:59:11	12° 59,996' N	088° 00,059' E	3084.5
SO305_27-3	MSS	2024/05/02 13:10:11	12° 59,997' N	088° 00,051' E	3081.0
SO305_27-4	CTD	2024/05/02 14:11:28	12° 59,586' N	087° 59,853' E	3085.7
SO305_27-5	CTD	2024/05/02 15:38:19	12° 59,579' N	087° 59,857' E	3084.2
SO305_27-6	WS	2024/05/02 16:26:01	12° 59,578' N	087° 59,851' E	3083.3
SO305_28-1	CTD	2024/05/02 23:22:09	12° 59,984' N	089° 00,097' E	3041.8
SO305_28-2	CTD	2024/05/03 02:06:34	12° 59,994' N	089° 00,095' E	3040.5
SO305_28-3	WS	2024/05/03 03:23:06	12° 59,989' N	089° 00,094' E	3044.1
SO305_29-1	CTD	2024/05/03 08:44:57	13° 30,657' N	088° 30,724' E	3022.7
SO305_29-2	MSS	2024/05/03 10:59:02	13° 30,657' N	088° 30,711' E	3017.8
SO305_30-1	CTD	2024/05/04 03:01:52	14° 00,000' N	087° 59,998' E	2972.1
SO305_30-2	CTD	2024/05/04 04:21:02	13° 59,998' N	088° 00,001' E	2971.5
SO305_30-3	CTD	2024/05/04 05:42:56	13° 59,999' N	087° 59,999' E	2970.0
SO305_30-4	CTD	2024/05/04 07:35:20	13° 59,998' N	088° 00,003' E	2970.2
SO305_30-5	CTD	2024/05/04 10:00:22	13° 59,996' N	088° 00,004' E	2970.4
SO305_30-6	DF	2024/05/04 12:00:11	14° 00,006' N	088° 00,000' E	2970.3
SO305_30-7	PUMP	2024/05/04 14:14:24	13° 59,650' N	087° 59,123' E	2972.3
SO305_30-8	CTD	2024/05/04 17:21:53	13° 59,655' N	087° 59,124' E	2969.5
SO305_30-9	CTD	2024/05/04 19:13:02	13° 59,643' N	087° 59,125' E	2969.7
SO305_30-10	CTD	2024/05/04 21:59:24	13° 59,646' N	087° 59,124' E	2970.1
SO305_30-11	MSS	2024/05/04 23:11:55	13° 59,649' N	087° 59,123' E	2969.9
SO305_30-12	CTD	2024/05/05 00:03:47	13° 59,653' N	087° 59,119' E	2970.6
SO305_30-13	BOAT	2024/05/05 00:59:47	13° 59,650' N	087° 59,124' E	2972.0
SO305_30-14	WS	2024/05/05 02:37:06	13° 59,643' N	087° 59,122' E	2972.2
SO305_30-15	TMF	2024/05/05 03:31:48	13° 59,643' N	087° 59,122' E	2972.2
SO305_31-1	CTD	2024/05/05 10:21:20	14° 29,934' N	087° 00,037' E	2981.3
SO305_31-2	MSS	2024/05/05 12:42:14	14° 29,942' N	087° 00,023' E	2979.5
SO305_32-1	CTD	2024/05/05 21:31:03	15° 00,025' N	085° 45,032' E	2940.8
SO305_32-2	CTD	2024/05/05 23:11:47	14° 59,996' N	085° 45,007' E	2851.3
SO305_32-3	MSS	2024/05/06 00:01:32	15° 00,001' N	085° 44,999' E	2941.2
SO305_32-4	CTD	2024/05/06 02:24:29	14° 59,439' N	085° 44,731' E	2934.3
SO305_32-5	CTD	2024/05/06 05:31:11	14° 59,434' N	085° 44,738' E	2932.0
SO305_32-6	MSS	2024/05/06 06:33:14	14° 59,405' N	085° 44,726' E	2931.2
SO305_32-7	PUMP	2024/05/06 07:25:24	14° 58,652' N	085° 44,285' E	2936.4
SO305_32-8	CTD	2024/05/06 11:14:13	14° 58,645' N	085° 44,290' E	2938.4
SO305_32-9	MSS	2024/05/06 12:26:27	14° 58,650' N	085° 44,283' E	2937.8
SO305_32-10	CTD	2024/05/06 13:21:49	14° 58,147' N	085° 43,919' E	2937.5
SO305_32-11	CTD	2024/05/06 14:44:43	14° 58,151' N	085° 43,920' E	2938.9
SO305_32-12	WS	2024/05/06 15:41:06	14° 58,153' N	085° 43,916' E	2937.0
SO305_32-13	CTD	2024/05/06 16:53:29	14° 58,143' N	085° 43,919' E	2935.7
SO305_32-14	MSS	2024/05/06 18:17:24	14° 58,142' N	085° 43,923' E	2934.9
SO305_32-15	CTD	2024/05/06 19:07:53	14° 57,712' N	085° 43,606' E	2934.6
SO305_33-1	DF	2024/05/07 10:48:55	13° 59,145' N	088° 12,752' E	2970.1
SO305_33-2	CTD	2024/05/07 12:51:34	13° 59,279' N	088° 13,754' E	2975.0
SO305_33-3	TMF	2024/05/07 13:35:29	13° 59,215' N	088° 13,644' E	2973.1
SO305_34-1	CTD	2024/05/08 05:41:57	15° 00,020' N	086° 59,958' E	2888.5
SO305_34-2	MSS	2024/05/08 08:13:47	15° 00,025' N	086° 59,954' E	2901.0

SO305_34-3	CTD	2024/05/08 09:07:21	15° 00,120' N	086° 59,932' E	2894.5
SO305_34-4	WS	2024/05/08 10:14:24	15° 00,118' N	086° 59,932' E	2887.4
SO305_35-1	CTD	2024/05/08 16:53:05	15° 00,019' N	087° 59,852' E	2834.3
SO305_35-2	CTD	2024/05/08 18:10:15	15° 00,017' N	087° 59,850' E	2832.9
SO305_35-3	MSS	2024/05/08 20:22:14	15° 00,013' N	087° 59,851' E	2834.9
SO305_35-4	CTD	2024/05/08 21:12:06	15° 00,025' N	087° 59,850' E	2834.4
SO305_35-5	WS	2024/05/08 22:06:25	15° 00,022' N	087° 59,848' E	2832.0
SO305_36-1	CTD	2024/05/09 03:28:32	14° 59,985' N	088° 44,749' E	2844.7
SO305_36-2	MSS	2024/05/09 06:21:39	14° 59,954' N	088° 44,758' E	2843.9
SO305_36-3	CTD	2024/05/09 07:21:44	14° 59,862' N	088° 44,543' E	2847.8
SO305_36-4	CTD	2024/05/09 08:49:26	14° 59,090' N	088° 43,406' E	2841.9
SO305_36-5	WS	2024/05/09 09:58:47	14° 59,093' N	088° 43,405' E	2841.2
SO305_37-1	CTD	2024/05/09 15:56:25	15° 00,016' N	089° 36,018' E	2713.9
SO305_37-2	MSS	2024/05/09 18:03:54	15° 00,016' N	089° 36,022' E	2718.5
SO305_37-3	CTD	2024/05/09 18:55:02	15° 00,145' N	089° 36,139' E	2712.8
SO305_37-4	CTD	2024/05/09 21:27:36	15° 00,142' N	089° 36,135' E	2710.4
SO305_37-5	MSS	2024/05/09 22:46:15	15° 00,142' N	089° 36,133' E	2712.9
SO305_37-6	BOAT	2024/05/09 23:58:09	15° 00,148' N	089° 36,130' E	2713.8
SO305_37-7	PUMP	2024/05/10 02:28:08	15° 00,142' N	089° 36,144' E	2714.6
SO305_37-8	CTD	2024/05/10 06:01:49	15° 02,129' N	089° 37,896' E	2704.8
SO305_37-9	MSS	2024/05/10 07:22:55	15° 02,255' N	089° 37,946' E	2722.7
SO305_37-10	CTD	2024/05/10 08:29:05	15° 04,356' N	089° 38,853' E	2724.6
SO305_37-11	CTD	2024/05/10 10:31:53	15° 04,344' N	089° 38,859' E	2747.4
SO305_37-12	CTD	2024/05/10 11:31:20	15° 04,353' N	089° 38,852' E	2722.4
SO305_37-13	CTD	2024/05/10 13:10:34	15° 04,352' N	089° 38,855' E	2722.8
SO305_37-14	WS	2024/05/10 14:14:18	15° 04,354' N	089° 38,860' E	2723.0
SO305_38-1	WS	2024/05/10 19:57:17	16° 00,018' N	089° 35,980' E	2561.5
SO305_38-2	CTD	2024/05/10 21:02:07	15° 59,998' N	089° 36,004' E	2591.0
SO305_38-3	MSS	2024/05/10 23:10:31	15° 59,999' N	089° 35,998' E	2577.4
SO305_38-4	CTD	2024/05/11 00:08:28	15° 59,998' N	089° 35,999' E	2574.8
SO305_38-5	CTD	2024/05/11 01:12:54	16° 00,001' N	089° 35,993' E	2556.1
SO305_38-6	CTD	2024/05/11 02:20:24	15° 59,998' N	089° 36,000' E	2561.3
SO305_38-7	CTD	2024/05/11 03:20:32	16° 00,008' N	089° 36,006' E	2560.3

Abbreviations:
VMADCP_38kHz: Vessel-mounted ADCP 38 kHz
VMADCP_75kHz: Vessel-mounted ADCP 75 kHz
PS: Sub bottom profiler
FBOX: FerryBox
EM122: Multi Beam Echo Sounder EM122
CTD: CTD/Rosette with 22 Bottles
TMF: Towed-fish
MSS: Microstruture probe
WS: GoFlo bottles
MOOR: Mooring
DF: Drifting particle (sediment) traps
BOAT: Zodiac
PUMP: Submersible pump
FLOAT: Argo float

7 Data and Sample Storage and Availability

The GEOMAR data management group operates the "Ocean Science Information System" (OSIS) as a central information and research data exchange program for marine research projects of GEOMAR and Kiel University. It is publicly accessible and can be used by all cruise participants, including national and international collaborators. OSIS brings together information about expeditions, experiments and numerical models with peer-reviewed publications and available research data. The view of all information in OSIS is publicly accessible, while access to current data in ongoing research projects can be restricted for a definable period of time (moratorium). Alternatively, the submission status of the datasets, including the responsible researcher as contact person, is visible to the public and can promote collaboration with interested researchers. Two GEOMAR data managers are PANGAEA data curators and can advise cruise participants on the preparation of data publication in a "World Data Centre" (e.g. PANGAEA), which then ensures long-term archiving and access to the research data. This data publication process will be based on the files available in OSIS and will therefore be transparent for all reviewers and other researchers. In collaboration with PANGAEA and the "Union for the Application of International Geosample Numbers" (IGSN), the data and samples are made globally traceable, thereby increasing their scientific value and usability. Links to data publishers or PIs provide contact information for external scientists. Seismic, bathymetric and/or hydroacoustic, video and raw image data as well as processed seismic data are archived in GEOMAR's IT storage infrastructure. The processed data will be made publicly available as published data in PANGAEA with the consent of the researcher. Metadata, including contact and access information are provided by OSIS.

The chief scientist and all PIs involved in SO305 BIOCAT-IIOE2 will adhere to the schedule below, which regulates the availability of all information and research data. After SO305 BIOCAT-IIOE2, the GEOMAR data management group will support and guide the researchers in the data sharing and publication process.

- Availability of metadata in OSIS (https://portal.geomar.de/osis):
  2 weeks after completion of the cruise and the associated experiments
- Availability of data in OSIS (https://portal.geomar.de/osis):
  12 months after completion of the cruise and associated experiments
- Availability of data in a WDC/PANGAEA (http://www.pangaea.de or as a compilation at http://www.pangaea.de/search?q=campaign:CRUISENAME):
  2 years after completion of the cruise and associated experiments.

Table 8.1 Definition of Data Responsibility for SO305 BIOCAT-IIOE2.

Data	PI, Affiliation, Email address
O_2, nutrients, trace gases: N_2O, CH_4, NO (underway, depth profiles)	H. Bange, GEOMAR, hbange@geomar.de
CTD, O_2 sensor, microstructure, ADCP, UVP	R. Czeschel, GEOMAR, rczeschel@geomar.de R. Kiko, GEOMAR, rkiko@geomar.de
N cycle processes: N isotopes	B. Gaye, U Hamburg, birgit.gaye@uni-hamburg.de
Organic material: DOM, POM etc.	A. Engel, GEOMAR, aengel@geomar.de
N cycle processes: rates, microbiology, metagenomics, O_2 sensor (MicroTail)	C. Löscher, SDU, DK, cloescher@biology.sdu.dk
Trace elements	M. Gledhill, GEOMAR, mgledhill@geomar.de
Atmospheric measurements: aerosols, trace gases (O_3, SO_2, NO_x)	M. van Pinxteren, TROPOS, Leipzig, manuela@tropos.de
Trace gases: dissolved and atmospheric DMS, isoprene, halogenated compounds etc.	C. Marandino, GEOMAR, cmarandino@geomar.de; B. Quack, bquack@geomar.de

8 Acknowledgements

We acknowledge the financial support of SO305 BIOCAT-IIOE2 by the German Federal Ministry for Education and Research (BMBF) with grants FKZ 03G0305A (GEOMAR) and FKZ 03G0305B (University of Hamburg). TROPOS (grant# HE3086/60-1) and the University of Oldenburg received funding for SO305 from the German Science Foundation (DFG). Hereon (Geesthacht) generously supported the participation of Leon Schmidt in SO305 BIOCAT-IIOE2. Last but not least, the University of Southern Denmark generously supported the participation of the four colleagues from Odense (DK). The Leitstelle Deutsche Forschungsschiffe (German Research Fleet Coordination Centre) at the University of Hamburg provided excellent support during the preparation of SO305 BIOCAT-IIOE2. We thank the Master Tilo Birnbaum and the crew of R/V SONNE for their never-ending excellent support during SO305.

9 References

Al-Hashem, A.A., Beck, A.J., Krisch, S., Menzel Barraqueta, J.L., Steffens, T., Achterberg, E.P., 2022. Particulate trace metal sources, cycling, and distributions on the southwest African shelf. Global Biogeochemical Cycles 36 (11), e2022GB007453.

Amakawa, H., Alibo, D.S., Nozaki, Y., 2000. Nd isotopic composition and REE pattern in the surface waters of the eastern Indian Ocean and its adjacent seas. Geochim Cosmochim Acta 64 (10), 1715-1727.

Anifowose, A., Sakugawa, H., 2017. Determination of daytime flux of nitric oxide radical (NO•) at an inland sea–atmospheric boundary in Japan. J. Aquat. Pollut. Toxicol 1 (2), 10.

Arévalo-Martínez, D.L., Beyer, M., Krumbholz, M., Piller, I., Kock, A., Steinhoff, T., Körtzinger, A., Bange, H.W., 2013. A new method for continuous measurements of oceanic and atmospheric N_2O, CO and CO_2: performance of off-axis integrated cavity output spectroscopy (OA-ICOS) coupled to non-dispersive infrared detection (NDIR). Ocean Sci. 9 (6), 1071-1087.

Arnosti, C., 2011. Microbial extracellular enzymes and the marine carbon cycle. Annual review of marine science 3 (1), 401-425.

Avery, A.M., Williams, L.R., Fortner, E.C., Robinson, W.A., Onasch, T.B., 2020. Particle detection using the dual-vaporizer configuration of the soot particle Aerosol Mass Spectrometer (SP-AMS). Aerosol Science and Technology 55 (3), 254-267.

Bakker, D.C.E., Bange, H.W., Gruber, N., Johannessen, T., Upstill-Goddard, R.C., Borges, A.V., Delille, B., Löscher, C.R., Naqvi, S.W.A., Omar, A.M., Santana-Casiano, J.M., 2014. Air-sea interactions of natural long-lived greenhouse gases (CO_2, N_2O, CH_4) in a changing climate. In: Liss, P.S., Johnson, M.T. (Eds.), Ocean-Atmosphere Interactions of Gases and Particles. Springer, Heidelberg, pp. 113-169.

Balasubramanian, R., Karthikeyan, S., Potter, J., Wurl, O., Durville, C., 2013. Chemical characterization of aerosols in the equatorial atmosphere over the Indian Ocean. Atmospheric Environment 78, 268-276.

Baltar, F., Arístegui, J., Gasol, J.M., Sintes, E., Van Aken, H.M., Herndl, G.J., 2010. High dissolved extracellular enzymatic activity in the deep central Atlantic Ocean. Aquatic Microbial Ecology 58 (3), 287-302.

Bange, H.W., Mongwe, P., Shutler, J.D., Arévalo-Martínez, D.L., Bianchi, D., Lauvset, S.K., Liu, C., Löscher, C.R., Martins, H., Rosentreter, J.A., Schmale, O., Steinhoff, T., Upstill-Goddard, R.C., Wanninkhof, R., Wilson, S.T., Xie, H., 2024. Advances in understanding of air–sea exchange and cycling of greenhouse gases in the upper ocean. Elementa: Science of the Anthropocene 12 (1), doi: 10.1525/elementa.2023.00044.

Bibi, Z., Coe, H., Brooks, J., Williams, P.I., Reyes-Villegas, E., Priestley, M., Percival, C.J., Allan, J.D., 2021. A new approach to discriminate different black carbon sources by utilising fullerene and metals in positive matrix factorisation analysis of high-resolution soot particle aerosol mass spectrometer data. Atmospheric Chemistry and Physics 21 (13), 10763-10777.

Birks, J.W., Turnipseed, A.A., Andersen, P.C., Williford, C.J., Strunk, S., Carpenter, B., Ennis, C.A., 2020. Portable calibrator for NO based on the photolysis of N 2 O and a combined NO 2/NO/O3 source for field calibrations of air pollution monitors. Atmospheric Measurement Techniques 13 (2), 1001-1018.

Böhlke, J. K., Smith, R. L., Hannon, J. E., 2007. Isotopic analysis of N and O in nitrite and nitrate by sequential selective bacterial reduction to N2O, Analytical Chemistry, 79, 5888-5895. https://doi.org/10.1021/ac070176k.

Bristow, L.A., Callbeck, C.M., Larsen, M., Altabet, M.A., Dekaezemacker, J., Forth, M., Gauns, M., Glud, R.N., Kuypers, M.M.M., Lavik, G., Milucka, J., Naqvi, S.W.A., Pratihary, A., Revsbech, N.P., Thamdrup, B., Treusch, A.H., Canfield, D.E., 2017. N2 production rates limited by nitrite availability in the Bay of Bengal oxygen minimum zone. Nature Geosci 10 (1), 24-29.

Canonaco, F., Crippa, M., Slowik, J.G., Baltensperger, U., Prévôt, A.S., 2013. SoFi, an IGOR-based interface for the efficient use of the generalized multilinear engine (ME-2) for the source apportionment: ME-2 application to aerosol mass spectrometer data. Atmospheric Measurement Techniques 6 (12), 3649-3661.Canonaco et al., 2013. 'SoFi, an IGOR-based interface for the efficient use of the generalized multilinear engine (ME-2) for the source apportionment: ME-2 application to aerosol mass spectrometer data', Atmos. Meas. Tech., 6: 3649-61.

Crutzen, P., Ramanathan, V., 2001. Foreword [to special section on Indian Ocean Experiment (INDOEX)]. J. Geophys. Res.-A, 106: 28369-70, pp. 28369-28370.

Curray, J.R., Emmel, F.J., Moore, D.G., 2002. The Bengal Fan: morphology, geometry, stratigraphy, history and processes. Marine and Petroleum Geology 19 (10), 1191-1223.

Cutter, G.A., Anderson, P., Codispoti, L., Croot, P., Francois, R., Lohan, M.C., Obata, H., Rutgers van der Loeff, M., 2014. Sampling and sample-handling protocols for GEOTRACES cruises, GEOTRACES.

Dähnke, K., Emeis, K.-C., Johannsen, A., Nagel, B., 2010. Stable isotope composition and turnover of nitrate in the German Bight. Marine Ecology Progress Series 408, 7–18. https://doi.org/10.3354/meps08558.

Farley, R., Bernays, N., Jaffe, D.A., Ketcherside, D., Hu, L., Zhou, S., Collier, S., Zhang, Q., 2022. Persistent Influence of Wildfire Emissions in the Western United States and Characteristics of Aged Biomass Burning Organic Aerosols under Clean Air Conditions. Environmental Science & Technology 56 (6), 3645-3657.

Fontanez, K.M., Eppley, J.M., Samo, T.J., Karl, D.M., DeLong, E.F., 2015. Microbial community structure and function on sinking particles in the North Pacific Subtropical Gyre. Frontiers in Microbiology 6, 469.

Frank, M., 2002. Radiogenic isotopes: Tracers of past ocean circulation and erosional input. Rev. Geophys. 40 (1), doi:10.1029/2000RG000094.

Gauns, M., Madhupratap, M., Ramaiah, N., Jyothibabu, R., Fernandes, V., Paul, J.T., Kumar, S.P., 2005. Comparative accounts of biological productivity characteristics and estimates of carbon fluxes in the Arabian Sea and the Bay of Bengal. Deep Sea Research Part II: Topical Studies in Oceanography 52 (14-15), 2003-2017.

Gaye, B., Nagel, B., Dähnke, K., Rixen, T., and Emeis, K. C., 2013. Evidence of parallel denitrification and nitrite oxidation in the ODZ of the Arabian Sea from paired stable isotopes of nitrate and nitrite, Global Biogeochemical Cycles 27, 1-13, doi: 10.1002/2011GB004115.

Gledhill, M., Hollister, A., Seidel, M., Zhu, K., Achterberg, E.P., Dittmar, T., Koschinsky, A., 2022. Trace metal stoichiometry of dissolved organic matter in the Amazon plume. Science Advances 8, eabm2249, doi: 10.1126/sciadv.abm2249.

Goldstein, S.J., Jacobsen, S.B., 1987. The Nd and Sr isotopic systematics of river-water dissolved material: Implications for the sources of Nd and Sr in seawater. Chemical Geology: Isotope Geoscience section 66 (3-4), 245-272.

Granger, J., Sigman, D.M., Needoba, J.A., Harrison, P.J., 2004. Coupled nitrogen and oxygen isotope fractionation of nitrate during assimilation by cultures of marine phytoplankton. Limnology and Oceanography 49 1763–1773, doi: 10.4319/lo.2004.49.5.1763.

Grasshoff, K., Kremling, K., Ehrhardt, M., 1999. Methods of seawater analysis. Wiley-VCH, New York.

Guazzotti, S., Suess, D., Coffee, K., Quinn, P., Bates, T., Wisthaler, A., Hansel, A., Ball, W., Dickerson, R., Neusüß, C., 2003. Characterization of carbonaceous aerosols outflow from India and Arabia: Biomass/biofuel burning and fossil fuel combustion. Journal of Geophysical Research: Atmospheres 108 (D15).

Hamilton, D.S., Moore, J.K., Arneth, A., Bond, T.C., Carslaw, K.S., Hantson, S., Ito, A., Kaplan, J.O., Lindsay, K., Nieradzik, L., Rathod, S.D., Scanza, R.A., Mahowald, N.M., 2020. Impact of changes to the atmospheric soluble iron deposition flux on ocean biogeochemical cycles in the Anthropocene. Global Biogeochemical Cycles 34 e2019GB006448, doi: 10.1029/2019GB006448.

Harms, N.C., Lahajnar, N., Gaye, B., Rixen, T., Dähnke, K., Ankele, M., Schwarz-Schampera, U., Emeis, K.C., 2019. Nutrient distribution and nitrogen and oxygen isotopic composition of nitrate in water masses of the subtropical southern Indian Ocean. Biogeosciences 16, 2715-2732, doi: 10.5194/bg-16-2715-2019.

Hathorne, E.C., Frank, M., Mohan, P., 2020. Rare earth elements in Andaman Island surface seawater: geochemical tracers for the monsoon? Frontiers in Marine Science 6, 767, doi: 10.3389/fmars.2019.00767.

Hawkins, L., Russell, L., Covert, D., Quinn, P., Bates, T., 2010. Carboxylic acids, sulfates, and organosulfates in processed continental organic aerosol over the southeast Pacific Ocean during VOCALS-REx 2008. Journal of Geophysical Research: Atmospheres 115 (D13).

Holmes, R.M., Aminot, A., Kérouel, R., Hooker, B.A., Peterson, B.J., 1999. A simple and precise method for measuring ammonium in marine and freshwater ecosystems. Canadian Journal of Fisheries and Aquatic Sciences 56 (10), 1801-1808.

Hoppe, H.-G., 1983. Significance of exoenzymatic activities in the ecology of brackish water: measurements by means of methylumbelliferyl-substrates. Marine Ecology Progress Series, 299-308; doi: 10.3354/meps011299.

Huang, S., Wu, Z., Poulain, L., van Pinxteren, M., Merkel, M., Assmann, D., Herrmann, H., Wiedensohler, A., 2018. Source apportionment of the organic aerosol over the Atlantic Ocean from 53∘ N to 53∘ S: significant contributions from marine emissions and long-range transport. Atmospheric Chemistry and Physics 18 (24), 18043-18062.

IPCC, 2021. Climate Change 2021: The Physical Science Basis. Contribution of Working Group I to the Sixth Assessment Report of the Intergovernmental Panel on Climate Change. Cambridge University Press, Cambridge, UK and New York, NY, USA; doi: 10.1017/9781009157896, 2021.

Jia, Y., Hahn, J., Quack, B., Jones, E., Brehon, M., Tegtmeier, S., 2023. Anthropogenic bromoform at the extratropical tropopause. Geophysical Research Letters 50 (9), e2023GL102894.

Kanakidou, M., Seinfeld, J., Pandis, S., Barnes, I., Dentener, F.J., Facchini, M.C., Van Dingenen, R., Ervens, B., Nenes, A., Nielsen, C., 2005. Organic aerosol and global climate modelling: a review. Atmospheric Chemistry and Physics 5 (4), 1053-1123.

Kumar, M.D., Naqvi, S., George, M., Jayakumar, D., 1996. A sink for atmospheric carbon dioxide in the northeast Indian Ocean. Journal of Geophysical Research: Oceans 101 (C8), 18121-18125.

Kuypers, M.M.M., Marchant, H.K., Kartal, B., 2018. The microbial nitrogen-cycling network. Nat Rev Microbiol 16, 263-276.

Liss, P.S., Johnson, M.T. (Eds.), 2014. Ocean-atmosphere interactions of gases and particles. Springer, Heidelberg.

Marconi, D., Weigand, M. A., Rafter, P. A., McIlvin, M. R., Forbes, M., Casciotti, K. L., Sigman, D. M., 2015. Nitrate isotope distributions on the US GEOTRACES North Atlantic cross-basin section: Signals of polar nitrate sources and low latitude nitrogen cycling. Marine Chemistry 177 (1), 143-156, doi: 10.1016/j.marchem.2015.06.007.

McCave, I. N., 1984. Size spectra and aggregation of suspended particles in the ocean, Deep-Sea Research 31, 329-352, doi: 10.1016/0198-0149(84)90088-8.

Mehlmann, M., Quack, B., Atlas, E., Hepach, H., Tegtmeier, S., 2020. Natural and anthropogenic sources of bromoform and dibromomethane in the oceanographic and biogeochemical regime of the subtropical North East Atlantic. Environmental Science: Processes & Impacts 22 (3), 679-707.

Moffett, J.W., Goeffert, T.J., Naqvi, S.W.A., 2007. Reduced iron associated with secondary nitrite maxima in the Arabian Sea. Deep-Sea Research Part I 54, 1341–1349.

Narvekar, J., Prasanna Kumar, S., 2014. Mixed layer variability and chlorophyll a biomass in the Bay of Bengal. Biogeosciences 11 (14), 3819-3843.

Norton, J.M., Stark, J.M., 2011. Chapter Fifteen - Regulation and Measurement of Nitrification in Terrestrial Systems. In: Klotz, M.G. (Eds.), Methods in Enzymology, pp. 343-368, Academic Press; doi: 10.1016/B978-0-12-381294-0.00015-8.

Nozaki, Y., Alibo, D.S., 2003. Importance of vertical geochemical processes in controlling the oceanic profiles of dissolved rare earth elements in the northeastern Indian Ocean. Earth and Planetary Science Letters 205 (3-4), 155-172.

Ogulei, D., Hopke, P.K., Chalupa, D.C., Utell, M.J., 2007. Modeling source contributions to submicron particle number concentrations measured in Rochester, New York. Aerosol Science and Technology 41 (2), 179-201.

Onasch, T., Trimborn, A., Fortner, E., Jayne, J., Kok, G., Williams, L., Davidovits, P., Worsnop, D., 2012. Soot particle aerosol mass spectrometer: development, validation, and initial application. Aerosol Science and Technology 46 (7), 804-817.

Paatero, P., 1999. The multilinear engine—a table-driven, least squares program for solving multilinear problems, including the n-way parallel factor analysis model. Journal of Computational and Graphical Statistics 8 (4), 854-888.

Pachauri, R.K., Allen, M.R., Barros, V.R., Broome, J., Cramer, W., Christ, R., Church, J.A., Clarke, L., Dahe, Q., Dasgupta, P., 2014. Climate change 2014: synthesis report. Contribution of Working Groups I, II and III to the fifth assessment report of the Intergovernmental Panel on Climate Change. IPCC.

Phillips, H.E., Menezes, V.V., Nagura, M., McPhaden, M.J., Vinayachandran, P.N., Beal, L.M., 2024. Indian Ocean circulation. In: Ummenhofer, C.C., Hood, R.R. (Eds.), The Indian Ocean and its role in the global climate system. Elsevier, Amsterdam, pp. 169-203.

Rapp, I., Schlosser, C., Rusiecka, D., Gledhill, M., Achterberg, E.P., 2017. Automated preconcentration of Fe, Zn, Cu, Ni, Cd, Pb, Co, and Mn in seawater with analysis using high-resolution sector field inductively-coupled plasma mass spectrometry. Analytica Chimica Acta 976, 1–13, doi: 10.1016/j.aca.2017.05.008

Resplandy, L., Lévy, M., McGillicuddy Jr., D. J., 2019. Effects of eddy-driven subduction on ocean biological carbon pump. Global Biogeochemical Cycles 33, 1071-1084, doi: 10.1029/2018GB006125.

Rixen, T., Cowie, G., Gaye, B., Goes, J., do Rosário Gomes, H., Hood, R.R., Lachkar, Z., Schmidt, H., Segschneider, J., Singh, A., 2020. Reviews and syntheses: Present, past, and future of the oxygen minimum zone in the northern Indian Ocean. Biogeosciences 17 (23), 6051-6080.

Sanders, T., Laanbroek, H.J., 2018. The distribution of sediment and water column nitrification potential in the hyper-turbid Ems estuary. Aquatic Sciences 80, 1-13.

Saunois, M., Stavert, A.R., Poulter, B., Bousquet, P., Canadell, J.G., Jackson, R.B., Raymond, P.A., Dlugokencky, E.J., Houweling, S., Patra, P.K., Ciais, P., Arora, V.K., Bastviken, D., Bergamaschi, P., Blake, D.R., Brailsford, G., Bruhwiler, L., Carlson, K.M., Carrol, M., Castaldi, S., Chandra, N., Crevoisier, C., Crill, P.M., Covey, K., Curry, C.L., Etiope, G., Frankenberg, C., Gedney, N., Hegglin, M.I., Höglund-Isaksson, L., Hugelius, G., Ishizawa, M., Ito, A., Janssens-Maenhout, G., Jensen, K.M., Joos, F., Kleinen, T., Krummel, P.B., Langenfelds, R.L., Laruelle, G.G., Liu, L., Machida, T., Maksyutov, S., McDonald, K.C., McNorton, J., Miller, P.A., Melton, J.R., Morino, I., Müller, J., Murguia-Flores, F., Naik, V., Niwa, Y., Noce, S., O'Doherty, S., Parker, R.J., Peng, C., Peng, S., Peters, G.P., Prigent, C., Prinn, R., Ramonet, M., Regnier, P., Riley, W.J., Rosentreter, J.A., Segers, A., Simpson, I.J., Shi, H., Smith, S.J., Steele, L.P., Thornton, B.F., Tian, H., Tohjima, Y., Tubiello, F.N., Tsuruta, A., Viovy, N., Voulgarakis, A., Weber, T.S., van Weele, M., van der Werf, G.R., Weiss, R.F., Worthy, D., Wunch, D., Yin, Y., Yoshida, Y., Zhang, W., Zhang, Z., Zhao, Y., Zheng, B., Zhu, Q., Zhu, Q., Zhuang, Q., 2020. The Global Methane Budget 2000–2017. Earth Syst. Sci. Data 12 (3), 1561-1623.

Sengupta, D., Bharath Raj, G., Shenoi, S., 2006. Surface freshwater from Bay of Bengal runoff and Indonesian throughflow in the tropical Indian Ocean. Geophysical Research Letters 33 (22), doi: 10.1029/2006GL027573.

Sigman, D.M., Granger, J., DiFiore, P.J., Lehmann, M.M., Ho, R., Cane, G., Van Geen, A., 2005. Coupled nitrogen and oxygen isotope measurements of nitrate along the eastern North Pacific margin. Global Biogeochemical Cycles 19 (4), doi: 10.1029/2005GB002458.

Sigman, D. M., Fripat, F., 2019. Nitrogen Isotopes in the Ocean. In Encyclopedia of Ocean Sciences (Third Edition), ed. Cochran, J. K., Bokuniewicz, H. J., Yager, P. L., 263-278, Academic Press; doi: 10.1016/B978-0-12-409548-9.11605-7.

Silver, M. W., Coale, S. L., Pilskaln, C. H., Steinberg, D. R., 1998. Giant aggregates: Importance as microbial centers and agents of material flux in the mesopelagic zone. Limnology and Oceanography 43, 498-507, doi: 10.4319/lo.1998.43.3.0498.

Singh, S.P., Singh, S.K., Goswami, V., Bhushan, R., Rai, V.K., 2012. Spatial distribution of dissolved neodymium and εNd in the Bay of Bengal: Role of particulate matter and mixing of water masses. Geochim Cosmochim Acta 94, 38-56, doi: 10.1016/j.gca.2012.07.017.

Srivastava, D., Favez, O., Petit, J.-E., Zhang, Y., Sofowote, U., Hopke, P., Bonnaire, N., Perraudin, E., Gros, V., Villenave, E., 2019. Speciation of organic fractions does matter for aerosol source apportionment. Part 3: Combining off-line and on-line measurements. Science of The Total Environment 690, 944-955.

Steiner, Z., Sarkar, A., Prakash, S., Vinaychandran, P., Turchyn, A.V., 2020. Dissolved strontium, Sr/Ca ratios, and the abundance of Acantharia in the Indian and Southern Oceans. ACS Earth and Space Chemistry 4 (6), 802-811.

Sun, X., Frey, C., Garcia-Robledo, E., Jayakumar, A., Ward, B. B., 2021. Correction: Microbial niche differentiation explains nitrite oxidation in marine oxygen minimum zones. ISME J. 15, 2492, doi: 10.1038/s41396-021-01032-7.

Tian, H., Xu, R., Canadell, J.G., Thompson, R.L., Winiwarter, W., Suntharalingam, P., Davidson, E.A., Ciais, P., Jackson, R.B., Janssens-Maenhout, G., Prather, M.J., Regnier, P., Pan, N., Pan, S., Peters, G.P., Shi, H., Tubiello, F.N., Zaehle, S., Zhou, F., Arneth, A., Battaglia, G., Berthet, S., Bopp, L., Bouwman, A.F., Buitenhuis, E.T., Chang, J., Chipperfield, M.P., Dangal, S.R.S., Dlugokencky, E., Elkins, J.W., Eyre, B.D., Fu, B., Hall, B., Ito, A., Joos, F., Krummel, P.B., Landolfi, A., Laruelle, G.G., Lauerwald, R., Li, W., Lienert, S., Maavara, T., MacLeod, M., Millet, D.B., Olin, S., Patra, P.K., Prinn, R.G., Raymond, P.A., Ruiz, D.J., van der Werf, G.R., Vuichard, N., Wang, J., Weiss, R.F., Wells, K.C., Wilson, C., Yang, J., Yao, Y., 2020. A comprehensive quantification of global nitrous oxide sources and sinks. Nature 586 (7828), 248-256.

Turner, D.R., Croot, P.L., Dickson, A.G., Gledhill, M., 2024. Physicochemical controls on seawater, in: The Oceans and Marine Geochemistry, Treatise on Geochemistry. Elsevier Academic Press Inc.

Villamayor, J., Iglesias-Suarez, F., Cuevas, C.A., Fernandez, R.P., Li, Q., Abalos, M., Hossaini, R., Chipperfield, M.P., Kinnison, D.E., Tilmes, S., 2023. Very short-lived halogens amplify ozone depletion trends in the tropical lower stratosphere. Nature Climate Change 13 (6), 554-560.

Ward, B.B. Chapter thirteen - Measurement and Distribution of Nitrification Rates in the Oceans. In Methods in Enzymology, ed. M.G. Klotz, 307-323: Academic Press, doi: 10.1016/B978-0-12-381294-0.00013-4.

Yamamoto, H., Yokouchi, Y., Otsuki, A., Itoh, H., 2001. Depth profiles of volatile halogenated hydrocarbons in seawater in the Bay of Bengal. Chemosphere 45 (3), 371-377.

Yu, Z., Colin, C., Meynadier, L., Douville, E., Dapoigny, A., Reverdin, G., Wu, Q., Wan, S., Song, L., Xu, Z., 2017. Seasonal variations in dissolved neodymium isotope composition in the Bay of Bengal. Earth and Planetary Science Letters 479, 310-321, doi: 10.1016/j.epsl.2017.09.022.

Zhu, K., Hopwood, M.J., Groenenberg, J.E., Engel, A., Achterberg, E.P., Gledhill, M., 2021. Influence of pH and dissolved organic matter on iron speciation and apparent iron solubility in the Peruvian shelf and slope region. Environmental Science & Technology 55 (13), 9372-9383, doi: 10.1021/ACS.EST.1C02477.

Ziska, F., Quack, B., Abrahamsson, K., Archer, S., Atlas, E., Bell, T., Butler, J., Carpenter, L.J., Jones, C., Harris, N., 2013. Global sea-to-air flux climatology for bromoform, dibromomethane and methyl iodide. Atmospheric Chemistry and Physics 13 (17), 8915-8934.

10 Abbreviations

ADCP stands for Acoustic Doppler Current Profiler.

CTD stands for conductivity, temperature and depth.

Ro stands for rosette (’Kranzwasserschöpfer).

11 Appendices

Table 11.1 Underway CTD (uCTD) station list.

Ship station	uCTD station	Date/Time [UTC]	Latitude	Longitude	Speed (kn)
SO305_0_Underway-8	1	22.04.2024, 12:47	05° 14.703' N	087° 59.999' E	8.2
SO305_0_Underway-8	2	22.04.2024, 13:34	05° 21.191' N	088° 00.001' E	8.3
SO305_0_Underway-9	3	23.04.2024, 11:10	05° 09.199' N	088° 11.202' E	8
SO305_0_Underway-9	4	23.04.2024, 13:05	05° 24.402' N	088° 09.665' E	8.1
SO305_0_Underway-9	5	23.04.2024, 14:02	05° 32.087' N	088° 08.888' E	8
SO305_0_Underway-9	6	23.04.2024, 15:07	05° 40.606' N	088° 08.032' E	8
SO305_0_Underway-9	7	23.04.2024, 16:08	05° 48.810' N	088° 07.205' E	7.9
SO305_0_Underway-9	8	23.04.2024, 17:03	05° 56.087' N	088° 06.468' E	7.9
SO305_0_Underway-9	9	23.04.2024, 18:03	06° 04.132' N	088° 05.659' E	8.1
SO305_0_Underway-9	10	23.04.2024, 19:04	06° 12.368' N	088° 04.821' E	8
SO305_0_Underway-9	11	23.04.2024, 20:00	06° 19.817' N	088° 04.059' E	8.2
SO305_0_Underway-9	12	23.04.2024, 21:00	06° 27.997' N	088° 03.238' E	8.1
SO305_0_Underway-9	13	23.04.2024, 22:07	06° 36.971' N	088° 02.328' E	8.2
SO305_0_Underway-9	14	23.04.2024, 23:02	06° 44.533' N	088° 01.561' E	8.1
SO305_0_Underway-9	15	24.04.2024, 00:04	06° 52.766' N	088° 00.728' E	8.1

Table 11.2 MSS station list.

Ship Station	MSS Station	Date/Time [UTC]	Latitude	Longitude
SO305_2-2	1	17.04.2024, 08:28	00° 59.993' S	088° 40.211' E
SO305_5-2	2	18.04.2024, 23:21	00° 30.003' N	088° 40.143' E
SO305_6-2	3	19.04.2024, 07:24	01° 00.073' N	088° 40.321' E
SO305_7-2	4	19.04.2024, 22:50	02° 00.002' N	087° 59.994' E
SO305_8-2	5	20.04.2024, 09:48	02° 59.996' N	087° 59.992' E
SO305_9-2	6	20.04.2024, 22:20	03° 59.988' N	087° 59.994' E
SO305_10-4	7	21.04.2024, 11:34	05° 00.001' N	088° 00.005' E
SO305_10-9	8	21.04.2024, 19:49	04° 59.995' N	087° 59.915' E
SO305_10-11	9	22.04.2024, 01:39	05° 00.265' N	088° 00.129' E
SO305_10-15	10	22.04.2024, 08:46	04° 59.802' N	087° 59.992' E
SO305_11-3	11	22.04.2024, 21:19	05° 59.995' N	087° 59.999' E
SO305_13-2	12	24.04.2024, 01:56	07° 00.041' N	087° 59.981' E
SO305_14-2	13	24.04.2024, 17:57	07° 59.965' N	087° 59.963' E
SO305_15-2	14	25.04.2024, 06:23	09° 00.073' N	088° 00.048' E
SO305_16-2	15	25.04.2024, 19:49	10° 00.106' N	088° 00.065' E
SO305_17-1	16	26.04.2024, 04:55	10° 59.966' N	088° 00.044' E
SO305_18-3	17	26.04.2024, 21:12	11° 59.985' N	087° 59.992' E
SO305_18-10	18	27.04.2024, 08:52	12° 00.197' N	087° 59.985' E
SO305_18-14	19	27.04.2024, 14:10	12° 00.573' N	088° 00.231' E
SO305_18-17	20	27.04.2024, 17:51	12° 00.832' N	088° 01.103' E
SO305_19-2	21	28.04.2024, 03:35	12° 12.285' N	087° 01.547' E
SO305_20-2	22	28.04.2024, 12:50	12° 30.010' N	085° 59.985' E
SO305_22-2	23	29.04.2024, 22:13	12° 44.534' N	085° 04.503' E
SO305_23-2	24	30.04.2024, 09:52	12° 59.988' N	084° 00.002' E
SO305_24-2	25	01.05.2024, 00:17	13° 00.080' N	085° 00.051' E
SO305_25-2	26	01.05.2024, 11:28	13° 00.072' N	086° 00.011' E
SO305_26-2	27	02.05.2024, 00:06	13° 00.091' N	086° 59.991' E
SO305_27-3	28	02.05.2024, 13:13	12° 59.992' N	088° 00.046' E
SO305_29-2	29	03.05.2024, 10:59	13° 30.656' N	088° 30.706' E
SO305_30-11	30	04.05.2024, 23:13	13° 59.648' N	087° 59.124' E
SO305_31-2	31	05.05.2024, 12:44	14° 29.935' N	087° 00.011' E
SO305_32-3	32	06.05.2024, 00:02	14° 59.994' N	085° 44.991' E
SO305_32-6	33	06.05.2024, 06:35	14° 59.391' N	085° 44.717' E
SO305_32-9	34	06.05.2024, 12:29	14° 58.645' N	085° 44.280' E
SO305_32-14	35	06.05.2024, 18:17	14° 58.141' N	085° 43.922' E
SO305_34-2	36	08.05.2024, 08:15	15° 00.023' N	086° 59.954' E
SO305_35-3	37	08.05.2024, 20:22	15° 00.013' N	087° 59.852' E
SO305_36-2	38	09.05.2024, 06:24	14° 59.945' N	088° 44.738' E
SO305_37-2	39	09.05.2024, 18:04	15° 00.016' N	089° 36.022' E
SO305_37-5	40	09.05.2024, 22:48	15° 00.143' N	089° 36.132' E
SO305_37-9	41	10.05.2024, 07:49	15° 03.147' N	089° 38.325' E
SO305_38-3	42	10.05.2024, 23:12	15° 59.998' N	089° 35.997' E

Table 11.3 List of samples of halogenated methanes.

Cast	Station	Bottle	bedfordnumber	depth	pressure	latitude	longitude	year	month	day	hour	minute
2	2_1	1	SO305_1_0023	4278.2	4345.8	-1.000	88.670	2024	4	17	5	48
2	2_1	5	SO305_1_0027	2994.1	3032.3	-1.000	88.670	2024	4	17	6	32
2	2_1	7	SO305_1_0029	1500.1	1513.8	-1.000	88.670	2024	4	17	7	7
2	2_1	8	SO305_1_0030	999.2	1007.1	-1.000	88.670	2024	4	17	7	16
2	2_1	10	SO305_1_0032	800.9	806.9	-0.999	88.670	2024	4	17	7	21
4	2_5	2	SO305_1_0063	500.9	504.3	-0.999	88.670	2024	4	17	14	43
4	2_5	4	SO305_1_0065	431.4	434.2	-0.999	88.670	2024	4	17	14	51
4	2_5	11	SO305_1_0072	195.6	196.8	-0.999	88.670	2024	4	17	15	4
4	2_5	13	SO305_1_0074	100.5	101.1	-0.999	88.670	2024	4	17	15	14
4	2_5	14	SO305_1_0075	80.2	80.7	-0.999	88.670	2024	4	17	15	15
4	2_5	15	SO305_1_0076	60	60.3	-0.999	88.670	2024	4	17	15	16
4	2_5	19	SO305_1_0080	50.8	51.1	-0.999	88.670	2024	4	17	15	17
4	2_5	20	SO305_1_0081	30.5	30.7	-0.999	88.670	2024	4	17	15	18
4	2_5	21	SO305_1_0082	10.5	10.6	-0.999	88.670	2024	4	17	15	19
6	4_1	4	SO305_1_0109	4481.8	4554.7	-0.025	88.670	2024	4	18	2	17
6	4_1	6	SO305_1_0111	3000.1	3038.5	-0.025	88.670	2024	4	18	2	43
6	4_1	7	SO305_1_0112	2000.9	2021.7	-0.025	88.670	2024	4	18	3	1
6	4_1	8	SO305_1_0113	1500.4	1514.2	-0.025	88.670	2024	4	18	3	9
6	4_1	9	SO305_1_0114	1001.2	1009.2	-0.025	88.670	2024	4	18	3	18
6	4_1	18	SO305_1_0123	715.4	720.6	-0.025	88.670	2024	4	18	3	26
6	4_1	22	SO305_1_0127	501.1	504.5	-0.026	88.670	2024	4	18	3	32
7	4_2	7	SO305_1_0134	341.1	343.3	-0.026	88.670	2024	4	18	5	6
7	4_2	10	SO305_1_0137	200.9	202.1	-0.026	88.670	2024	4	18	5	10
7	4_2	14	SO305_1_0141	100.9	101.5	-0.026	88.670	2024	4	18	5	13
7	4_2	16	SO305_1_0143	81.2	81.7	-0.026	88.670	2024	4	18	5	14
7	4_2	21	SO305_1_0148	61.3	61.7	-0.026	88.670	2024	4	18	5	16
7	4_2	22	SO305_1_0149	50.8	51.1	-0.026	88.670	2024	4	18	5	17
8	4_3	1	SO305_1_0150	31	31.1	-0.026	88.670	2024	4	18	6	33
8	4_3	6	SO305_1_0155	2.1	2.1	-0.026	88.670	2024	4	18	6	35
10	6_1	4	SO305_1_0197	4348.8	4418.2	1.001	88.672	2024	4	19	5	47
10	6_1	5	SO305_1_0198	3001.8	3040.1	1.001	88.672	2024	4	19	6	11
10	6_1	6	SO305_1_0199	2001.1	2021.8	1.001	88.672	2024	4	19	6	28
10	6_1	7	SO305_1_0200	1500.9	1514.7	1.001	88.672	2024	4	19	6	38
10	6_1	8	SO305_1_0201	1000.4	1008.3	1.001	88.672	2024	4	19	6	47
10	6_1	15	SO305_1_0208	759.8	765.4	1.001	88.672	2024	4	19	6	53
10	6_1	19	SO305_1_0212	501.3	504.7	1.001	88.672	2024	4	19	6	59
10	6_1	22	SO305_1_0215	370.9	373.3	1.001	88.672	2024	4	19	7	2
11	6_3	6	SO305_1_0221	200.8	202	0.998	88.662	2024	4	19	8	38
11	6_3	8	SO305_1_0223	171.2	172.2	0.998	88.662	2024	4	19	8	40
11	6_3	10	SO305_1_0225	101.3	101.9	0.998	88.662	2024	4	19	8	42
11	6_3	15	SO305_1_0230	69.6	70	0.998	88.662	2024	4	19	8	44
11	6_3	22	SO305_1_0237	1.6	1.6	0.998	88.662	2024	4	19	8	48
13	7_1	1	SO305_1_0238	4247.6	4314.4	2.000	88.000	2024	4	19	20	42
13	7_1	3	SO305_1_0240	3001.9	3040.3	2.000	88.000	2024	4	19	21	7
13	7_1	4	SO305_1_0241	2000.1	2020.9	2.000	88.000	2024	4	19	21	26
13	7_1	5	SO305_1_0242	1001.4	1009.3	2.000	88.000	2024	4	19	21	45
13	7_1	9	SO305_1_0246	690.9	695.9	2.000	88.000	2024	4	19	21	54
13	7_1	11	SO305_1_0248	501.7	505.1	2.000	88.000	2024	4	19	21	59
13	7_1	13	SO305_1_0250	360.5	362.9	2.000	88.000	2024	4	19	22	3
13	7_1	15	SO305_1_0252	200.5	201.7	2.000	88.000	2024	4	19	22	7
13	7_1	17	SO305_1_0254	101	101.6	2.000	88.000	2024	4	19	22	11
13	7_1	18	SO305_1_0255	81	81.5	2.000	88.000	2024	4	19	22	12
13	7_1	19	SO305_1_0256	70.3	70.7	2.000	88.000	2024	4	19	22	13
13	7_1	20	SO305_1_0257	51.4	51.7	2.000	88.000	2024	4	19	22	15
13	7_1	21	SO305_1_0258	31.2	31.3	2.000	88.000	2024	4	19	22	16
13	7_1	22	SO305_1_0259	4.7	4.8	2.000	88.000	2024	4	19	22	18
14	8_1	4	SO305_1_0263	4191.3	4256.7	3.000	88.000	2024	4	20	8	9
14	8_1	5	SO305_1_0264	3000	3038.3	3.000	88.000	2024	4	20	8	30
14	8_1	6	SO305_1_0265	2001	2021.8	3.000	88.000	2024	4	20	8	48
14	8_1	7	SO305_1_0266	1501.2	1515	3.000	88.000	2024	4	20	8	57
14	8_1	8	SO305_1_0267	1000.4	1008.4	3.000	88.000	2024	4	20	9	6
14	8_1	14	SO305_1_0273	759	764.6	3.000	88.000	2024	4	20	9	11
14	8_1	18	SO305_1_0277	498.8	502.1	3.000	88.000	2024	4	20	9	17
15	8_3	3	SO305_1_0284	339.4	341.6	2.996	87.996	2024	4	20	11	4
15	8_3	7	SO305_1_0288	229.1	230.5	2.996	87.996	2024	4	20	11	8
15	8_3	9	SO305_1_0290	150.3	151.2	2.996	87.996	2024	4	20	11	11
15	8_3	10	SO305_1_0291	99.7	100.3	2.996	87.996	2024	4	20	11	12
15	8_3	16	SO305_1_0297	55.1	55.4	2.996	87.996	2024	4	20	11	15
15	8_3	22	SO305_1_0303	2.4	2.4	2.996	87.996	2024	4	20	11	18
16	9_1	1	SO305_1_0304	3978.7	4038.9	4.000	88.000	2024	4	20	20	32
16	9_1	2	SO305_1_0305	3000.2	3038.6	4.000	88.000	2024	4	20	20	50
16	9_1	3	SO305_1_0306	2001.8	2022.7	4.000	88.000	2024	4	20	21	8
16	9_1	4	SO305_1_0307	1501.5	1515.3	4.000	88.000	2024	4	20	21	18
16	9_1	5	SO305_1_0308	1001.1	1009.1	4.000	88.000	2024	4	20	21	28
16	9_1	9	SO305_1_0312	670.9	675.7	4.000	88.000	2024	4	20	21	36
16	9_1	11	SO305_1_0314	500.8	504.2	4.000	88.000	2024	4	20	21	40
16	9_1	15	SO305_1_0318	200.7	201.9	4.000	88.000	2024	4	20	21	48
16	9_1	16	SO305_1_0319	150.2	151.1	4.000	88.000	2024	4	20	21	49
16	9_1	17	SO305_1_0320	101	101.5	4.000	88.000	2024	4	20	21	51
16	9_1	18	SO305_1_0321	81.9	82.3	4.000	88.000	2024	4	20	21	52

16	9 1	19	SO305 1 0322	62	62.4	4.000	88.000	2024	4	20	21	53
16	9 1	20	SO305 1 0323	51.1	51.4	4.000	88.000	2024	4	20	21	54
16	9 1	21	SO305 1 0324	30.8	31	4.000	88.000	2024	4	20	21	55
16	9 1	22	SO305 1 0325	2.4	2.4	4.000	88.000	2024	4	20	21	57
18	10 3	4	SO305 1 0329	3943	4002.3	5.000	88.000	2024	4	21	10	3
18	10 3	7	SO305 1 0332	1501.3	1515.1	5.000	88.000	2024	4	21	10	47
18	10 3	8	SO305 1 0333	1000.2	1008.2	5.000	88.000	2024	4	21	10	55
18	10 3	9	SO305 1 0334	900.2	907.2	5.000	88.000	2024	4	21	10	58
18	10 3	16	SO305 1 0341	590.8	594.9	5.000	88.000	2024	4	21	11	5
18	10 3	18	SO305 1 0343	501.3	504.7	5.000	88.000	2024	4	21	11	8
19	10 5	8	SO305 1 0355	135.1	135.9	5.000	87.999	2024	4	21	12	57
19	10 5	15	SO305 1 0362	55.1	55.4	5.000	87.999	2024	4	21	13	2
21	10 8	12	SO305 1 0403	151.2	152.1	5.000	87.999	2024	4	21	19	25
21	10 8	16	SO305 1 0407	60.3	60.7	5.000	87.999	2024	4	21	19	29
21	10 8	18	SO305 1 0409	51.1	51.4	5.000	87.999	2024	4	21	19	30
21	10 8	19	SO305 1 0410	31.4	31.6	5.000	87.999	2024	4	21	19	32
21	10 8	20	SO305 1 0411	11.9	12	5.000	87.999	2024	4	21	19	33
21	10 8	21	SO305 1 0412	4.2	4.2	5.000	87.999	2024	4	21	19	35
24	10 16	12	SO305 1 0469	140.8	141.7	4.997	88.000	2024	4	22	10	26
24	10 16	16	SO305 1 0473	56.1	56.4	4.997	88.000	2024	4	22	10	30
24	10 16	18	SO305 1 0475	50.6	50.9	4.997	88.000	2024	4	22	10	30
24	10 16	19	SO305 1 0476	25.5	25.6	4.997	88.000	2024	4	22	10	32
24	10 16	21	SO305 1 0478	1.6	1.6	4.997	88.000	2024	4	22	10	34
25	11 1	4	SO305 1 0483	3864.6	3922.1	6.000	88.000	2024	4	22	19	43
25	11 1	5	SO305 1 0484	3001.2	3039.7	6.000	88.000	2024	4	22	19	59
25	11 1	6	SO305 1 0485	2000.3	2021.2	6.000	88.000	2024	4	22	20	19
25	11 1	7	SO305 1 0486	1501.5	1515.4	6.000	88.000	2024	4	22	20	28
25	11 1	8	SO305 1 0487	1001.2	1009.3	6.000	88.000	2024	4	22	20	38
25	11 1	14	SO305 1 0493	500	503.4	6.000	88.000	2024	4	22	20	50
26	11 4	5	SO305 1 0506	208.9	210.2	6.000	88.000	2024	4	22	22	27
26	11 4	7	SO305 1 0508	151.2	152.1	6.000	88.000	2024	4	22	22	30
26	11 4	9	SO305 1 0510	101	101.6	6.000	88.000	2024	4	22	22	32
26	11 4	10	SO305 1 0511	76.4	76.9	6.000	88.000	2024	4	22	22	33
26	11 4	15	SO305 1 0516	46.5	46.7	6.000	88.000	2024	4	22	22	35
26	11 4	16	SO305 1 0517	30.8	31	6.000	88.000	2024	4	22	22	36
26	11 4	17	SO305 1 0518	11	11	6.000	88.000	2024	4	22	22	38
26	11 4	22	SO305 1 0523	3.3	3.3	6.000	88.000	2024	4	22	22	39
29	13 3	5	SO305 1 0572	3729.3	3783.7	7.010	88.007	2024	4	24	4	20
29	13 3	6	SO305 1 0573	2999.3	3037.8	7.010	88.007	2024	4	24	4	33
29	13 3	8	SO305 1 0575	1500.7	1514.6	7.010	88.007	2024	4	24	5	0
29	13 3	9	SO305 1 0576	1000.3	1008.4	7.010	88.007	2024	4	24	5	9
29	13 3	17	SO305 1 0584	500.3	503.7	7.010	88.007	2024	4	24	5	20
30	13 4	1	SO305 1 0590	300.5	302.4	7.010	88.007	2024	4	24	6	35
30	13 4	4	SO305 1 0593	150.8	151.7	7.010	88.007	2024	4	24	6	39
30	13 4	5	SO305 1 0594	100.6	101.1	7.010	88.007	2024	4	24	6	41
30	13 4	6	SO305 1 0595	76.5	77	7.010	88.007	2024	4	24	6	42
30	13 4	7	SO305 1 0596	62.3	62.6	7.010	88.007	2024	4	24	6	43
30	13 4	12	SO305 1 0601	51.3	51.6	7.010	88.007	2024	4	24	6	44
30	13 4	13	SO305 1 0602	31.7	31.9	7.010	88.007	2024	4	24	6	45
30	13 4	14	SO305 1 0603	10.9	10.9	7.010	88.007	2024	4	24	6	47
30	13 4	19	SO305 1 0608	2.9	2.9	7.010	88.007	2024	4	24	6	48
31	14 1	1	SO305 1 0612	3622.2	3674.2	8.000	87.999	2024	4	24	16	27
31	14 1	5	SO305 1 0616	2000.6	2021.6	7.999	87.999	2024	4	24	16	56
31	14 1	6	SO305 1 0617	1500.9	1514.9	7.999	87.999	2024	4	24	17	5
31	14 1	7	SO305 1 0618	1000.7	1008.8	7.999	87.999	2024	4	24	17	14
31	14 1	13	SO305 1 0624	400.9	403.6	7.999	87.999	2024	4	24	17	28
31	14 1	16	SO305 1 0627	180.9	182	8.000	87.999	2024	4	24	17	33
31	14 1	18	SO305 1 0629	81.7	82.2	8.000	87.999	2024	4	24	17	37
31	14 1	19	SO305 1 0630	50.6	50.9	8.000	87.999	2024	4	24	17	38
31	14 1	20	SO305 1 0631	42.7	42.9	8.000	87.999	2024	4	24	17	39
31	14 1	21	SO305 1 0632	30	30.2	8.000	87.999	2024	4	24	17	40
31	14 1	22	SO305 1 0633	2.9	2.9	8.000	87.999	2024	4	24	17	42
33	15 1	5	SO305 1 0660	3494.3	3543.5	9.001	88.001	2024	4	25	4	50
33	15 1	6	SO305 1 0661	3000.7	3039.4	9.001	88.001	2024	4	25	5	0
33	15 1	7	SO305 1 0662	2000.5	2021.5	9.001	88.001	2024	4	25	5	19
33	15 1	8	SO305 1 0663	1500.4	1514.4	9.001	88.001	2024	4	25	5	29
33	15 1	9	SO305 1 0664	1000.9	1009	9.001	88.001	2024	4	25	5	39
33	15 1	15	SO305 1 0670	499.8	503.3	9.001	88.001	2024	4	25	5	51
33	15 1	19	SO305 1 0674	433.8	436.7	9.001	88.001	2024	4	25	5	53
33	15 1	21	SO305 1 0676	360.1	362.5	9.001	88.001	2024	4	25	5	56
34	15 3	8	SO305 1 0685	200	201.2	9.001	88.001	2024	4	25	7	48
34	15 3	10	SO305 1 0687	99.6	100.2	9.001	88.001	2024	4	25	7	51
34	15 3	11	SO305 1 0688	80.8	81.3	9.001	88.001	2024	4	25	7	52
34	15 3	15	SO305 1 0692	64.8	65.1	9.001	88.001	2024	4	25	7	53
34	15 3	17	SO305 1 0694	31	31.2	9.001	88.001	2024	4	25	7	55
34	15 3	18	SO305 1 0695	11.3	11.4	9.001	88.001	2024	4	25	7	56
34	15 3	22	SO305 1 0699	2	2	9.001	88.001	2024	4	25	7	57
36	16 1	1	SO305 1 0722	3387.2	3434.2	10.001	88.001	2024	4	25	18	21
36	16 1	2	SO305 1 0723	2998.8	3037.6	10.001	88.001	2024	4	25	18	29
36	16 1	3	SO305 1 0724	2000.4	2021.5	10.001	88.001	2024	4	25	18	48
36	16 1	5	SO305 1 0726	1002.5	1010.6	10.001	88.001	2024	4	25	19	7
36	16 1	11	SO305 1 0732	450.2	453.2	10.001	88.001	2024	4	25	19	21
36	16 1	15	SO305 1 0736	240.3	241.9	10.001	88.001	2024	4	25	19	27

36	16 1	17	SO305 1 0738	100.7	101.3	10.001	88.001	2024	4	25	19	31
36	16 1	18	SO305 1 0739	81.9	82.4	10.001	88.001	2024	4	25	19	32
36	16 1	19	SO305 1 0740	75	75.4	10.001	88.001	2024	4	25	19	34
36	16 1	21	SO305 1 0742	31.4	31.5	10.001	88.001	2024	4	25	19	37
36	16 1	22	SO305 1 0743	3.7	3.7	10.001	88.001	2024	4	25	19	39
38	17 1	1	SO305 1 0766	3299.6	3344.7	10.991	88.001	2024	4	26	7	13
38	17 1	2	SO305 1 0767	2000.2	2021.4	10.991	88.001	2024	4	26	7	39
38	17 1	4	SO305 1 0769	1500.3	1514.4	10.991	88.001	2024	4	26	7	50
38	17 1	5	SO305 1 0770	1000	1008.2	10.991	88.001	2024	4	26	8	0
38	17 1	10	SO305 1 0775	501	504.5	10.991	88.001	2024	4	26	8	12
38	17 1	11	SO305 1 0776	400.3	403	10.991	88.001	2024	4	26	8	14
38	17 1	15	SO305 1 0780	200.8	202.1	10.991	88.001	2024	4	26	8	22
38	17 1	18	SO305 1 0783	81.6	82.1	10.991	88.001	2024	4	26	8	27
38	17 1	19	SO305 1 0784	71.7	72.1	10.991	88.001	2024	4	26	8	27
38	17 1	21	SO305 1 0786	31.5	31.7	10.991	88.001	2024	4	26	8	30
38	17 1	22	SO305 1 0787	3.1	3.1	10.991	88.001	2024	4	26	8	32
39	18 2	6	SO305 1 0793	2000.9	2022.1	12.000	88.000	2024	4	26	20	16
39	18 2	10	SO305 1 0797	1493.9	1507.9	12.000	88.000	2024	4	26	20	27
39	18 2	11	SO305 1 0798	1000.9	1009.1	12.000	88.000	2024	4	26	20	36
39	18 2	22	SO305 1 0809	500.7	504.2	12.000	88.000	2024	4	26	20	52
40	18 4	5	SO305 1 0814	442.4	445.4	12.004	88.005	2024	4	26	22	30
40	18 4	7	SO305 1 0816	356.5	358.9	12.004	88.005	2024	4	26	22	33
40	18 4	10	SO305 1 0819	201.2	202.4	12.004	88.005	2024	4	26	22	39
40	18 4	14	SO305 1 0823	81	81.5	12.004	88.005	2024	4	26	22	46
40	18 4	15	SO305 1 0824	71.4	71.8	12.004	88.005	2024	4	26	22	47
40	18 4	16	SO305 1 0825	51	51.3	12.004	88.005	2024	4	26	22	49
40	18 4	17	SO305 1 0826	31.1	31.3	12.004	88.005	2024	4	26	22	51
40	18 4	18	SO305 1 0827	11.2	11.2	12.004	88.005	2024	4	26	22	52
40	18 4	22	SO305 1 0831	3.9	3.9	12.004	88.005	2024	4	26	22	54
42	18 9	17	SO305 1 0870	71.2	71.7	12.002	87.999	2024	4	27	8	33
42	18 9	18	SO305 1 0871	50.8	51.1	12.002	87.999	2024	4	27	8	34
42	18 9	19	SO305 1 0872	31	31.2	12.002	87.999	2024	4	27	8	35
42	18 9	20	SO305 1 0873	11.4	11.5	12.002	87.999	2024	4	27	8	36
42	18 9	22	SO305 1 0875	2.2	2.2	12.002	87.999	2024	4	27	8	37
47	18 16	17	SO305 1 0980	73.3	73.7	12.014	88.018	2024	4	27	17	31
47	18 16	18	SO305 1 0981	50.4	50.7	12.014	88.018	2024	4	27	17	32
47	18 16	19	SO305 1 0982	30.8	31	12.014	88.018	2024	4	27	17	33
47	18 16	20	SO305 1 0983	10.7	10.8	12.014	88.018	2024	4	27	17	35
47	18 16	22	SO305 1 0985	1.7	1.8	12.014	88.018	2024	4	27	17	35
49	20 1	1	SO305 1 1008	3216.8	3260.4	12.500	86.000	2024	4	28	11	31
49	20 1	6	SO305 1 1013	2000.1	2021.4	12.500	86.000	2024	4	28	11	53
49	20 1	7	SO305 1 1014	1500	1514.1	12.500	86.000	2024	4	28	12	2
49	20 1	8	SO305 1 1015	1000.5	1008.7	12.500	86.000	2024	4	28	12	11
49	20 1	16	SO305 1 1023	501.2	504.7	12.500	86.000	2024	4	28	12	23
50	20 2	1	SO305 1 1030	201.6	202.9	12.503	85.993	2024	4	28	13	51
50	20 2	6	SO305 1 1035	171.1	172.1	12.503	85.993	2024	4	28	13	53
50	20 2	9	SO305 1 1038	100.5	101.1	12.503	85.993	2024	4	28	13	57
50	20 2	14	SO305 1 1043	80.7	81.1	12.503	85.993	2024	4	28	13	58
50	20 2	15	SO305 1 1044	50.8	51.1	12.503	85.993	2024	4	28	14	1
50	20 2	16	SO305 1 1045	30.7	30.9	12.503	85.993	2024	4	28	14	2
50	20 2	17	SO305 1 1046	11	11	12.503	85.993	2024	4	28	14	3
50	20 2	22	SO305 1 1051	1.5	1.5	12.503	85.993	2024	4	28	14	4
53	22 1	13	SO305 1 1108	230.1	231.5	12.742	85.075	2024	4	29	21	48
53	22 1	17	SO305 1 1112	86.1	86.6	12.742	85.075	2024	4	29	21	53
53	22 1	18	SO305 1 1113	80.9	81.4	12.742	85.075	2024	4	29	21	54
53	22 1	19	SO305 1 1114	50.7	51	12.742	85.075	2024	4	29	21	56
53	22 1	20	SO305 1 1115	30.9	31.1	12.742	85.075	2024	4	29	21	57
53	22 1	21	SO305 1 1116	11.2	11.2	12.742	85.075	2024	4	29	21	59
53	22 1	22	SO305 1 1117	4.5	4.5	12.742	85.075	2024	4	29	22	0
54	23 1	5	SO305 1 1122	3273.9	3318.7	13.000	84.000	2024	4	30	8	21
54	23 1	9	SO305 1 1126	2000.1	2021.4	13.000	84.000	2024	4	30	8	46
54	23 1	10	SO305 1 1127	1500.2	1514.4	13.000	84.000	2024	4	30	8	57
54	23 1	14	SO305 1 1131	1000.5	1008.8	13.000	84.000	2024	4	30	9	7
54	23 1	17	SO305 1 1134	699.8	705	13.000	84.000	2024	4	30	9	15
55	23 3	2	SO305 1 1141	500.4	503.9	12.984	83.997	2024	4	30	11	14
55	23 3	11	SO305 1 1150	249.1	250.7	12.984	83.997	2024	4	30	11	22
55	23 3	14	SO305 1 1153	168.3	169.4	12.984	83.997	2024	4	30	11	26
55	23 3	17	SO305 1 1156	90.6	91.1	12.984	83.997	2024	4	30	11	30
55	23 3	18	SO305 1 1157	80.5	81	12.984	83.997	2024	4	30	11	31
55	23 3	19	SO305 1 1158	55.9	56.2	12.984	83.997	2024	4	30	11	33
55	23 3	20	SO305 1 1159	30.7	30.9	12.984	83.997	2024	4	30	11	35
55	23 3	21	SO305 1 1160	10.9	11	12.984	83.997	2024	4	30	11	36
55	23 3	22	SO305 1 1161	1.3	1.3	12.984	83.997	2024	4	30	11	37
59	24 3	9	SO305 1 1236	171	172.1	12.991	84.991	2024	5	1	1	31
59	24 3	11	SO305 1 1238	83.9	84.4	12.991	84.991	2024	5	1	1	35
59	24 3	15	SO305 1 1242	84.4	84.9	12.991	84.991	2024	5	1	1	35
59	24 3	16	SO305 1 1243	50.9	51.2	12.991	84.991	2024	5	1	1	37
59	24 3	17	SO305 1 1244	30.6	30.7	12.991	84.991	2024	5	1	1	39
59	24 3	18	SO305 1 1245	11.4	11.5	12.991	84.991	2024	5	1	1	40
59	24 3	22	SO305 1 1249	3.3	3.3	12.991	84.991	2024	5	1	1	41
61	25 1	5	SO305 1 1254	3167.3	3209.8	13.001	86.000	2024	5	1	10	12
61	25 1	9	SO305 1 1258	2000.3	2021.6	13.001	86.000	2024	5	1	10	34
61	25 1	13	SO305 1 1262	1500.7	1514.8	13.001	86.000	2024	5	1	10	43

61	25 1	19	SO305 1 1268	700.9	706.1	13.001	86.000	2024	5	1	10	59
61	25 1	20	SO305 1 1269	700.7	705.9	13.001	86.000	2024	5	1	10	59
62	25 3	15	SO305 1 1286	121.4	122.2	13.000	85.998	2024	5	1	12	52
62	25 3	17	SO305 1 1288	80.9	81.4	13.000	85.998	2024	5	1	12	54
62	25 3	19	SO305 1 1290	50.7	51	13.000	85.998	2024	5	1	12	56
62	25 3	20	SO305 1 1291	29.8	30	13.000	85.998	2024	5	1	12	58
62	25 3	21	SO305 1 1292	11	11.1	13.000	85.998	2024	5	1	12	59
62	25 3	22	SO305 1 1293	1.9	1.9	13.000	85.998	2024	5	1	13	0
65	26 3	4	SO305 1 1341	220.9	222.3	12.996	86.996	2024	5	2	1	19
65	26 3	11	SO305 1 1348	100.4	101	12.996	86.996	2024	5	2	1	24
65	26 3	15	SO305 1 1352	73.2	73.7	12.996	86.996	2024	5	2	1	25
65	26 3	16	SO305 1 1353	50.2	50.5	12.996	86.996	2024	5	2	1	27
65	26 3	17	SO305 1 1354	31.1	31.3	12.996	86.996	2024	5	2	1	28
65	26 3	18	SO305 1 1355	10.4	10.5	12.996	86.996	2024	5	2	1	29
65	26 3	22	SO305 1 1359	3.8	3.8	12.996	86.995	2024	5	2	1	31
66	26 4	12	SO305 1 1371	202.4	203.7	12.996	86.996	2024	5	2	2	32
68	27 2	4	SO305 1 1385	3050.5	3090.6	13.000	88.001	2024	5	2	11	59
68	27 2	9	SO305 1 1390	2000.3	2021.6	13.000	88.001	2024	5	2	12	18
68	27 2	13	SO305 1 1394	1500.4	1514.6	13.000	88.001	2024	5	2	12	27
68	27 2	14	SO305 1 1395	999.7	1007.9	13.000	88.001	2024	5	2	12	36
68	27 2	20	SO305 1 1401	700	705.2	13.000	88.001	2024	5	2	12	44
69	27 4	10	SO305 1 1413	330.9	333.1	12.993	87.998	2024	5	2	14	33
69	27 4	17	SO305 1 1420	90.5	91	12.993	87.998	2024	5	2	14	44
69	27 4	18	SO305 1 1421	72.3	72.7	12.993	87.998	2024	5	2	14	45
69	27 4	19	SO305 1 1422	50.6	50.9	12.993	87.998	2024	5	2	14	46
69	27 4	20	SO305 1 1423	30.3	30.4	12.993	87.998	2024	5	2	14	48
69	27 4	21	SO305 1 1424	10.4	10.5	12.993	87.998	2024	5	2	14	49
69	27 4	22	SO305 1 1425	1.9	1.9	12.993	87.998	2024	5	2	14	50
71	28 1	4	SO305 1 1451	3002.8	3042	13.000	89.002	2024	5	3	0	23
71	28 1	9	SO305 1 1456	2000.7	2022	13.000	89.002	2024	5	3	0	43
71	28 1	10	SO305 1 1457	1500.1	1514.3	13.000	89.002	2024	5	3	0	53
71	28 1	11	SO305 1 1458	1000.1	1008.3	13.000	89.002	2024	5	3	1	3
71	28 1	19	SO305 1 1466	501	504.5	13.000	89.002	2024	5	3	1	17
72	28 2	1	SO305 1 1470	423.8	426.7	13.000	89.002	2024	5	3	2	25
72	28 2	10	SO305 1 1479	135.3	136.2	13.000	89.002	2024	5	3	2	34
72	28 2	11	SO305 1 1480	99.6	100.2	13.000	89.002	2024	5	3	2	35
72	28 2	15	SO305 1 1484	80.4	80.8	13.000	89.002	2024	5	3	2	37
72	28 2	16	SO305 1 1485	50.7	51	13.000	89.002	2024	5	3	2	38
72	28 2	17	SO305 1 1486	31	31.2	13.000	89.002	2024	5	3	2	40
72	28 2	18	SO305 1 1487	9.9	10	13.000	89.002	2024	5	3	2	41
72	28 2	22	SO305 1 1491	2.4	2.4	13.000	89.002	2024	5	3	2	42
76	30 3	1	SO305 1 1558	1000.1	1008.4	14.000	88.000	2024	5	4	6	8
76	30 3	7	SO305 1 1564	500.2	503.7	14.000	88.000	2024	5	4	6	20
76	30 3	13	SO305 1 1570	200.4	201.6	14.000	88.000	2024	5	4	6	28
76	30 3	16	SO305 1 1573	100.8	101.4	14.000	88.000	2024	5	4	6	32
76	30 3	17	SO305 1 1574	80.6	81.1	14.000	88.000	2024	5	4	6	33
76	30 3	18	SO305 1 1575	75.8	76.3	14.000	88.000	2024	5	4	6	34
76	30 3	19	SO305 1 1576	50.8	51.2	14.000	88.000	2024	5	4	6	36
76	30 3	20	SO305 1 1577	30.9	31.1	14.000	88.000	2024	5	4	6	37
76	30 3	21	SO305 1 1578	11	11.1	14.000	88.000	2024	5	4	6	38
76	30 3	22	SO305 1 1579	2	2	14.000	88.000	2024	5	4	6	39
77	30 4	4	SO305 1 1583	2938	2976	14.000	88.000	2024	5	4	8	32
77	30 4	8	SO305 1 1587	2000.2	2021.6	14.000	88.000	2024	5	4	8	49
77	30 4	9	SO305 1 1588	1500.6	1514.8	14.000	88.000	2024	5	4	8	59
79	30 8	13	SO305 1 1636	209.7	211.1	13.994	87.985	2024	5	4	18	8
79	30 8	16	SO305 1 1639	100.6	101.2	13.994	87.985	2024	5	4	18	12
79	30 8	18	SO305 1 1641	80.8	81.3	13.994	87.985	2024	5	4	18	14
79	30 8	19	SO305 1 1642	51.2	51.5	13.994	87.985	2024	5	4	18	15
79	30 8	20	SO305 1 1643	31.4	31.6	13.994	87.985	2024	5	4	18	17
79	30 8	21	SO305 1 1644	11.4	11.5	13.994	87.985	2024	5	4	18	19
79	30 8	22	SO305 1 1645	3.3	3.3	13.994	87.985	2024	5	4	18	20
83	31 1	1	SO305 1 1712	2940.7	2978.8	14.499	87.000	2024	5	5	11	22
83	31 1	3	SO305 1 1714	1501.1	1515.4	14.499	87.000	2024	5	5	11	48
83	31 1	9	SO305 1 1720	500.2	503.7	14.499	87.000	2024	5	5	12	9
83	31 1	11	SO305 1 1722	321.1	323.2	14.499	87.000	2024	5	5	12	14
83	31 1	14	SO305 1 1725	225.3	226.8	14.499	87.000	2024	5	5	12	18
83	31 1	17	SO305 1 1728	100.5	101.1	14.499	87.000	2024	5	5	12	22
83	31 1	18	SO305 1 1729	76.3	76.8	14.499	87.000	2024	5	5	12	24
83	31 1	19	SO305 1 1730	50.2	50.5	14.499	87.000	2024	5	5	12	25
83	31 1	20	SO305 1 1731	30.8	31	14.499	87.000	2024	5	5	12	27
83	31 1	21	SO305 1 1732	10.5	10.6	14.499	87.000	2024	5	5	12	28
83	31 1	22	SO305 1 1733	2.8	2.8	14.499	87.000	2024	5	5	12	29
86	32 4	4	SO305 1 1781	2900.5	2937.9	14.991	85.745	2024	5	6	3	45
86	32 4	8	SO305 1 1785	2000.7	2022.1	14.991	85.746	2024	5	6	4	2
86	32 4	9	SO305 1 1786	1500.3	1514.6	14.991	85.746	2024	5	6	4	11
86	32 4	10	SO305 1 1787	1000.1	1008.4	14.991	85.746	2024	5	6	4	20
86	32 4	16	SO305 1 1793	501	504.6	14.991	85.746	2024	5	6	4	34
87	32 5	4	SO305 1 1803	150.4	151.4	14.991	85.746	2024	5	6	5	59
87	32 5	10	SO305 1 1809	nan	nan	nan	nan	nan	nan	nan	nan	nan
87	32 5	14	SO305 1 1813	89.9	90.5	14.991	85.746	2024	5	6	6	6
87	32 5	19	SO305 1 1818	50.5	50.8	14.991	85.746	2024	5	6	6	10
87	32 5	20	SO305 1 1819	30.8	31	14.991	85.746	2024	5	6	6	11
87	32 5	21	SO305 1 1820	11.4	11.4	14.991	85.746	2024	5	6	6	12

87	32 5	22	SO305 1 1821	3.1	3.1	14.991	85.746	2024	5	6	6	13
91	32 14	13	SO305 1 1900	169.3	170.4	14.969	85.732	2024	5	6	17	54
91	32 14	16	SO305 1 1903	101.7	102.3	14.969	85.732	2024	5	6	17	58
91	32 14	17	SO305 1 1904	86.8	87.4	14.969	85.732	2024	5	6	18	0
91	32 14	19	SO305 1 1906	40	40.2	14.969	85.732	2024	5	6	18	2
91	32 14	20	SO305 1 1907	30.2	30.4	14.969	85.732	2024	5	6	18	3
91	32 14	21	SO305 1 1908	10.6	10.6	14.969	85.732	2024	5	6	18	5
91	32 14	22	SO305 1 1909	4	4.1	14.969	85.732	2024	5	6	18	6
97	35 2	8	SO305 1 2027	2000.8	2022.3	15.000	87.998	2024	5	8	19	24
97	35 2	9	SO305 1 2028	1501	1515.3	15.000	87.998	2024	5	8	19	34
97	35 2	10	SO305 1 2029	1000	1008.3	15.000	87.998	2024	5	8	19	43
97	35 2	15	SO305 1 2034	501.2	504.7	15.000	87.998	2024	5	8	19	57
97	35 2	17	SO305 1 2036	401	403.7	15.000	87.998	2024	5	8	20	1
97	35 2	21	SO305 1 2040	345.4	347.8	15.000	87.998	2024	5	8	20	2
98	35 4	2	SO305 1 2043	200.8	202.1	15.000	87.998	2024	5	8	21	28
98	35 4	8	SO305 1 2049	100.8	101.4	15.000	87.997	2024	5	8	21	33
98	35 4	12	SO305 1 2053	83.1	83.6	15.000	87.997	2024	5	8	21	35
98	35 4	16	SO305 1 2057	53.7	54	15.000	87.997	2024	5	8	21	37
98	35 4	17	SO305 1 2058	31.5	31.7	15.000	87.998	2024	5	8	21	39
98	35 4	18	SO305 1 2059	10.6	10.6	15.000	87.998	2024	5	8	21	40
98	35 4	19	SO305 1 2060	4.1	4.1	15.000	87.998	2024	5	8	21	42
102	37 1	1	SO305 1 2130	2678.8	2711.9	NaN	89.600	2024	5	9	16	51
102	37 1	8	SO305 1 2137	2001.1	2022.5	NaN	89.600	2024	5	9	17	5
102	37 1	12	SO305 1 2141	1500.6	1514.9	NaN	89.600	2024	5	9	17	15
102	37 1	13	SO305 1 2142	1000.8	1009.1	NaN	89.600	2024	5	9	17	25
102	37 1	19	SO305 1 2148	500.9	504.4	NaN	89.600	2024	5	9	17	41
103	37 3	1	SO305 1 2152	300.2	302.2	NaN	89.602	2024	5	9	19	9
103	37 3	3	SO305 1 2154	220.9	222.3	NaN	89.602	2024	5	9	19	12
103	37 3	8	SO305 1 2159	101.1	101.7	NaN	89.602	2024	5	9	19	21
103	37 3	12	SO305 1 2163	71.3	71.8	NaN	89.602	2024	5	9	19	23
103	37 3	16	SO305 1 2167	41.3	41.6	NaN	89.602	2024	5	9	19	25
103	37 3	17	SO305 1 2168	31.5	31.7	NaN	89.602	2024	5	9	19	26
103	37 3	18	SO305 1 2169	11.4	11.5	NaN	89.602	2024	5	9	19	28
103	37 3	22	SO305 1 2173	3.1	3.2	NaN	89.602	2024	5	9	19	30
105	37 5	1	SO305 1 2196	999.5	1007.9	NaN	89.632	2024	5	10	6	29
105	37 5	7	SO305 1 2202	500.6	504.1	NaN	89.632	2024	5	10	6	42
105	37 5	9	SO305 1 2204	399.1	401.8	NaN	89.631	2024	5	10	6	45
105	37 5	16	SO305 1 2211	125.8	126.6	NaN	89.632	2024	5	10	6	56
105	37 5	17	SO305 1 2212	101	101.6	NaN	89.632	2024	5	10	6	57
105	37 5	18	SO305 1 2213	61.1	61.4	NaN	89.632	2024	5	10	6	59
105	37 5	19	SO305 1 2214	50.4	50.7	NaN	89.632	2024	5	10	7	0
105	37 5	20	SO305 1 2215	31.1	31.2	NaN	89.632	2024	5	10	7	2
105	37 5	21	SO305 1 2216	10.5	10.6	NaN	89.632	2024	5	10	7	3
105	37 5	22	SO305 1 2217	1.8	1.8	NaN	89.632	2024	5	10	7	4
110	38 2	1	SO305 1 2306	2523.4	2553.8	NaN	89.600	2024	5	10	21	54
110	38 2	6	SO305 1 2311	2000.7	2022.3	NaN	89.600	2024	5	10	22	7
110	38 2	7	SO305 1 2312	1501	1515.4	NaN	89.600	2024	5	10	22	17
110	38 2	14	SO305 1 2319	501	504.6	NaN	89.600	2024	5	10	22	43
111	38 4	8	SO305 1 2335	139.3	140.2	NaN	89.600	2024	5	11	0	26
111	38 4	11	SO305 1 2338	80	80.4	NaN	89.600	2024	5	11	0	31
111	38 4	12	SO305 1 2339	51	51.3	NaN	89.600	2024	5	11	0	33
111	38 4	13	SO305 1 2340	36	36.2	NaN	89.600	2024	5	11	0	34
111	38 4	19	SO305 1 2346	4.2	4.2	NaN	89.600	2024	5	11	0	39

Table 11.4 List of underway samples of halogenated methanes.

Date/Time UTC	Date/Time Local	Number
16.04.2024 12:00	16.04.2024 18:00	30520004
16.04.2024 18:00	17.04.2024 00:00	30520010
17.04.2024 00:00	17.04.2024 06:00	30520016
17.04.2024 06:00	17.04.2024 12:00	30520022
17.04.2024 12:00	17.04.2024 18:00	30520028
17.04.2024 18:00	18.04.2024 00:00	30520034
18.04.2024 00:00	18.04.2024 06:00	30520040
18.04.2024 06:00	18.04.2024 12:00	30520046
18.04.2024 12:00	18.04.2024 18:00	30520052
18.04.2024 18:00	19.04.2024 00:00	30520058
19.04.2024 00:00	19.04.2024 06:00	30520064
19.04.2024 06:00	19.04.2024 12:00	30520070
19.04.2024 12:00	19.04.2024 18:00	30520076
19.04.2024 18:00	20.04.2024 00:00	30520082
20.04.2024 00:00	20.04.2024 06:00	30520088
20.04.2024 06:00	20.04.2024 12:00	30520094
20.04.2024 12:00	20.04.2024 18:00	30520100
20.04.2024 18:00	21.04.2024 00:00	30520106
21.04.2024 00:00	21.04.2024 06:00	30520112
21.04.2024 06:00	21.04.2024 12:00	30520118
21.04.2024 12:00	21.04.2024 18:00	30520124
22.04.2024 00:00	22.04.2024 06:00	30520136
22.04.2024 06:00	22.04.2024 12:00	30520142
22.04.2024 12:00	22.04.2024 18:00	30520148
22.04.2024 18:00	23.04.2024 00:00	30520154
23.04.2024 00:00	23.04.2024 06:00	30520160
23.04.2024 06:00	23.04.2024 12:00	30520166
23.04.2024 12:00	23.04.2024 18:00	30520172
24.04.2024 00:00	24.04.2024 06:00	30520184
24.04.2024 06:00	24.04.2024 12:00	30520190
24.04.2024 12:00	24.04.2024 18:00	30520196
25.04.2024 00:00	25.04.2024 06:00	30520208
25.04.2024 06:00	25.04.2024 12:00	30520214
25.04.2024 12:00	25.04.2024 18:00	30520220
26.04.2024 00:00	26.04.2024 06:00	30520232
26.04.2024 06:00	26.04.2024 12:00	30520238
26.04.2024 12:00	26.04.2024 18:00	30520244
26.04.2024 18:00	27.04.2024 00:00	30520250
27.04.2024 00:00	27.04.2024 06:00	30520256
27.04.2024 06:00	27.04.2024 12:00	30520262
27.04.2024 12:00	27.04.2024 18:00	30520268
28.04.2024 00:00	28.04.2024 06:00	30520280
28.04.2024 06:00	28.04.2024 12:00	30520286
28.04.2024 12:00	28.04.2024 18:00	30520292
29.04.2024 00:00	29.04.2024 06:00	30520304
29.04.2024 06:00	29.04.2024 12:00	30520310
29.04.2024 12:00	29.04.2024 18:00	30520316
29.04.2024 18:00	30.04.2024 00:00	30520322
30.04.2024 00:00	30.04.2024 06:00	30520328
30.04.2024 03:00	30.04.2024 09:00	30520331
30.04.2024 06:00	30.04.2024 12:00	30520334
30.04.2024 12:00	30.04.2024 18:00	30520340
30.04.2024 18:00	01.05.2024 00:00	30520346
01.05.2024 00:00	01.05.2024 06:00	30520352
01.05.2024 06:00	01.05.2024 12:00	30520358
01.05.2024 12:00	01.05.2024 18:00	30520364
02.05.2024 00:00	02.05.2024 06:00	30520376
02.05.2024 06:00	02.05.2024 12:00	30520382
02.05.2024 12:00	02.05.2024 18:00	30520388
02.05.2024 18:00	03.05.2024 00:00	30520394
03.05.2024 00:00	03.05.2024 06:00	30520400
03.05.2024 06:00	03.05.2024 12:00	30520406
03.05.2024 12:00	03.05.2024 18:00	30520412
04.05.2024 06:00	04.05.2024 12:00	30520430
04.05.2024 12:00	04.05.2024 18:00	30520436
04.05.2024 18:00	05.05.2024 00:00	30520442
05.05.2024 00:00	05.05.2024 06:00	30520448
05.05.2024 06:00	05.05.2024 12:00	30520454
05.05.2024 12:00	05.05.2024 18:00	30520460
05.05.2024 18:00	06.05.2024 00:00	30520466
06.05.2024 00:00	06.05.2024 06:00	30520472
06.05.2024 06:00	06.05.2024 12:00	30520478
06.05.2024 12:00	06.05.2024 18:00	30520484
07.05.2024 00:00	07.05.2024 06:00	30520496
07.05.2024 06:00	07.05.2024 12:00	30520502
07.05.2024 12:00	07.05.2024 18:00	30520508
08.05.2024 00:00	08.05.2024 06:00	30520520
08.05.2024 06:00	08.05.2024 12:00	30520526
08.05.2024 12:00	08.05.2024 18:00	30520532
08.05.2024 18:00	09.05.2024 00:00	30520538

09.05.2024 00:00	09.05.2024 06:00	30520544
09.05.2024 06:00	09.05.2024 12:00	30520550
09.05.2024 12:00	09.05.2024 18:00	30520556
10.05.2024 06:00	10.05.2024 12:00	30520574
10.05.2024 12:00	10.05.2024 18:00	30520580
11.05.2024 07:00	11.05.2024 13:00	30520599

Table 11.5 List of underway air samples.

			Canister numbers		
Date/Time UTC	Date/Time Local	Number		Double	Kiel
16.04.2024 18:00	17.04.2024 00:00	30520010	914		781
17.04.2024 18:00	18.04.2024 00:00	30520034	720	956	916
18.04.2024 12:00	18.04.2024 18:00	30520052	907	851	677
18.04.2024 18:00	19.04.2024 00:00	30520058	919		
19.04.2024 13:00	19.04.2024 19:00	30520077	726	802	689/921
19.04.2024 18:00	20.04.2024 00:00	30520082	692		
20.04.2024 06:00	20.04.2024 12:00	30520094	548		
20.04.2024 18:00	21.04.2024 00:00	30520106	737	918	945
21.04.2024 09:00	21.04.2024 15:00	30520121	543		
21.04.2024 18:00	22.04.2024 00:00	30520130	992	780	675
22.04.2024 09:00	22.04.2024 15:00	30520145	790		790
22.04.2024 18:00	23.04.2024 00:00	30520154	540		
23.04.2024 13:00	23.04.2024 19:00	30520173	903		
24.04.2024 07:00	24.04.2024 13:00	30520191	763		
24.04.2024 12:00	24.04.2024 18:00	30520196	836		
24.04.2024 18:00	25.04.2024 00:00	30520202	779		
25.04.2024 09:00	25.04.2024 15:00	30520217	535	593	969
25.04.2024 12:00	25.04.2024 18:00	30520220	530		
25.04.2024 18:00	26.04.2024 00:00	30520226	566		
26.04.2024 12:00	26.04.2024 18:00	30520244	799	855	927
26.04.2024 18:00	27.04.2024 00:00	30520250	613		
27.04.2024 07:00	27.04.2024 13:00	30520263	952	958	661
27.04.2024 12:00	27.04.2024 18:00	30520268	718		
27.04.2024 18:00	28.04.2024 00:00	30520274	917		
28.04.2024 06:00	28.04.2024 12:00	30520286	589		
28.04.2024 12:00	28.04.2024 18:00	30520292	935		
28.04.2024 18:00	29.04.2024 00:00	30520298	808		
29.04.2024 07:00	29.04.2024 13:00	30520311	744		
29.04.2024 12:00	29.04.2024 18:00	30520316	750		
29.04.2024 18:00	30.04.2024 00:00	30520322	913		
30.04.2024 08:00	30.04.2024 14:00	30520336	567	560	
30.04.2024 13:00	30.04.2024 19:00	30520341	762		
30.04.2024 18:00	01.05.2024 00:00	30520346	923		
01.05.2024 09:00	01.05.2024 15:00	30520361	820		
01.05.2024 12:00	01.05.2024 18:00	30520364	685		
01.05.2024 18:00	02.05.2024 00:00	30520370	577	759	544
02.05.2024 08:00	02.05.2024 14:00	30520384	747		
02.05.2024 12:00	02.05.2024 18:00	30520388	782		
02.05.2024 18:00	03.05.2024 00:00	30520394	550		
03.05.2024 09:00	03.05.2024 15:00	30520409	809		
03.05.2024 12:00	03.05.2024 18:00	30520412	978	412	
03.05.2024 23:00	04.05.2024 05:00	30520423	963		
04.05.2024 13:00	04.05.2024 19:00	30520437	940	804	
05.05.2024 07:00	05.05.2024 13:00	30520455	971	791	999
05.05.2024 12:00	05.05.2024 18:00	30520460	766		
05.05.2024 18:00	06.05.2024 00:00	30520466	756		
06.05.2024 06:00	06.05.2024 12:00	30520478	667		
06.05.2024 12:00	06.05.2024 18:00	30520484	605		
06.05.2024 20:00	07.05.2024 02:00	30520492	925		
07.05.2024 07:00	07.05.2024 13:00	30520503	911		581
07.05.2024 12:00	07.05.2024 18:00	30520508	857		
08.05.2024 09:00	08.05.2024 15:00	30520529	678		
08.05.2024 12:00	08.05.2024 18:00	30520532	704		
08.05.2024 19:00	09.05.2024 01:00	30520539	646		662
09.05.2024 09:00	09.05.2024 15:00	30520553	973		854
09.05.2024 19:00	10.05.2024 01:00	30520563	694		
10.05.2024 10:00	10.05.2024 16:00	30520578	611		
10.05.2024 17:00	10.05.2024 23:00	30520585	725		942
10.05.2024 18:00	11.05.2024 00:00	30520586	722		
10.05.2024 20:00	11.05.2024 02:00	30520588	946	906	850
11.05.2024 02:00	11.05.2024 08:00	30520594	691	753	949
11.05.2024 06:00	11.05.2024 12:00	30520598	770	795	964
11.05.2024 08:00	11.05.2024 14:00	30520600	658	777	

Table 11.6 List of underway pigment samples.

Sample	Bedford ID	Date	Time	Filtered	Sample Bottle	Remarks	
SO305	So305_2_0004	16.04.202	12:00	2L	1	More then 1h filtration	
SO305	SO305_2_0010	16.04.202	18:00	2L	3		
SO305	SO305_2_0016	17.04.202	00:00	2L	6	300 mbar	
SO305	SO305_2_0022	17.04.202	06:00	2L	3		
SO305	SO305_1_0072	17.04.202		2L	1	Flow-cyto A+B zu voll	
SO305	SO305_1_0075	17.04.202		2L	2		
SO305	SO305_1_0076	17.04.202		1.8L	3		
SO305	SO305_1_0080	17.04.202		1.6L	4		
SO305	SO305_1_0081	17.04.202		2L	5		
SO305	SO305_1_0082	17.04.202		2L	6		
SO305	SO305_2_0028	17.04.202	12:00	2L	1		
SO305	SO305_2_0034	17.04.202	18:00	2L	4	Filter kurz trocken gesaugt	
SO305	SO305_2_0040	18.04.202	00:00	2L	6		
SO305	SO305_2_0046	18.04.202	06:00	2L	5		
SO305	SO305_1_0137	18.04.202		1.152L	1		
SO305	SO305_1_0143	18.04.202		2L	2		
SO305	SO305_1_0147	18.04.202		2L	3		
SO305	SO305_1_0149	18.04.202		2L	4		
SO305	SO305_1_0150	18.04.202		2L	5		
SO305	SO305_1_0155	18.04.202		2L	6		
SO305	SO305_2_0052	18.04.202	12:00	2L	3		
SO305	SO305_2_0058	18.04.202	18:00	2L	3		
SO305	SO305_1_0186	19.04.202	00:00	2L	1		
SO305	SO305_1_0189	19.04.202	00:00	2L	2		
SO305	SO305_1_0190	19.04.202	00:00	2L	3		
SO305	SO305_1_0191	19.04.202	00:00	2L	4		
SO305	SO305_1_0192	19.04.202	00:00	2L	5		
SO305	SO305_1_0193	19.04.202	00:00	2L	6		
SO305	SO305_2_0070	19.04.202	06:00	2L	1		
SO305	SO305_1_0221	19.04.202		2L	1		
SO305	SO305_1_0225	19.04.202		2L	2		
SO305	SO305_1_0229	19.04.202		2L	3		
SO305	SO305_1_0231	19.04.202		2L	4		
SO305	SO305_1_0232	19.04.202		2L	5		
SO305	SO305_1_0237	19.04.202		2L	6		
SO305	SO305_2_0076	19.04.202	12:00	2L	3		
SO305	SO305_2_0082	19.04.202	18:00	2L	4	Pigmentfilter der Probe SO305_2_0082 in	
SO305	SO305_1_0252	20.04.202	05:15	2L	1		
SO305	SO305_1_0255	20.04.202	05:15	2L	2		
SO305	SO305_1_0256	20.04.202	05:15	2L	3		
SO305	SO305_1_0257	20.04.202	05:15	2L	4		
SO305	SO305_1_0258	20.04.202	05:15	2L	5		
SO305	SO305_1_0259	20.04.202	05:15	2L	6	Nur Flow Cyto	
SO305	SO305_1_0259	20.04.202	05:15	2L	6	Nur Pigmentfilter	
SO305	SO305_2_0094	20.04.202	06:00	2L	3		
SO305	SO305_1_0288	20.04.202		2L	1		
SO305	SO305_1_0291	20.04.202		2L	2		
SO305	SO305_1_0292	20.04.202		2L	3		
SO305	SO305_1_0297	20.04.202		2L	4		
SO305	SO305_1_0298	20.04.202		2L	5		
SO305	SO305_1_0303	20.04.202		2L	6		
SO305	SO305_2_0100	20.04.202	12:00	2L	-	Kühlschrank für 1.5h	
SO305	SO305_2_0106	20.04.202	18:00	2L	6		
SO305	SO305_1_0318	20.04.202	22:40	2L	1		
SO305	SO305_1_0321	20.04.202	22:40	2L	2		
SO305	SO305_1_0322	20.04.202	22:40	2L	3		
SO305	SO305_1_0323	20.04.202	22:40	2L	4		
SO305	SO305_1_0324	20.04.202	22:40	2L	5		
SO305	SO305_1_0325	20.04.202	22:40	2L	6		
SO305	SO305_2_0112	21.04.202	00:00	2L	-		
SO305	SO305_2_0118	21.04.202	06:00	2L	4		
SO305	SO305_2_0124	21.04.202	12:00	2L	-		
SO305	SO305_1_0362	21.04.202	13:00	2L	1		
SO305	SO305_1_0364	21.04.202	13:00	2L	2		
SO305	SO305_1_0365	21.04.202	13:00	2L	3		
SO305	SO305_1_0352	21.04.202	13:00	820	4		
SO305	SO305_1_0355	21.04.202	13:00	2L	5		
SO305	SO305_1_0357	21.04.202	13:00	2L	6		
SO305	SO305_2_0130	21.04.202	06:00	2L	2		
SO305	SO305_1_0406	22.04.202	01:30	2L	1		
SO305	SO305_1_0407	22.04.202	01:30	2L	2		
SO305	SO305_1_0409	22.04.202	01:30	2L	3		
SO305	SO305_1_0410	22.04.202	01:30	2L	4		
SO305	SO305_1_0411	22.04.202	01:30	2L	5		
SO305	SO305_1_0412	22.04.202	01:30	2L	6		
SO305	SO305_2_0136	22.04.202	00:03	2L	4		
SO305	SO305_X_0001	22.04.202		2L	Braunglasflasc	Zodiac	
SO305	SO305_1_0428	22.04.202	04:30	2L	1		
SO305	SO305_1_0429	22.04.202	04:30	2L	2		
SO305	SO305_1_0431	22.04.202	04:30	2L	3		
SO305	SO305_1_0432	22.04.202	04:30	2L	4		

SO305	SO305_1_0433	22.04.202	04:30	2L	5		
SO305	SO305_1_0434	22.04.202	04:30	2L	6	Fiter lag nicht richtig drauf. 50mL weniger	
SO305	SO305_2_0142	22.04.202	06:30	2L	1	nach starkem Regen	
SO305	SO305_1_0472	22.04.202		2L	1		
SO305	SO305_1_0473	22.04.202		2L	2		
SO305	SO305_1_0475	22.04.202		2L	3		
SO305	SO305_1_0476	22.04.202		2L	4		
SO305	SO305_1_0477	22.04.202				Nicht geschlossen	
SO305	SO305_1_0478	22.04.202		2L	6		
SO305	SO305_2_0148	22.04.202	12:00	2L	-		
SO305	SO305_2_0154	22.04.202	18:00	2L	6		
SO305	SO305_1_0506	22.04.202	22:00	2L	1		
SO305	SO305_1_0511	22.04.202	22:00	2L	2		
SO305	SO305_1_0516	22.04.202	22:00	2L	3		
SO305	SO305_1_0517	22.04.202	22:00	2L	4		
SO305	SO305_1_0518	22.04.202	22:00	2L	5		
SO305	SO305_1_0523	22.04.202	22:00	2L	6		
SO305	SO305_2_0160	23.04.202	00:00	2L	-		
SO305	SO305_2_0166	23.04.202	06:00	2L	2		
SO305	SO305_2_0172	23.04.202	12:00	2L	-		
SO305	SO305_2_0184	24.04.202	00:00	2L	-		
SO305	SO305_2_0190	24.04.202	06:00	2L	2		
SO305	SO305_1_0592	24.04.202		2L	1	Filter lag nicht richtig drauf	
SO305	SO305_1_0594	24.04.202		2L	2		
SO305	SO305_1_0595	24.04.202		2L	3		
SO305	SO305_1_0596	24.04.202		2L	4		
SO305	SO305_1_0601	24.04.202		2L	5		
SO305	SO305_1_0608	24.04.202		2L	6		
SO305	SO305_2_0196	24.04.202	12:00	2L	-		
SO305	SO305_1_0627	24.04.202	17:00	2L	1		
SO305	SO305_1_0629	24.04.202	17:00	2L	2		
SO305	SO305_1_0630	24.04.202	17:00	2L	3		
SO305	SO305_1_0631	24.04.202	17:00	2L	4		
SO305	SO305_1_0632	24.04.202	17:00	2L	5		
SO305	SO305_1_0633	24.04.202	17:00	2.1L	6		
SO305	SO305_2_0208	25.04.202	00:00	2L	-		
SO305	SO305_2_0214	25.04.202	06:00	2L	5		
SO305	SO305_1_0685	25.04.202	08:00	2L	1		
SO305	SO305_1_0687	25.04.202	08:00	2L	2		
SO305	SO305_1_0688	25.04.202	08:00	2L	3		
SO305	SO305_1_0692	25.04.202	08:00	2L	4	Position dichtet nicht richtig ab, Disc	
SO305	SO305_1_0694	25.04.202	08:00	2L	5		
SO305	SO305_1_0699	25.04.202	08:00	2L	6		
SO305	SO305_2_0220	25.04.202	12:00	2L	-		
SO305	SO305_1_0736	25.04.202	19:00	2L	1		
SO305	SO305_1_0739	25.04.202	19:00	2L	2		
SO305	SO305_1_0740	25.04.202	19:00	2L	3		
SO305	SO305_1_0741	25.04.202	19:00			Nicht geschlossen	
SO305	SO305_1_0742	25.04.202	19:00	2L	5		
SO305	SO305_1_0743	25.04.202	19:00	2L	6		
SO305	SO305_2_0226	25.04.202	18:00	2L	-		
SO305	SO305_2_0232	26.04.202	00:00	2L	-		
SO305	SO305_2_0238	26.04.202	06:00	2L	2		
SO305	SO305_1_0781	26.04.202		2L	1		
SO305	SO305_1_0783	26.04.202		2L	2		
SO305	SO305_1_0784	26.04.202		2L	3		
SO305	SO305_1_0785	26.04.202		2L	4		
SO305	SO305_1_0786	26.04.202		2L	5		
SO305	SO305_1_0787	26.04.202		2L	6		
SO305	SO305_2_0244	26.04.202	12:00	2L	-		
SO305	SO305_2_0250	26.04.202	18:00	2L	-		
SO305	SO305_1_0823	26.04.202	23:00	2L	1		
SO305	SO305_1_0824	26.04.202	23:00	2L	2		
SO305	SO305_1_0825	26.04.202	23:00	2L	3	Flow-cyto C in 129C aber A+ B in 145	
SO305	SO305_1_0826	26.04.202	23:00	2L	4		
SO305	SO305_1_0827	26.04.202	23:00	2L	5		
SO305	SO305_1_0831	26.04.202	23:00	2L	6		
SO305	SO305_X_0002	27.04.202	02:45	2L	3	Zodiac	
SO305	SO305_1_0869	27.04.202	08:30	2L	1		
SO305	SO305_1_0870	27.04.202	08:30	2L	2		
SO305	SO305_1_0871	27.04.202	08:30	2L	3		
SO305	SO305_1_0872	27.04.202	08:30	2L	4		
SO305	SO305_1_0873	27.04.202	08:30	2L	5		
SO305	SO305_1_0875	27.04.202	08:30	2L	6		
SO305	SO305_1_0935	27.04.202	14:00	2L	1		
SO305	SO305_1_0936	27.04.202	14:00	2L	2		
SO305	SO305_1_0937	27.04.202	14:00	2L	3		
SO305	SO305_1_0938	27.04.202	14:00	2L	4		
SO305	SO305_1_0939	27.04.202	14:00	2L	5		
SO305	SO305_1_0940	27.04.202	14:00	2L	6		
SO305	SO305_1_0979	27.04.202	18:00	2L	1		
SO305	SO305_1_0980	27.04.202	18:00	2L	2		
SO305	SO305_1_0981	27.04.202	18:00	2L	3		

SO305	SO305_1_0982	27.04.202	18:00	2L	4		
SO305	SO305_1_0983	27.04.202	18:00	2L	5		
SO305	SO305_1_0985	27.04.202	18:00	2L	6		
SO305	SO305_2_0280	28.04.202	00:00	2L	-	Filter war nicht mittig	
SO305	SO305_1_1002	28.04.202	03:00	2L	1		
SO305	SO305_1_1003	28.04.202	03:00	2L	2	Filter nicht mittig	
SO305	SO305_1_1004	28.04.202	03:00	2L	3		
SO305	SO305_1_1006	28.04.202	03:00	2L	5		
SO305	SO305_1_1007	28.04.202	03:00	2L	6		
SO305	SO305_2_0286	28.04.202	06:00	2L	3		
SO305	SO305_1_1035	28.04.202	14:00	2L	1		
SO305	SO305_1_1043	28.04.202	14:00	2L	2		
SO305	SO305_1_1044	28.04.202	14:00	2L	3		
SO305	SO305_1_1045	28.04.202	14:00	2L	4		
SO305	SO305_1_1046	28.04.202	14:00	2L	5		
SO305	SO305_1_1051	28.04.202	14:00	2L	6		
SO305	SO305_2_0304	29.04.202	00:00	2L	-		
SO305	SO305_2_0310	29.04.202	06:00	2L	5	filter was dry for short	
SO305	SO305_2_0316	29.04.202	12:00	2L	-		
SO305	SO305_2_0322	29.04.202	18:00	2L	3		
SO305	SO305_1_1112	29.04.202	22:00	2L	1		
SO305	SO305_1_1113	29.04.202	22:00	2L	2		
SO305	SO305_1_1114	29.04.202	22:00	2L	3		
SO305	SO305_1_1115	29.04.202	22:00	2L	4		
SO305	SO305_1_1116	29.04.202	22:00	2L	5		
SO305	SO305_1_1117	29.04.202	22:00	2L	6		
SO305	SO305_2_0328	30.04.202	00:00	2L	-		
SO305	SO305_2_0334	30.04.202	06:00	2L	5		
SO305	SO305_1_1156	30.04.202		2L	1		
SO305	SO305_1_1157	30.04.202		2L	2		
SO305	SO305_1_1158	30.04.202		2L	3	Probe wahrscheinlich unbrauch bar, undicht	
SO305	SO305_1_1159	30.04.202		2L	4		
SO305	SO305_1_1160	30.04.202		2L	5	Druck zwischendurch bei 0,5 bar	
SO305	SO305_1_1161	30.04.202		2L	6		
SO305	SO305_2_0346	30.04.202	18:00	2L	5		
SO305	SO305_2_0352	01.05.202	00:00	2L	-		
SO305	SO305_1_1238	01.05.202	02:00	2L	1		
SO305	SO305_1_1242	01.05.202	02:00	2L	2		
SO305	SO305_1_1243	01.05.202	02:00	2L	3		
SO305	SO305_1_1244	01.05.202	02:00	2L	4		
SO305	SO305_1_1245	01.05.202	02:00	2L	5		
SO305	SO305_1_1249	01.05.202	02:00	2L	6		
SO305	SO305_2_0358	01.05.202	06:00	2L	5	druck zwischendurch bei 0.4 bar	
SO305	SO305_2_0364	01.05.202	12:00	2L	-		
SO305	SO305_1_1288	01.05.202	12:20	2L	1		
SO305	SO305_1_1289	01.05.202	12:20	2L	2		
SO305	SO305_1_1290	01.05.202	12:20	2L	3		
SO305	SO305_1_1291	01.05.202	12:20	2L	4		
SO305	SO305_1_1292	01.05.202	12:20	2L	5		
SO305	SO305_1_1293	01.05.202	12:20	2L	6		
SO305	SO305_2_0370	01.05.202	18:00	2L	4		
SO305	SO305_2_0376	02.05.202	00:00	2L	-		
SO305	SO305_1_1348	02.05.202	01:45	2L	1		
SO305	SO305_1_1352	02.05.202	01:45	2L	2		
SO305	SO305_1_1353	02.05.202	01:45	2L	3		
SO305	SO305_1_1354	02.05.202	01:45	2L	4		
SO305	SO305_1_1355	02.05.202	01:45	2L	5		
SO305	SO305_1_1359	02.05.202	01:45	2L	6		
SO305	SO305_2_0382	02.05.202	06:00	2L	5		
SO305	SO305_2_0388	02.05.202	12:00	2L	-		
SO305	SO305_1_1420	02.05.202			1		
SO305	SO305_1_1421	02.05.202			2		
SO305	SO305_1_1422	02.05.202			3		
SO305	SO305_1_1423	02.05.202			4		
SO305	SO305_1_1424	02.05.202			5		
SO305	SO305_1_1425	02.05.202			6		
SO305	SO305_2_0394	02.05.202	18:00	2L	5	no Filter on Rack. Only flow cyto	
SO305	SO305_2_0400	02.05.202	00:00	2L	-		
SO305	SO305_1_1480	03.05.202	02:30	2L	1		
SO305	SO305_1_1484	03.05.202	02:30	2L	2		
SO305	SO305_1_1485	03.05.202	02:30	2L	3		
SO305	SO305_1_1486	03.05.202	02:30	2L	4		
SO305	SO305_1_1487	03.05.202	02:30	2L	5		
SO305	SO305_1_1491	03.05.202	02:30	2L	6		
SO305	SO305_2_0406	03.05.202	06:00	2L	5		
SO305	SO305_1_1508	03.05.202	11:30	2L	1		
SO305	SO305_1_1509	03.05.202	11:30	2L	2		
SO305	SO305_1_1510	03.05.202	11:30	2L	3		
SO305	SO305_1_1511	03.05.202	11:30	2L	4		
SO305	SO305_1_1512	03.05.202	11:30	2L	5		
SO305	SO305_1_1513	03.05.202	11:30	2L	6		
SO305	SO305_2_0412	03.05.202	12:00	2L	-		
SO305	SO305_1_1573	04.05.202	06:45	2L	1		

SO305	SO305_1_1575	04.05.202	06:45	2L	2		
SO305	SO305_1_1576	04.05.202	06:45	2L	3		
SO305	SO305_1_1577	04.05.202	06:45	2L	4		
SO305	SO305_1_1578	04.05.202	06:45	2L	5		
SO305	SO305_1_1579	04.05.202	06:45	2L	6		
SO305	SO305_1_1617	04.05.202	11:30	2L	1		
SO305	SO305_1_1619	04.05.202	11:30	2L	2	Filterrand undeutlich. Rack saß nicht	
SO305	SO305_1_1620	04.05.202	11:30	2L	3		
SO305	SO305_1_1621	04.05.202	11:30	2L	4		
SO305	SO305_1_1622	04.05.202	11:30	2L	5		
SO305	SO305_1_1623	04.05.202	11:30	2L	6		
SO305	SO305_1_1639	04.05.202	17:30	2L	1		
SO305	SO305_1_1641	04.05.202	17:30	2L	2		
SO305	SO305_1_1642	04.05.202	17:30	2L	3		
SO305	SO305_1_1643	04.05.202	17:30	2L	4		
SO305	SO305_1_1644	04.05.202	17:30	2L	5		
SO305	SO305_1_1645	04.05.202	17:30	2L	6		
SO305	SO305_1_1683	04.05.202	23:30	2L	1		
SO305	SO305_1_1685	04.05.202	23:30	2L	2		
SO305	SO305_1_1686	04.05.202	23:30	2L	3		
SO305	SO305_1_1687	04.05.202	23:30	2L	4		
SO305	SO305_1_1688	04.05.202	23:30	2L	5		
SO305	SO305_1_1689	04.05.202	23:30	2L	6		
SO305	SO305_2_0454	05.05.202	06:00	2L	-		
SO305	SO305_1_1728	05.05.202	13:00	2L	1		
SO305	SO305_1_1729	05.05.202	13:00	2L	2		
SO305	SO305_1_1730	05.05.202	13:00	2L	3		
SO305	SO305_1_1731	05.05.202	13:00	2L	4		
SO305	SO305_1_1732	05.05.202	13:00	2L	5		
SO305	SO305_1_1733	05.05.202	13:00	2L	6		
SO305	SO305_2_0460	05.05.202	12:00	2L	-		
SO305	SO305_2_0466	05.05.202	18:00	2L	4		
SO305	SO305_1_1749	05.05.202	22:40	2L	1		
SO305	SO305_1_1750	05.05.202	22:40	2L	2		
SO305	SO305_1_1752	05.05.202	22:40	2L	3		
SO305	SO305_1_1754	05.05.202	22:40	2L	5		
SO305	SO305_1_1755	05.05.202	22:40	2L	6		
SO305	SO305_2_0472	06.05.202	00:00	2L	-		
SO305	SO305_1_1809	06.05.202	06:15	2L	1		
SO305	SO305_1_1813	06.05.202	06:15	2L	2		
SO305	SO305_1_1818	06.05.202	06:15	2L	3		
SO305	SO305_1_1819	06.05.202	06:15	2L	4		
SO305	SO305_1_1820	06.05.202	06:15	2L	5		
SO305	SO305_1_1821	06.05.202	06:15	2L	6		
SO305	SO305_1_1838	06.05.202	12:15	2L	1		
SO305	SO305_1_1839	06.05.202	12:15	2L	2		
SO305	SO305_1_1840	06.05.202	12:15	2L	3		
SO305	SO305_1_1841	06.05.202	12:15	2L	4		
SO305	SO305_1_1842	06.05.202	12:15	2L	5		
SO305	SO305_1_1843	06.05.202	12:15	2L	6		
SO305	SO305_1_1903	06.05.202	17:30	2L	1		
SO305	SO305_1_1904	06.05.202	17:30	2L	2		
SO305	SO305_1_1906	06.05.202	17:30	2L	3		
SO305	SO305_1_1907	06.05.202	17:30	2L	4		
SO305	SO305_1_1908	06.05.202	17:30	2L	5		
SO305	SO305_1_1909	06.05.202	17:30	2L	6		
SO305	SO305_2_0496	07.05.202	00:00	2L	-		
SO305	SO305_2_0502	07.05.202	06:00	2L	-		
SO305	SO305_2_0508	07.05.202	12:00	2L	-		
SO305	SO305_2_0514	07.05.202	18:00	2L	-		
SO305	SO305_2_0520	08.05.202	00:00	2L	-		
SO305	SO305_2_0526	08.05.202	06:00	2L	-		
SO305	SO305_1_1983	08.05.202	10:00	2L	1		
SO305	SO305_1_1986	08.05.202	10:00	2L	2		
SO305	SO305_1_1990	08.05.202	10:00	2L	3		
SO305	SO305_1_1992	08.05.202	10:00	2L	4		
SO305	SO305_1_1993	08.05.202	10:00	2L	5		
SO305	SO305_1_1994	08.05.202	10:00	2L	6		
SO305	SO305_2_0532	08.05.202	12:00	2L	-		
SO305	SO305_2_0538	08.05.202	18:00	2L	-		
SO305	SO305_1_2049	08.05.202	22:00	2L	1		
SO305	SO305_1_2053	08.05.202	22:00	2L	2		
SO305	SO305_1_2057	08.05.202	22:00	2L	3		
SO305	SO305_1_2058	08.05.202	22:00	2L	4		
SO305	SO305_1_2059	08.05.202	22:00	2L	5		
SO305	SO305_1_2060	08.05.202	22:00	2L	6		
SO305	SO305_2_0544	09.05.202	00:00	2L	-		
SO305	SO305_2_0550	09.05.202	06:00	2L	-		
SO305	SO305_1_2096	09.05.202	08:10	2L	1		
SO305	SO305_1_2097	09.05.202	08:10	2L	2		
SO305	SO305_1_2101	09.05.202	08:10	2L	3		
SO305	SO305_1_2102	09.05.202	08:10	2L	4		
SO305	SO305_1_2103	09.05.202	08:10	2L	5		

SO305	**SO305_1_2107**	**09.05.202**	**08:10**	**2L**	**6**		
SO305	**SO305_2_0556**	**09.05.202**	**12:00**	**2L**	**-**		
SO305	**SO305_2_0562**	**09.05.202**	**18:00**	**2L**	**-**		
SO305	**SO305_1_2159**	**09.05.202**	**20:00**	**2L**	**1**		
SO305	**SO305_1_2163**	**09.05.202**	**20:00**	**2L**	**2**		
SO305	**SO305_1_2167**	**09.05.202**	**20:00**	**2L**	**3**		
SO305	**SO305_1_2168**	**09.05.202**	**20:00**	**2L**	**4**		
SO305	**SO305_1_2169**	**09.05.202**	**20:00**	**2L**	**5**		
SO305	**SO305_1_2173**	**09.05.202**	**20:00**	**2L**	**6**		
SO305	**SO305_1_2190**	**09.05.202**	**22:45**	**2L**	**1**		
SO305	**SO305_1_2191**	**09.05.202**	**22:45**	**2L**	**2**		
SO305	**SO305_1_2192**	**09.05.202**	**22:45**	**2L**	**3**		
SO305	**SO305_1_2193**	**09.05.202**	**22:45**	**2L**	**4**		
SO305	**SO305_1_2194**	**09.05.202**	**22:45**	**2L**	**5**		
SO305	**SO305_1_2195**	**09.05.202**	**22:45**	**2L**	**6**		
SO305	**SO305_2_0568**	**10.05.202**	**00:00**	**2L**	**-**		
SO305	**Zodiac**	**10.05.202**	**02:00**	**2L**	**Braunglasflasc**	**Zodiac 2m**	
SO305	**SO305_1_2212**	**10.05.202**			**1**		
SO305	**SO305_1_2213**	**10.05.202**			**2**		
SO305	**SO305_1_2214**	**10.05.202**			**3**		
SO305	**SO305_1_2215**	**10.05.202**			**4**		
SO305	**SO305_1_2216**	**10.05.202**			**5**		
SO305	**SO305_1_2217**	**10.05.202**			**6**		
SO305	**SO305_1_2278**	**10.05.202**	**12:20**	**2L**	**1**	**sehr lange gelaufen wegen Pumpenproblem**	
SO305	**SO305_1_2279**	**10.05.202**	**12:20**	**2L**	**2**	**sehr lange gelaufen wegen Pumpenproblem**	
SO305	**SO305_1_2280**	**10.05.202**	**12:20**	**2L**	**3**	**sehr lange gelaufen wegen Pumpenproblem**	
SO305	**SO305_1_2281**	**10.05.202**	**12:20**	**2L**	**4**	**leaked, sehr lange gelaufen wegen**	
SO305	**SO305_1_2282**	**10.05.202**	**12:20**	**2L**	**5**	**sehr lange gelaufen wegen Pumpenproblem**	
SO305	**SO305_1_2283**	**10.05.202**	**12:20**	**2L**	**6**	**leaked, sehr lange gelaufen wegen**	
SO305	**SO305_2_0592**	**11.05.202**	**00:00**	**2L**	**-**		
SO305	**SO305_1_2338**	**11.05.202**	**01:45**	**2L**	**1**		
SO305	**SO305_1_2339**	**11.05.202**	**01:45**	**2L**	**2**		
SO305	**SO305_1_2340**	**11.05.202**	**01:45**	**2L**	**3**		
SO305	**SO305_1_2346**	**11.05.202**	**01:45**	**2L**	**6**		

Table 11.7 List of samples from drifting sediment traps.

Date	Time [UTC]	Station	CTD/ TRAP cast	depth [m]	POC/N, TPC, PAA, PCHO, lipids, POP, BSi, TEP, CSP	mass, micro-plastics	gel traps	meta-g (DNA)	meta-t (RNA), EEA	flow cytom.
22.04.24	05:10	SO305/10-13	CTD #1 deploy Cast 023	5	x					x
22.04.24	05:10	SO305/10-13		50	x			x	x	x
22.04.24	05:10	SO305/10-13		100	x					x
22.04.24	05:10	SO305/10-13		150	x					x
22.04.24	05:10	SO305/10-13		200	x					x
22.04.24	05:10	SO305/10-13		300	x			x	x	x
22.04.24	05:10	SO305/10-13		400	x					x
22.04.24	05:10	SO305/10-13		500	x					x
22.04.24	05:10	SO305/10-13		600	x			x	x	x
23.04.24	09:31	SO305/12-2	CTD #1 recover Cast 027	5	x					x
23.04.24	09:31	SO305/12-2		50	x			x	x	x
23.04.24	09:31	SO305/12-2		100	x					x
23.04.24	09:31	SO305/12-2		150	x					x
23.04.24	09:31	SO305/12-2		200	x			x	x	x
23.04.24	09:31	SO305/12-2		300	x					x
23.04.24	09:31	SO305/12-2		400	x					x
23.04.24	09:31	SO305/12-2		500	x			x	x	x
23.04.24	09:31	SO305/12-2		600	x					x
23.04.24	08:48	SO305/12-1	**TRAP #1**	50	x	x	x		x	
23.04.24	08:48	SO305/12-1		100	x	x	x			
23.04.24	08:48	SO305/12-1		150	x	x	x			
23.04.24	08:48	SO305/12-1		200	x	x	x			
23.04.24	08:48	SO305/12-1		300	x	x				
23.04.24	08:48	SO305/12-1		400	x	x	x			
23.04.24	08:48	SO305/12-1		500	x	x	x			
23.04.24	08:48	SO305/12-1		600	x	x			x	
27.04.24	07:40	SO305/18-8	CTD #2 deploy Cast 041	5	x					x
27.04.24	07:40	SO305/18-8		50	x			x	x	x
27.04.24	07:40	SO305/18-8		100	x					x
27.04.24	07:40	SO305/18-8		150	x					x
27.04.24	07:40	SO305/18-8		200	x			x	x	x
27.04.24	07:40	SO305/18-8		300	x					x
27.04.24	07:40	SO305/18-8		400	x					x
27.04.24	07:40	SO305/18-8		500	x			x	x	x
27.04.24	07:40	SO305/18-8		600	x					x
29.04.24	04:00	SO305/21-2	CTD #2 recover Cast 052	5	x					x
29.04.24	04:00	SO305/21-2		50	x			x	x	x
29.04.24	04:00	SO305/21-2		100	x					x
29.04.24	04:00	SO305/21-2		150	x					x

29.04.24	04:00	SO305/21-2		200	x			x	x	x
29.04.24	04:00	SO305/21-2		300	x					x
29.04.24	04:00	SO305/21-2		400	x					x
29.04.24	04:00	SO305/21-2		500	x			x	x	x
29.04.24	04:00	SO305/21-2		600	x					x
29.04.24	08:48	SO305/21-1	**TRAP #2**	50	x	x	x			
29.04.24	08:48	SO305/21-1		100	x	x	x		x	
29.04.24	08:48	SO305/21-1		150	x	x	x			
29.04.24	08:48	SO305/21-1		200	x	x	x			
29.04.24	08:48	SO305/21-1		300	x	x			x	
29.04.24	08:48	SO305/21-1		400	x	x	x			
29.04.24	08:48	SO305/21-1		500	x	x	x			
29.04.24	08:48	SO305/21-1		600	x	x			x	
05.05.24	00:05	SO305/30-12	CTD #3 deploy Cast 082	5	x					x
05.05.24	00:05	SO305/30-12		50	x			x	x	x
05.05.24	00:05	SO305/30-12		100	x					x
05.05.24	00:05	SO305/30-12		150	x					x
05.05.24	00:05	SO305/30-12		200	x					x
05.05.24	00:05	SO305/30-12		300	x			x	x	x
05.05.24	00:05	SO305/30-12		400	x					x
05.05.24	00:05	SO305/30-12		500	x					x
05.05.24	00:05	SO305/30-12		600	x			x	x	x
05.05.24	23:50	SO305/32-2	Extra CTD 1 24h St. no trap Cast 085	5	x					x
05.05.24	23:50	SO305/32-2		50	x			x	x	x
05.05.24	23:50	SO305/32-2		100	x					x
05.05.24	23:50	SO305/32-2		150	x					x
05.05.24	23:50	SO305/32-2		200	x			x	x	x
05.05.24	23:50	SO305/32-2		300	x					x
05.05.24	23:50	SO305/32-2		400	x					x
05.05.24	23:50	SO305/32-2		500	x			x	x	x
05.05.24	23:50	SO305/32-2		600	x					x
07.05.24	12:51	SO305/33-2	CTD #3 recover Cast 093	5	x					x
07.05.24	12:51	SO305/33-2		50	x			x	x	x
07.05.24	12:51	SO305/33-2		100	x					x
07.05.24	12:51	SO305/33-2		150	x					x
07.05.24	12:51	SO305/33-2		200	x			x	x	x
07.05.24	12:51	SO305/33-2		300	x					x
07.05.24	12:51	SO305/33-2		400	x					x
07.05.24	12:51	SO305/33-2		500	x			x	x	x
07.05.24	12:51	SO305/33-2		600	x					x
07.05.24	11:05	SO305/33-1	**TRAP #3**	50	x	x	x		x	
07.05.24	11:05	SO305/33-1		100	x	x	x			
07.05.24	11:05	SO305/33-1		150	x	x	x			
07.05.24	11:05	SO305/33-1		200	x	x	x			

07.05.24	11:05	SO305/33-1		300	x	x			x	
07.05.24	11:05	SO305/33-1		400	x	x	x			
07.05.24	11:05	SO305/33-1		500	x	x	x			
07.05.24	11:05	SO305/33-1		600	x	x			x	
11.05.24	02:45	SO305/38-6	Extra CTD 2 no trap Cast 113	5	x					x
11.05.24	02:45	SO305/38-6		50	x			x	x	x
11.05.24	02:45	SO305/38-6		100	x					x
11.05.24	02:45	SO305/38-6		150	x					x
11.05.24	02:45	SO305/38-6		200	x					x
11.05.24	02:45	SO305/38-6		300	x			x	x	x
11.05.24	02:45	SO305/38-6		400	x					x
11.05.24	02:45	SO305/38-6		500	x					x
11.05.24	02:45	SO305/38-6		600	x			x	x	x